Scalar Field Theories of Nucleon Interactions

Frank A. Dick, B.S., M.S.

A Dissertation
Submitted to the Faculty
of the

Worcester Polytechnic Institute

in partial fulfillment of the requirements for the
Degree of Doctor of Philosophy
in
Physics

May, 2007

APPROVED:

_____

Professor John W. Norbury, Dissertation Advisor

_____

Professor P.K. Aravind, Co-Advisor

_____

Professor Khin Maung Maung, Committee Member

Acknowledgements

Contents

List of Figures

List of Tables

Abstract

This dissertation documents the results of two related efforts. Firstly, a model of nucleon-nucleon (NN) interactions is developed based on scalar field theory. Secondly, the relativistic 2-body Bethe-Salpeter equation (BSE) is generalized to handle inelastic processes in the ladder approximation.

Scalar field theory describes the behavior of scalar particles, particles with spin 0. In the present work scalar field theory is used to describe NN interactions mediated by pion exchange. The scalar theory is applied to nucleons despite the fact that nucleons are fermions, spin $1/2$ particles best described by four-component Dirac spinor fields. Nevertheless, the scalar theory is shown to give a good fit to experiment for the total cross sections for several reactions [1]. The results are consistent with more elaborate spinor models involving one boson exchange (OBE). The results indicate that the spin and isospin of nucleons can to some extent be ignored under certain conditions. Being able to ignore spin and isospin greatly reduces the complexity of the model.

A limitation of the scalar theory is that it does not distinguish between particle and anti-particle. Consequently one must decide how to interpret the s-channel diagrams generated by the theory, diagrams which involve particle creation and annihilation. The issue is resolved by extending the scalar theory to include electric charge, and formulating NN interactions in terms of complex scalar fields, which are able to describe both particles and anti-particles.

A generalized Bethe-Salpeter equation (GBSE) is developed to handle inelastic processes in the ladder approximation. The GBSE, formulated using the scalar theory, is new, and introduces a systematic method for analyzing families of coupled reactions. A formalism is developed centered around the amplitude matrix $\mathcal{M}'$ defined for a given Lagrangian. $\mathcal{M}'$ gives the amplitudes of a family

of reactions that arise from the Lagrangian. The formalism demonstrates how these amplitudes, to 2nd order, segregate into independent groups of coupled BSE's. The GBSE formalism is applied to the coupled BSE (CBSE) of Faassen and Tjon (FT) [2] for the reaction $N + N \rightarrow N + \Delta$, showing that the CBSE is missing a coupling channel, and in the expansion, under counts ladder diagrams. A proof is given of the equivalence of the series of ladder diagrams generated by $\mathcal{M}'$ and the S-matrix. A section on future work discusses several projects for further development and application of the GBSE.

1 Introduction

The objectives of the present work are twofold:

1. By merit of its simplicity, use scalar field theory to develop a model of nucleon-nucleon interactions.

2. Extend the model by using the Bethe-Salpeter equation (BSE) to sum over all orders of meson exchanges.

This introduction explains the rationale behind these objectives, and summarizes our chosen paths of investigation.

1.1 Applicability of Scalar Theory to Nucleon Interactions

The application of scalar theory to nucleon-nucleon (NN) interactions dates back to the work of Hideki Yukawa [3], who in 1935 proposed an early field theory for the NN interaction involving a potential based on the exchange of a massive scalar particle, now known as the pion. Yukawa used spinor fields for the nucleons, but scalar fields also lead to the Yukawa potential. It can be shown that the more modern quantum field theory, originally formulated by Feynman [4], Schwinger and Tomanaga in the late 1940s, when applied to scalar fields, leads to the Yukawa potential ([5] pg. 26). Wanders [6] has shown that the Bethe-Salpeter equation (BSE) for scalar fields, when taken to the non-relativistic limit, is equivalent to the Schrödinger equation with a Yukawa potential. In a literature search one can find articles in which the nucleon is represented by a scalar field. Researchers use the scalar theory for its simplicity, avoiding the encumbrances of the spinor formulation in order to to clarify relations that are not dependent on spin [7, 8, 9, 10]. Sauli and Adam use the complex scalar field [11]. An extensive review of BSE studies involving scalar theory is found in [12]. Scalar theory is often used as a first attempt to analyze NN interactions, for the reason that in its simplest form, it ignores both spin and isospin, thus avoids the analytical complexities involved when treating spin and isospin states and transitions. In

such applications, scalar theory has also been shown to serve as a useful approximation in describing the phenomena. This statement is validated by application of the present work [1].

1.2 Effective Field Theories

Particle field theories, in their most elaborate forms, take into account all available attributes of the particles. In addition to mass, the theories include particle spin, isospin, and various charges. The most fundamental charges are the electro-weak or flavor charge and the strong or color charge. These charges enter into the so-called standard model, which consists of the electro-weak theory, sometimes called quantum flavor dynamics (QFD), and the strong theory, called quantum chromo-dynamics (QCD). QFD describes the interaction of quarks and leptons through the exchange of the photon and the W+/- and Z bosons, while QCD describes the interaction of quarks through the exchange of gluons. The complexities of these theories are such that an accurate and detailed description of nucleon interactions at all energies has not yet been achieved [13]. Consequently, simplified theories, often called effective field theories, have been developed. These theories are aimed at reducing the complexity of the model while demonstrating the ability to accurately predict particle behavior for specified conditions (e.g., over particular energy ranges). Many theories are semi-empirical in nature, with parameters that can be adjusted to fit experiment.

The simplest dynamical particle field theory considers only two particle attributes, the inertia or mass m, and a "charge" or coupling strength g that is independent of the mass. The particle mass enters into the free particle Lagrangian, while the coupling strength enters into the interaction Lagrangian. With the attribute of spin being absent from the theory, the particles are treated as spin 0 particles or scalars, and are represented by scalar fields. The interactions are mediated by a neutral spin 0 particle, also represented by a scalar field.

9

1.3 Scalar Model of Nucleon Interactions

The scalar theory may be applied to nucleons. Nucleon interactions involve the strong nuclear force. The interactions are termed hadronic interactions, and particles involved in hadronic interactions are called hadrons. In the scalar model, the hadronic interaction is effected by the exchange of scalar mesons between nucleons. More fundamentally, hadronic interactions are mediated by gluons, which are exchanged by the quark constituents of the hadrons. Thus the nucleon-meson model is seen to be an effective field theory that replaces the underlying quark-gluon interaction with the simpler nucleon-meson interaction.

The nucleon's hadronic "charge" is represented by a coupling constant that specifies the strength of the hadronic interaction. The simplest description of the interaction is written as a product of three fields $A(x)$, $B(x)$ and $C(x)$ and coupling constants g_{AAC} and g_{ABC}. The interaction Lagrangian density

$$\mathcal{L} \;=\; -g_{AAC}A(x)A(x)C(x) - g_{ABC}A(x)B(x)C(x) \tag{1}$$

states that the intensity of interaction of the three particles is proportional to an energy density determined by the product of the field strengths *at the same point in 4-space*, scaled by the coupling constants. The A field represents nucleons, the B field the Δ baryon, and the C field the meson. The lightest meson is the pion, also called the π-meson or simply the π. The pion is involved in long to short range interactions (low to high energies). At medium range (medium energies) heavier mesons become involved in the nucleon-nucleon interactions. Various models work with as many as six mesons, the π, ρ, η, ϵ, δ, and the ω.

Although the scalar model recognizes only two particle attributes, this model is sufficient to determine scattering amplitudes, from which decay rates and differential and total cross sections are derived. The scalar model may be optimized by parameterizing the coupling constant and adjusting this parameter to improve the fit between theoretical and experimental differential and total cross sections. Parametrization of the coupling constant is justified by the fact that in high energy particle interactions, coupling constants depend on

the momentum of the interaction, and are known as running coupling constants.

In the scalar theory of nucleons no distinction is made between the proton and neutron, nor between particle and anti-particle. As a result, one must decide how to interpret the s-channel Feynman diagrams, which describe interactions involving the annihilation of the initial state particles, and creation of the final state particles. We cannot interpret these diagrams as proton-proton annihilation, since such a process violates conservation of baryon number, and does not occur in nature. The issue is resolved by simply identifying one of the initial state particles as an anti-particle, and one of the final state particles as an anti-particle. Alternatively, one may adopt a model that accommodates anti-particles. The charged scalar model achieves this, but at the cost of added complexity. To include anti-particles, one must consider a third particle attribute, the electric charge.

1.4 Complex Scalar and Spinor Fields

The charged scalar model is formulated in terms of the complex scalar field. The complex field has two components, and thereby has the capacity to distinguish particles from anti-particles. In the model, the proton acquires an electric charge of $+1$, and the anti-proton a charge of -1. With the model's recognition of electric charge, protons also become distinct from neutrons, and the description of interactions must treat charge exchange mediated by charged pseudo-scalar mesons. The handling of charge exchange is dealt with using the isospin formalism, in which the proton and neutron form an isospin doublet. The description of interactions takes into account the isospin states of the initial and final state particles, and handles isospin transitions.

With the additional field components, the incorporation of the charged pseudo-scalar mesons and the inclusion of the isospin formalism, the step up from the scalar to complex scalar field is accompanied by a significant increase in the complexity of the model. The s-channel diagrams are explained in explicit fashion as describing the reaction between a nucleon and anti-nucleon. In view of one of our goals, namely to predict the cross sections of *nucleon-nucleon* interactions, the s-channel diagrams are not required by either the scalar

or the complex scalar model. The scalar model is, therefore, a reasonable choice for the given application, and the complexity of the charged scalar model is thereby avoided.

Nucleons are spin 1/2 particles, and the four component Dirac spinor fields, which by design account for both particles and anti-particles and their spin states, are more appropriate than scalar fields for describing the nucleons. However, by including the particle attribute of spin, the model must also include mesons capable of carrying spin and mediating spin transitions. The set of exchange particles must therefore expand again to include spin 1 vector mesons. The introduction of four-component spinor fields, the simultaneous treatment of spin and isospin states, and spin and isospin transitions, entail yet another significant increase in complexity of the model. In keeping with our stated goal, namely to assess how well the calculated cross sections of scalar theory fit experiment, we purposely avoid the complexities of the spinor field theory.

1.5   Current Theories of Nucleon-Nucleon Interactions

Beyond the attributes of mass, hadronic charge, electric charge and spin, current theories of nucleon-nucleon interactions consider additional degrees of freedom, that is, additional channels through which interactions can occur. So far we have considered *meson* degrees of freedom, in which the nucleons exchange the several types of mesons. The *isobar* degree of freedom arises from the formation of πN resonances in NN interactions. The *nucleon* degree of freedom proposed by Skyrme [14] arises from the *baryonic current* and characterization of baryons as *topological solitons*, in essence exchange particles. Long range and medium range nucleon interactions are successfully described by various models which take into account the hadronic degrees of freedom (meson, isobar and nucleon) [13]. These models are used to calculate cross sections, phase shifts, analyzing power, polarization and various spin observables, for comparison to experiment. So far, attempts to describe particle interactions in terms of the *quark* degrees of freedom, both as a stand-alone model or a hybrid model (quark and hadronic degrees of freedom combined) have not been altogether successful. The scalar theory is capable of embracing the meson, isobar and nucleon degrees of freedom.

The present work employs the meson and isobar degrees of freedom. The nucleon degree of freedom is also included in the application of the generalized Bethe-Salpeter equation to the 3-vertex model in section 4.16, where the nucleon degree of freedom takes the form of a nucleon kernel.

1.6   Summing Diagrams to all Orders

In Dick-Norbury [1] the one pion exchange (OPE) model is used to determine pion production cross sections. The OPE model is based on 2nd order diagrams. Diagrams of 4th and higher order are neglected. The 2nd order cutoff is convenient, but for nucleon interactions, higher order terms are significant, especially at higher energies. Greater accuracy in determining amplitudes is attained by including higher order diagrams, but the amount of calculation increases rapidly with order. The Bethe-Salpeter equation (BSE) offers a way of including higher order terms. The BSE couples the amplitude to itself, giving a compact expression for the sum over all orders of diagrams. The sum is performed in the *ladder approximation*, which is valid when the ladder diagrams dominate over loop diagrams and cross diagrams ([15], chap. 12). The BSE describes bound states and elastic scattering processes. For inelastic processes, a generalization of the BSE is needed. Section 4 details the development of a generalized BSE (GBSE) for inelastic processes in the ladder approximation. Section 5 *Future Work* outlines research topics for the continued development of the GBSE.

The next section launches the in-depth presentation with a summary of the theory of scalar fields.

2 Quantized Scalar Fields

The scalar field, also known as the Klein-Gordon field, is discussed in most if not all quantum field theory textbooks [5, 15, 16, 17, 18, 19, 20, 21, 22, 23, 24, 25, 26, 27, 28, 29]. This section draws primarily on the texts of Norbury [16], Aitchison [17], Peskin [18] and Maggiore [19], hereinafter referred to collectively as NAPM, and provides a summary of the theory of scalar fields. Several interaction Lagrangians are then defined and discussed as candidates for modeling the nucleon-nucleon interactions mediated by pion exchange. The Lagrangian $\mathcal{L} = -g_{AAC}AAC - g_{ABC}ABC$ given by (1) and formed from two types of interaction vertices is discussed in detail. This Lagrangian forms the basis for the work documented in the paper *Pion Cross Sections from Scalar Theory* [1], in which cross sections calculated from the scalar theory are fitted to experimentally determined cross sections. The paper draws on a second paper *Differential Cross Section Kinematics for 3-Dimensional Transport Codes* [30].

2.1 Overview of the Theory of Scalar Fields

The following sections provide an overview of the theory of scalar fields, and are followed by a derivation of 2nd order Feynman diagrams for the reaction $N + N \rightarrow N + \Delta$. We present the scalar field of a free particle, and quantize the field by expressing it in terms of particle creation and destruction operators. The free particle and interaction Lagrangians and Hamiltonians are defined in terms of these operators. The interaction Hamiltonian enters into the S-matrix, a perturbative expansion of terms to all orders in the coupling constant. Using Wick's theorem, the terms are translated into Feynman diagrams. The scattering amplitude then follows from the application of Feynman's rules.

2.1.1   The Klein-Gordon Equation and Free Particle Fields

The field ϕ of a free scalar particle of positive mass m is a real field that satisfies the Klein-Gordon equation (KGE)

$$(\Box + m^2)\phi \;=\; 0 \tag{2}$$

where

$$\phi \;=\; \phi(x) \tag{3}$$

$$\Box \;=\; \partial_\mu \partial^\mu \;=\; \frac{\partial^2}{\partial t^2} - \nabla^2 \tag{4}$$

and where x is a point in 4-space. The KGE may be derived from the relativistic energy relation

$$p^2 - m^2 \;=\; 0 \tag{5}$$

$$p^2 \;=\; E^2 - |\mathbf{p}|^2 \tag{6}$$

where $p = (E, \mathbf{p})$ is the 4-momentum of the particle. Substituting the quantum mechanical operators

$$E \;\to\; i\frac{\partial}{\partial t} \tag{7}$$

$$\mathbf{p} \;\to\; -i\nabla \tag{8}$$

into (5) and letting both sides operate on ϕ leads to (2). The KGE is also derivable from a stationary action principle using the action S and free particle Lagrangian density $\mathcal{L}$ (hereinafter referred to simply as the Lagrangian) given by

$$\mathcal{S} \;=\; \frac{1}{2}\int d^4x\,\mathcal{L} \tag{9}$$

$$\mathcal{L} \;=\; \partial_\mu \phi \partial^\mu \phi - m^2 \phi^2 \tag{10}$$

The real field ϕ is a superposition of planes waves $e^{\mp ip\cdot x}$ of the form

$$\phi(x) \;=\; \int \frac{d^3p}{(2\pi)^3\sqrt{2E_{\mathbf{p}}}}(a_{\mathbf{p}}e^{-ip\cdot x} + a_{\mathbf{p}}^\dagger e^{ip\cdot x}) \tag{11}$$

$$=\; \phi_+(x) + \phi_-(x) \tag{12}$$

15

where

$$\phi_+(x) \quad = \quad \int \frac{d^3p}{(2\pi)^3\sqrt{2E_{\mathbf{p}}}} a_{\mathbf{p}} e^{-ip\cdot x} \tag{13}$$

$$\phi_-(x) \quad = \quad \int \frac{d^3p}{(2\pi)^3\sqrt{2E_{\mathbf{p}}}} a_{\mathbf{p}}^\dagger e^{ip\cdot x} \tag{14}$$

$$E_{\mathbf{p}} \quad \equiv \quad \sqrt{\mathbf{p}^2 + m^2} \tag{15}$$

$$a_{\mathbf{p}} \quad = \quad a(\mathbf{p}) \tag{16}$$

$$a_{\mathbf{p}}^\dagger \quad = \quad a^\dagger(\mathbf{p}) \tag{17}$$

and where the factor $\sqrt{2E_{\mathbf{p}}}$ gives the normalization in the NAPM formalism.

2.1.2 Quantization of the Free Fields

In the quantized theory, the coefficients $a_{\mathbf{p}}$ and $a_{\mathbf{p}}^\dagger$ become destruction and creation operators, respectively, on particle states $|\mathbf{p}\rangle$ in Fock space. The state $|0\rangle$ is the vacuum state, and is defined by

$$a_{\mathbf{p}}|0\rangle \quad \equiv \quad 0 \tag{18}$$

$$\langle 0|a_{\mathbf{p}}^\dagger \quad \equiv \quad 0 \tag{19}$$

The state $|\mathbf{p}\rangle$ signifies the existence of a single particle of momentum $\mathbf{p}$, and is created by the creation operator acting on the vacuum state

$$|\mathbf{p}\rangle \quad = \quad \sqrt{2E_{\mathbf{p}}} a_{\mathbf{p}}^\dagger |0\rangle \tag{20}$$

$$\langle \mathbf{p}| \quad = \quad \sqrt{2E_{\mathbf{p}}} \langle 0|a_{\mathbf{p}} \tag{21}$$

The operators obey the commutation relation

$$[a_{\mathbf{p}}, a_{p'}^\dagger] \quad = \quad (2\pi)^3 \delta(\mathbf{p} - \mathbf{p}') \tag{22}$$

Some other useful results are

$$a_{\mathbf{p}}|\mathbf{p}'\rangle = (2\pi)^3 \sqrt{2E_{\mathbf{p}}} \delta^4(\mathbf{p} - \mathbf{p}')|0\rangle \tag{23}$$

$$\phi_+(x)|\mathbf{p}\rangle = e^{-ip\cdot x}|0\rangle \tag{24}$$

$$\langle\mathbf{p}'|\phi_-(x)\phi_+(y)|\mathbf{p}\rangle = e^{i(p'\cdot x - p\cdot y)} \tag{25}$$

$$\langle\mathbf{p}'|\phi_+(x)\phi_-(y)|\mathbf{p}\rangle = \langle\mathbf{p}'|\phi_-(x)\phi_+(y)|\mathbf{p}\rangle + i\Delta^+(x - y)\langle\mathbf{p}'|\mathbf{p}\rangle \tag{26}$$

The Hamiltonian density can be expressed in terms of the operators

$$\mathcal{H} = \int \frac{d^3p}{(2\pi)^3} E_{\mathbf{p}} \left(a_{\mathbf{p}}^\dagger a_{\mathbf{p}} + \frac{1}{2}[a_{\mathbf{p}}, a_{\mathbf{p}}^\dagger] \right) \tag{27}$$

The 2nd term makes an infinite contribution, and represents an infinite ground state energy. In quantum field theory, we are interested in the energy of states "above" the ground state, so we discard the infinite term. The term is formally removed by the process known as *normal ordering*. In a normal ordered product of operators, all annihilation operators are placed to the right of creation operators. A bracket of colons : : denotes a normal ordered product. For example, $: a_{\mathbf{p}} a_{\mathbf{p}}^\dagger := a_{\mathbf{p}}^\dagger a_{\mathbf{p}}$. The normal ordered Hamiltonian is

$$: \mathcal{H} : = \int \frac{d^3p}{(2\pi)^3} E_{\mathbf{p}} a_{\mathbf{p}}^\dagger a_{\mathbf{p}} \tag{28}$$

Wick's theorem presented below makes use of normal ordering to render a time ordered product into a collection of normal ordered products from which Feynman diagrams are readily extracted.

Particles of the scalar field are their own anti-particles. This is demonstrated at the end of section 3.1. This aspect of scalar fields requires care in interpreting the 2nd order s-channel diagram of NN interactions (see section 2.4.4).

2.1.3 The Interaction Lagrangian and Hamiltonian

The Lagrangian and Hamiltonian discussed so far describe free particles. To describe interacting particles we include an interaction term

$$\mathcal{H} = \mathcal{H}_0 + \mathcal{H}_I \tag{29}$$

17

where $\mathcal{H}_0$ is the free particle Hamiltonian and $\mathcal{H}_I$ is the interaction Hamiltonian. We shall work with Hamiltonians that are products of three fields, with no derivative coupling (e.g., $\nabla\phi$)

$$\mathcal{H}_I \;=\; -\mathcal{L}_I \;=\; g_{ABC}\phi_A(x_1)\phi_B(x_1)\phi_C(x_1) \tag{30}$$

where g_{ABC} is a coupling constant that represents the strength of the interaction between the fields. The interaction Lagrangian is discussed in detail in section 2.2. The interaction Hamiltonian enters into the S-matrix.

2.1.4 The S-Matrix and Scattering Amplitude

The Dyson scattering matrix or S-matrix determines the amplitude of a scattering process, given the interaction Hamiltonian and the initial and final states of the interacting particles. The S-matrix is a perturbation expansion containing terms to all orders in the interaction Hamiltonian. If the coupling constant is small, higher order terms may be neglected and the amplitude can be approximated by the first few terms in the series. The S-matrix is given by

$$
\begin{aligned}
S \;&=\; T\,\exp\left(-i\int d^4x\,\mathcal{H}_\mathcal{I}\right) \\
&=\; 1+\sum_{n=1}^{\infty}\frac{(-i)^n}{n!}\int d^4x_1\ldots d^4x_n\,T\left[\mathcal{H}_I(x_1)\ldots\mathcal{H}_I(x_n)\right] \\
&=\; 1+\sum_{n=1}^{\infty}S_n
\end{aligned}
\tag{31}
$$

where T is the time ordering operator, which ensures that the Hamiltonians, hence the fields, are ordered in time with the earliest to the right. We shall focus on S_2 and S_4, which produce 2nd and 4th order Feynman diagrams, respectively, given by

$$S_2 \;=\; \frac{(-i)^2}{2!}\int d^4x_1 d^4x_2\,T\left[\mathcal{H}_\mathcal{I}(x_1)\mathcal{H}_\mathcal{I}(x_2)\right] \tag{32}$$

$$S_4 \;=\; \frac{(-i)^4}{4!}\int d^4x_1\ldots d^4x_4\,T\left[\mathcal{H}_\mathcal{I}(x_1)\ldots\mathcal{H}_\mathcal{I}(x_4)\right] \tag{33}$$

$$\tag{34}$$

For two-body scattering, the scattering amplitude $\mathcal{M}$ is written in terms of S from the relation

$$S = 1 + (2\pi)^4 \delta^4(p_1 + p_2 - p_3 - p_4) i\mathcal{M} \tag{35}$$

where p_1 and p_2 are the 4-momenta of the initial state particles and p_3 and p_4 are the 4-momenta of the final state particles. Given initial and final particle states $|i\rangle$ and $\langle f|$

$$|i\rangle = |p_1, p_2\rangle \tag{36}$$

$$\langle f| = \langle p_3, p_4| \tag{37}$$

the scattering amplitude becomes

$$S_{fi} = \langle f|S|i\rangle$$

$$= 1 + (2\pi)^4 \delta^4(p_1 + p_2 - p_3 - p_4) i\mathcal{M}_{fi} \tag{38}$$

The scattering amplitude is used in [1] to calculate pion production cross sections.

2.1.5 The Feynman Propagator

The Feynman propagator is the vacuum expectation value (VEV) of the time ordered product of two fields, and is given by

$$\langle 0|T\{\phi(x_1)\phi(x_2)\}|0\rangle = D_F(x_1 - x_2)$$

$$= \int \frac{d^4 p}{(2\pi)^4} \frac{i}{p^2 - m^2 - i\epsilon} e^{ip(x_1 - x_2)} \tag{39}$$

In momentum space the propagator is

$$D_F(p) = \frac{i}{p^2 - m^2 - i\epsilon} \tag{40}$$

The Feynman propagator appears in Wick contractions, and is a vital component in the reduction of time ordered products of fields to Feynman diagrams.

2.1.6   Wick's Theorem and External Contractions

The application of Wick's theorem to terms in the S-matrix streamlines the process of determining Feynman diagrams. The method is augmented by using Peskin's external contractions [18]. Wick's theorem states that a time ordered product of fields is equal to the sum of a sequence of normal ordered products consisting of the product plus all contractions of the product

$$T\left\{\phi(x_1)\ldots\phi(x_n)\right\} \;=\; :\phi(x_1)\ldots\phi(x_n) + \textit{all possible contractions}: \qquad (41)$$

Contractions produce Feynman propagators. Given two fields $\phi(x_1)$ and $\phi(x_2)$ and initial and final vacuum states $|0\rangle$ and $\langle 0|$, the contraction of the two fields is indicated by a horizontal bracket

$$\langle 0|\overset{\frown}{\phi(x_1)\phi(x_2)}|0\rangle = D_F(x_1 - x_2) \qquad (42)$$

External state contractions are defined by

$$\overset{\frown}{\phi(x)|\mathbf{p}\rangle} \equiv e^{-ip\cdot x}|0\rangle \qquad (43)$$

$$\langle\mathbf{p}|\overset{\frown}{\phi(x)} \equiv \langle 0|e^{+ip\cdot x} \qquad (44)$$

The set of all possible contractions produces all possible time orderings. The S-matrix has a built in factor of $1/n!$ in the nth order term to cancel the $n!$ duplicate terms produced by generating all time orderings.

In applying Wick/Peskin contractions to bosonic fields as we do here, we encounter the vertex AAC in the Hamiltonian. This vertex contains two identical A fields, and we must apply the following rule for how the fields contract with the initial and final states, to prevent over-counting of diagrams:

An external state is allowed to contract to a vertex only once. If two identical fields appear at a vertex, the external state may contract to only one of the two.

This rule deals with one of several types of symmetry factors that occur when performing contractions ([18] chap. 4). In section 2.4 we apply the method of Wick/Peskin contractions to the time ordered products of fields appearing in the S-matrix.

2.2   Candidate Interaction Lagrangians

The Interaction Lagrangian densities (hereinafter referred to simply as Lagrangians) considered in this work have terms of the form $\phi_a(x)\phi_b(x)\phi_c(x)$, in which the product of the three fields ϕ_a, ϕ_b and ϕ_c signifies that the fields interact at a point x in space and time, a vertex. Lagrangians of this form, styled by Gross as "ϕ^3" theory ([15] chap. 12), are commonly used to describe the interaction of two real scalar particles and one virtual or exchange scalar particle. The present work shows that the ϕ^3 terms suffice to accurately determine the total cross sections of various NN interactions, in which, of course, the nucleons are treated as scalar particles.

We consider the suitability of the Lagrangians below for describing the reactions $N + N \to N + N$ and $N + N \to N + \Delta$, where N is a nucleon and Δ is the Δ baryon. We let $A(x) = N(x)$ be the field of the nucleon, $B(x) = \Delta(x)$ the field of the Δ baryon, and $C(x)$ the field of the exchange pion.

$$\mathcal{L}_1 = -g_{AAC}A_1(x)A_2(x)C(x) = -g_{AA}AAC \tag{45}$$

$$\mathcal{L}_4 = -g_{ABC}A(x)B(x)C(x) = -g_{AB}ABC \tag{46}$$

$$\mathcal{L}_2 = -g_{AAC}A_1(x)A_2(x)C(x) - g_{ABC}A(x)B(x)C(x)$$

$$= -g_{AA}AAC - g_{AB}ABC = -AAC - ABC \tag{47}$$

$$\mathcal{L}_3 = -g_{AAC}A_1(x)A_2(x)C(x) - g_{ABC}A(x)B(x)C(x) - g_{BBC}B_1(x)B_2(x)C(x)$$

$$= -g_{AA}AAC - g_{AB}ABC - g_{BB}BBC = -AAC - ABC - BBC \tag{48}$$

where $A(x)$, $B(x)$ and $C(x)$ are the scalar fields of particles A, B and C respectively, C is the exchange particle (more exactly, the field of the exchange particle) and the g's are the coupling constants (interaction strengths) of the three types of vertices AAC, ABC and

BBC. For shorthand, we drop the subscript C from the coupling constants, and suppress the dependence on 4-space coordinate x.

The table in figure 1 lists the four candidate Lagrangians (coupling constants omitted) along with the generic 2nd order diagrams generated by the Lagrangians. By "generic" we mean that the type of meson exchange, t-channel, u-channel or s-channel, is not specified. The table also lists the kernels (U) and propagators (G) from which ladder diagrams are constructed (see section 4 for the discussion of the generalized Bethe-Salpeter equation). Each 2nd order diagram may be rotated, flipped and twisted to produce all types of exchanges. If a diagram has identical particles in the initial (or final) state, there is also an associated exchange diagram (here the word "exchange" means that identical particles are "swapped" in either the initial or final state).

2.3   Lagrangians for Nucleon-Nucleon Interactions

The description of NN interactions requires at least two types of fields, one for the nucleon and one for the exchange particle, the pion. Only one type of nucleon is recognized, and no distinction is made between proton and neutron. By considering all nucleons the same, isospin is, in effect, ignored. Most models of nucleon-nucleon interactions take into account isospin, which differentiates between the two types of nucleons. The decision to ignore isospin is consistent with our thesis, namely to use as simplified a theory as possible, and to assess the ability of this theory to accurately describe NN interactions.

Letting the letter A represent the field of the nucleon and C represent the field of the pion, the interaction Lagrangian

$$\mathcal{L}_1 \;=\; -g_{AA}AAC \tag{49}$$

may be used to describe interactions between two nucleons at energies *below* the pion threshold. Figure 1 (top row) shows the two-vertex diagram that corresponds to the elastic interaction between two nucleons $A + A \rightarrow A + A$.

If the energy of interaction is sufficient, the interaction of two nucleons can produce a

Lagrangian | **2nd Order Diagrams Involving C Exchange** | **Kernels(U)** | **Propagators(G)**

$\mathcal{L}_1 = $ **-AAC** for energies below the one pion threshold

$U_A = $ [A], $U_C = $ [C]

$G_A^A = $ [A/A], $G_C^A = $ [A/C]
$G_A^C = $ [C/A], $G_C^C = $ [C/C]

$\mathcal{L}_4 = $ **-ABC** incomplete at all energies

Propagators for C kernels only

$U_C = $ [C]

$G_A^A = $ [A/A], $G_B^A = $ [A/B]
$G_A^B = $ [B/A], $G_B^B = $ [B/B]

$\mathcal{L}_2 = $ **-AAC - ABC** for energies above the one pion threshold but below the two pion threshold

Each of the three Lagrangians $\mathcal{L}_2$, $\mathcal{L}_3$ and $\mathcal{L}_4$ can produce three kernels and nine propagators.

Propagators for A and B kernels only

$U_A = $ [A], $U_B = $ [B]

$G_C^A = $ [A/C], $G_A^C = $ [C/A]
$G_C^B = $ [B/C], $G_B^C = $ [C/B]
$G_C^C = $ [C/C]

$\mathcal{L}_3 = $ **- AAC - ABC - BBC** for energies above the two pion threshold

Figure 1: Four Scalar Langrangians.

Delta baryon. Designating the Delta baryon field as B, the inelastic reaction $A+A \rightarrow A+B$ shown in figure 1 (third row) describes Delta baryon production. It is clear from the diagram that two types of vertices are required, AAC and ABC, and the interaction Lagrangian must take the form

$$\mathcal{L}_2 \quad = \quad -g_{AA}AAC - g_{AB}ABC \tag{50}$$

This "2-vertex" Lagrangian suffices to describe interactions at energies below the threshold for double Δ production. But even at the lower pion π threshold, a "virtual" Δ particle may be produced. This virtual Δ propagates between interaction vertices. Thus the 2-vertex Lagrangian becomes applicable at this lower threshold, the π threshold.

Above the $\Delta\Delta$ threshold, the reaction $A + A \rightarrow B + B$ is possible. The presence of two Δ particles suggests a third interaction vertex BBC, requiring the 3-vertex Lagrangian given by

$$\mathcal{L}_3 \quad = \quad -g_{AA}AAC - g_{AB}ABC - g_{BB}BBC \tag{51}$$

Above the double π threshold, two virtual Δ particles may propagate simultaneously. Thus the 3-vertex Lagrangian becomes applicable at the $\pi\pi$ threshold.

The 2-vertex Lagrangian forms the basis for the application of scalar theory to the determination of pion production cross sections [1]. In the next section we use the 2-vertex Lagrangian to determine the 2nd order Feynman diagrams for an inelastic process.

2.4   Second Order Diagrams of NN Interactions

The scalar theory developed in the preceding sections is used to derive the 2nd order Feynman diagrams for the inelastic process $N+N \rightarrow N+\Delta$. We use the interaction Hamiltonian defined by (50)

$$\mathcal{H}_I \quad = \quad -\mathcal{L}_I \quad = \quad g_{AA}AAC + g_{AB}ABC \tag{52}$$

which contains two types of vertices, AAC and ABC. This form has the versatility to describe the reaction $N + N \rightarrow N + \Delta$. In the remainder of the discussion, we use the

24

substitutions

$$N \rightarrow A$$

$$\Delta \rightarrow B$$

$$X \rightarrow B$$

and use C to represent the exchange pion (π). The letters A, B and C represent the fields of the particles

$$A \equiv A(x) \tag{53}$$

$$B \equiv B(x) \tag{54}$$

$$C \equiv C(x) \tag{55}$$

2.4.1 2nd Order Diagrams for $N + N \rightarrow N + \Delta$

The initial and final particle states of this reaction are

$$|i\rangle = |A_1 A_2\rangle \tag{56}$$

$$\langle f| = \langle A'B'| \tag{57}$$

where A_1 and A_2 label the initial state particles (nucleons) and A' and B' label the final state particles (nucleon and Δ baryon). Inserting the Hamiltonian (52) into the S_2 term of the S-matrix (32) and expanding the product of Hamiltonians

$$
\begin{aligned}
S_2 &= \frac{(-i)^2}{2!} \int d^4 x_1 d^4 x_2 T\left[\mathcal{H}_{\mathcal{I}}(x_1)\mathcal{H}_{\mathcal{I}}(x_2)\right] \\
&= \frac{(-i)^2}{2!} \int d^4 x_1 d^4 x_2 T[A(x_1)A(x_1)C(x_1) + A(x_1)B(x_1)C(x_1)] \times \\
&\quad [A(x_2)A(x_2)C(x_2) + A(x_2)B(x_2)C(x_2)] \\
&= \frac{(-i)^2}{2!} \int d^4 x_1 d^4 x_2 T[(AAC)_1(AAC)_2] + T[(AAC)_1(ABC)_2] + \\
&\quad T[(ABC)_1(AAC)_2] + T[(ABC)_1(ABC)_2]
\end{aligned}
\tag{58}
$$

gives four terms, each a product of six fields

$$(AAC)_1(AAC)_2$$

25

$$(ABC)_1(ABC)_2$$

$$(AAC)_1(ABC)_2$$

$$(ABC)_1(AAC)_2$$

The notation has been simplified by setting $A(x_1)B(x_1)C(x_1) \equiv (ABC)_1$, similarly for the other three terms, and hiding the coupling constants. In calculating the expectation value

$$\langle f|S_2|i\rangle \quad = \quad \langle A'B'|S_2|A_1A_2\rangle \tag{59}$$

we insert the sum of four terms

$$
\begin{aligned}
\langle f|T\left[\mathcal{H}_\mathcal{I}(x_1)\mathcal{H}_\mathcal{I}(x_2)\right]|i\rangle \quad &= \quad \langle A'B'|T[(AAC)_1(AAC)_2]|A_1A_2\rangle + \\
&= \quad \langle A'B'|T[(ABC)_1(ABC)_2]|A_1A_2\rangle + \\
&= \quad \langle A'B'|T[(AAC)_1(ABC)_2]|A_1A_2\rangle + \\
&= \quad \langle A'B'|T[(ABC)_1(AAC)_2]|A_1A_2\rangle \tag{60}
\end{aligned}
$$

and for each term, count the number of *A fields and states*, *B fields and states* and C fields (there are no C states). Each of these numbers must be an even number, since contractions will pair the fields and states. Consequently, the first two terms cannot contribute to the reaction. Both of these terms have an odd number of Bs. The last two terms have the correct number of fields and states, so (58) reduces to

$$
\begin{aligned}
\langle p_3\, p_4|S_2|p_1\, p_2\rangle \quad &= \quad \frac{(-i)^2 g_{AA}g_{AB}}{2!}\int d^4x_1 d^4x_2 \times \\
&\qquad \langle p_4\, p_3|T\{A_1\, B_1\, C_1\ A_2\, A_2\, C_2 + A_1\, A_1\, C_1\ A_2\, B_2\, C_2\}|p_1\, p_2\rangle
\end{aligned}
$$

$$\tag{61}$$

where the initial state particles have been labeled by their momenta p_1, p_2, the final state particles by their momenta p_3 and p_4, and the field subscripts 1 and 2 indicate at which vertex the field is taken. Also, the coupling constants g_{AA} and g_{AB} have been restored. We proceed to evaluate (61) by contracting each term in all possible ways. The two contributing

The two terms that contribute to $A + A \rightarrow A + B$:

(a) $\langle A'B' \,|\, (ABC)_1 \; (AAC)_2 \,|A_1A_2\rangle$

(b) $\langle A'B' \,|\, (AAC)_1 \; (ABC)_2 \,|A_1A_2\rangle$

Three ways to contract term (a) give three diagrams:

$\langle A'B' \,|\; (ABC)_1 \; (AAC)_2 \;|\; A_1A_2 \,\rangle$

$\langle A'B' \,|\; (ABC)_1 \; (AAC)_2 \;|\; A_1A_2 \,\rangle$

$\langle A'B' \,|\; (ABC)_1 \; (AAC)_2 \;|\; A_1A_2 \,\rangle$

s-channel

t-channel

u-channel
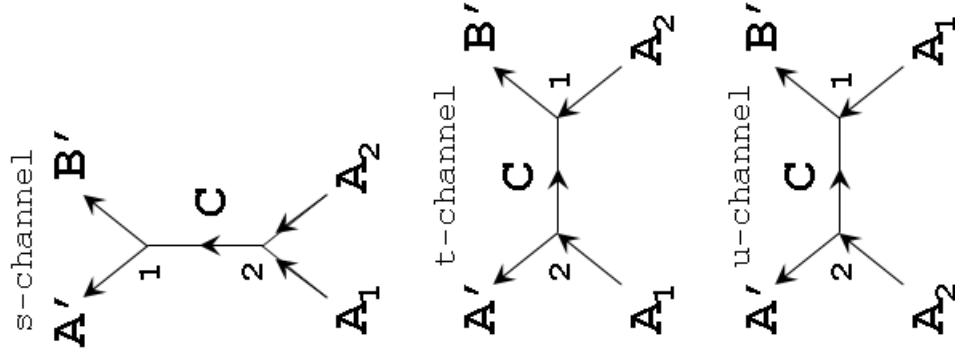
Figure 2: 2nd Order Diagrams for reaction $A + A \rightarrow A + B$.

terms labeled (a) and (b) are shown at the top of figure 2. The only sets of contractions that contribute to the reaction are those in which all fields and states are contracted. There are three contributing sets of contractions produced by each term. For the first term, the figure shows the three contributing sets of contractions and their corresponding Feynman diagrams. The B' state contracts with the B field in only one way, and the two C fields contract with each other in only one way. The A' state can contract in two ways, once to an A field at vertex 1, and once to an A field at vertex 2. When the A' state contracts to vertex 2, there are two ways the A_1 state can contract, once to vertex 1 and once to vertex 2.

The second term produces an identical group of diagrams. This is made obvious by considering that the vertex labels 1 and 2 are dummy labels, and may be reassigned (swapped) in the second term, showing its equivalence to the first term. Together the two terms produce two of each diagram. The factor of $1/2!$ in S_2 cancels the duplicates.

The diagrams may be read directly from the contracted terms. The contractions indicate to which vertices the externals states are attached. In the diagrams, time proceeds upward across the page. The initial state particles enter vertices from below, and the final state particles exit vertices from above. The second and third diagrams are referred to as the "direct" and "exchange" diagrams, the difference being in the placement of the initial states A_1 and A_2 at the vertices. The third diagram is obtained from the second by exchanging the two initial states.

Note that the exchange term owes its existence to the presence of two vertices in the Lagrangian $\mathcal{L} = -AAC - ABC$. In applying the Wick/Peskin contractions, it is immediately clear that having the two vertices ABC and AAC present gives the initial state particles A_1 and A_2 two places to which they can contract, which leads to direct and exchange terms. These contractions of symbols mirror the physical view. Two identical nucleons A_1 and A_2 interact by exchanging a meson. There are two possible outcomes for each particle: 1) exchange the pion and become a Delta baryon, or 2) exchange the pion and remain a

nucleon. In mathematical symbols, we "give" the particles these two possibilities by giving them two types of vertices to which they may connect, two types of interactions in which they may engage. Similarly in spinor theory, the Lagrangian consists of the sum of an interaction vertex and it's hermitian conjugate [31, 32]. Together, the two vertices provide for the existence of an exchange term.

2.4.2 Evaluation of $\langle f|S_2|i\rangle$

Each of the three diagrams (contracted terms) in figure 2 contributes to the expectation value $\langle f|S_2|i\rangle$. Labeling these contributions by the type of diagram s, t and u, we have $S_2 = S_{2s} + S_{2t} + S_{2u}$ and

$$
\begin{aligned}
\langle f|S_2|i\rangle &= \langle f|S_{2s}|i\rangle + \langle f|S_{2t}|i\rangle + \langle f|S_{2u}|i\rangle \\
&= \langle f|S_{2s,a}|i\rangle + \langle f|S_{2s,b}|i\rangle + \langle f|S_{2t,a}|i\rangle + \langle f|S_{2t,b}|i\rangle + \langle f|S_{2u,a}|i\rangle + \langle f|S_{2u,b}|i\rangle
\end{aligned}
\tag{62}
$$

In the last line the contributions from terms (a) and (b) are shown separately. Taking the fully contracted term $\langle f|S_{2s,a}|i\rangle$

$$
\langle f|S_{2s,a}|i\rangle = \frac{(-i)^2 g_{AA} g_{AB}}{2!} \int d^4x_1 d^4x_2 \langle p_3 p_4 | A_1 \, B_1 \, C_1 \, A_2 \, A_2 \, C_2 | p_1 p_2 \rangle
\tag{63}
$$

and substituting the propagator (42) for the internal C-contraction, and (43) and (44) for right and left external contractions gives

$$
\langle f|S_{2s,a}|i\rangle = \frac{(-i)^2 g_{AA} g_{AB}}{2!} \int d^4x_1 d^4x_2 D_F(x_1 - x_2) e^{ip_3 x_1} e^{ip_4 x_1} e^{-ip_1 x_2} e^{-ip_2 x_2}
\tag{64}
$$

Making the same substitutions for the fully contracted term $\langle f|S_{2s,b}|i\rangle$ gives

$$
\langle f|S_{2s,b}|i\rangle = \frac{(-i)^2 g_{AA} g_{AB}}{2!} \int d^4x_1 d^4x_2 D_F(x_2 - x_1) e^{ip_3 x_2} e^{ip_4 x_2} e^{-ip_1 x_1} e^{-ip_2 x_1}
\tag{65}
$$

Swapping the dummy vertex indices 1 and 2 in $\langle f|S_{2s,b}|i\rangle$ shows that the (b) term is identical to the (a) term $\langle f|S_{2s,a}|i\rangle$. Combining the two terms

$$
\langle f|S_{2s}|i\rangle = \langle f|S_{2s,a}|i\rangle + \langle f|S_{2s,b}|i\rangle = 2 \times \langle f|S_{2s,a}|i\rangle
\tag{66}
$$

and substituting (39) for the propagator $D_F(x_1 - x_2)$ leads to

$$
\begin{aligned}
\langle f|S_{2s}|i\rangle &= \frac{2(-i)^2 g_{AA}g_{AB}}{2!} \int d^4x_1 d^4x_2 \frac{d^4p}{(2\pi)^4} \frac{i}{p^2 - m^2 - i\epsilon} e^{ip(x_1 - x_2)} \times \\
&\quad e^{ix_1(p_3 + p_4)} e^{-ix_2(p_1 + p_2)} \\
&= \frac{2(-i)^2 g_{AA}g_{AB}}{2!} \int d^4x_1 d^4x_2 \frac{d^4p}{(2\pi)^4} \frac{i}{p^2 - m^2 - i\epsilon} e^{ix_1(p_3 + p_4 + p)} e^{-ix_2(p_1 + p_2 + p)}
\end{aligned}
$$

(67)

where m is the mass of the exchanged pion. As mentioned previously, there are two of each diagram, producing a factor of 2 in the numerator. From the s-channel diagram, where the arrows indicate the "flow" of 4-momentum, it is clear that

$$
p = p_1 + p_2 = p_3 + p_4 \tag{68}
$$

where p is the 4-momentum of the exchange particle, p_1 and p_2 are the 4-momenta of the initial state particles A_1 and A_2, respectively and p_3 and p_4 are the 4-momenta of the final state particles A' and B', respectively. The integrals over x_1 and x_2 convert the exponentials into δ functions of the momenta, and integration over p evaluates one of the delta functions with the result

$$
\langle f|S_{2s}|i\rangle = \frac{-ig_{AA}g_{AB}}{(p_1 + p_2)^2 - m^2 - i\epsilon} (2\pi)^4 \delta^4(p_1 + p_2 - p_3 - p_4) \tag{69}
$$

Similarly, the result for the second diagram, with

$$
p = p_1 - p_3 = p_4 - p_3 \tag{70}
$$

is

$$
\langle f|S_{2t}|i\rangle = \frac{-ig_{AA}g_{AB}}{(p_1 - p_3)^2 - m^2 - i\epsilon} (2\pi)^4 \delta^4(p_1 + p_2 - p_3 - p_4) \tag{71}
$$

and for the third diagram, with

$$
p = p_1 - p_4 = p_3 - p_2 \tag{72}
$$

is

$$\langle f|S_{2u}|i\rangle \;\; = \;\; \frac{-ig_{AA}g_{AB}}{(p_1-p_4)^2-m^2-i\epsilon}(2\pi)^4\delta^4(p_1+p_2-p_3-p_4) \tag{73}$$

Introducing the Mandelstam invariants

$$s \;\; \equiv \;\; (p_1+p_2)^2=(p_3+p_4)^2 \tag{74}$$

$$t \;\; \equiv \;\; (p_1-p_3)^2=(p_4-p_2)^2 \tag{75}$$

$$u \;\; \equiv \;\; (p_1-p_4)^2=(p_3-p_2)^2 \tag{76}$$

and combining the three results leads to

$$\langle f|S_2|i\rangle \;\; = \;\; -ig_{AA}g_{AB}(2\pi)^4\delta^4(p_1+p_2-p_3-p_4)\times$$
$$\left[\frac{1}{s-m^2-i\epsilon}+\frac{1}{t-m^2-i\epsilon}+\frac{1}{u-m^2-i\epsilon}\right] \tag{77}$$

Finally, substituting this result into (38) gives the amplitude

$$\mathcal{M}_2 \;\; = \;\; -g_{AA}g_{AB}\left[\frac{1}{s-m^2-i\epsilon}+\frac{1}{t-m^2-i\epsilon}+\frac{1}{u-m^2-i\epsilon}\right] \tag{78}$$

The amplitude for the reaction $N+N\to N+\Delta$ is the sum of s, t and u channel exchanges. However, the s-channel must be excluded from the amplitude for this reaction for reasons discussed in section 2.4.4.

2.4.3 Feynman's Rules

The steps for determining the scattering amplitude of an interaction process from the Feynman diagrams are condensed into a set of rules known as *Feynman's rules*. The procedure of the preceding section may be summarized as follows:

1. Perform Wick/Peskin contractions for a given particle interaction process and interaction Hamiltonian to determine the Feynman diagrams.

2. Apply Feynman's rules to each diagram and sum over all diagrams to determine the scattering amplitude.

Let us enumerate these steps in greater detail.

Apply Wick/Peskin contractions:

1. Write down the expression for $\langle f|S|i \rangle$ and expand the terms to the desired order (we used 2nd order above).

2. Find the terms that contribute to the process. This is done simply by counting the numbers of *fields and states* for each type of field and state (A, B, etc), and ascertaining that all the counts are even numbers.

3. For each contributing term, perform Wick/Peskin contractions to find all possible sets of contractions, making sure that in each set all fields and states are contracted.

4. Read the Feynman diagrams directly from the contracted terms.

5. For each diagram, apply Feynman's rules to determine the amplitude for that diagram.

6. Sum the amplitudes of all the diagrams.

Apply Feynman's rules for scalar theory:

1. For a given diagram, label the momenta for all external and internal lines, and assign arrows to all lines. For external lines the arrows indicate the movement of the initial and final state particles in time. For initial state particles, the arrows should point toward the vertices, and for final state particles they should point away from the vertices. The arrows also indicate the direction of the "flow" of 4-momentum.

2. For each vertex, assign the appropriate coupling factor $-ig_{xyz}$, where x, y, z label the fields that meet at the vertex.

3. For each internal line write a propagator factor $D_F(q) = i/(q^2 - m^2 - i\epsilon)$, where q is the momentum of the exchange particle represented by the line.

4. For each external line, write a factor $\exp(-ipx)$ for inbound particles, and $\exp(+ipx)$ for outbound particles.

5. For each vertex write a delta function factor $(2\pi)^4\delta^4(\sum p_i)$ to enforce conservation of 4-momentum at the vertex. For each line attached to the vertex, if the line is inbound p_i carries a $+$ sign, and if the line is outbound p_i carries a $-$ sign.

6. Integrate over all internal momenta, using the integral $\int d^4q_i/(2\pi)^4$ for each momentum q_i.

2.4.4 Interpretation of the s-channel in $N + N \to N + \Delta$ Scattering

In section 2.4.2 an s-channel diagram is generated for the reaction $A+A \to A+B$, along with the t and u-channel diagrams. Letting A represent a nucleon N and B the Δ baryon, the s-channel diagram represents the annihilation of two identical nucleons. This interpretation of the s-channel diagram is not correct, since such a reaction does not occur in nature. We have been led to this interpretation because scalar theory does not distinguish between particle and anti-particle. The correct interpretation is obtained by first considering a model that accommodates both particles and anti-particles, namely the charged scalar model.

The scalar model is compared to the charged scalar model at the end section 3.1, where fields are expressed in terms of annihilation and creation operators. There, the complex scalar model describes two types of fields, has two sets of annihilation and creation operators, and is able to distinguish between particle and anti-particle. In the charged scalar model the s-channel diagram describes the particle/anti-particle reaction $\bar{N} + N \to \bar{N} + \Delta$. The scalar model should be consistent with the charged scalar model, therefore the s-channel diagram should be interpreted as describing the particle/anti-particle reaction. Then both models give t and u-channel diagrams for the reaction $N + N \to N + \Delta$, and give the s-channel diagram for the reaction $\bar{N} + N \to \bar{N} + \Delta$. In the comparison of the scalar model to experiment [1] only the t and u-channel diagrams are used.

3 Extension to Complex Scalar Fields

In applying scalar theory to nucleons, we purposely ignore spin and isospin, and treat all nucleons (protons and neutrons) as identical. We then ask the question "To what extent is scalar theory able to determine cross sections of nucleon-nucleon interactions"? Since scalar theory does not distinguish between particle and anti-particle, we must either include electric charge, or decide how to interpret s-channel diagrams, which involve pair creation and annihilation. Do we say that in a proton-proton interaction, the protons can annihilate? We cannot, since such a process does not occur in nature. Wishing to keep the scalar theory as simple as possible by not including charge, we view s-channel diagrams as having particle/anti-particle pairs in both the initial and final states. In this way, we are able to achieve some success in fitting calculated cross sections to measured cross sections [1].

The simplest way to extend the capabilities of the scalar model is to consider the electric charge of the particles. This enables us to present a theory that recognizes anti-particles (e.g., protons and anti-protons, neutrons and anti-neutrons). However by including charge, we can no longer consider the proton and neutron to be identical nucleons. The charged scalar model must include the isospin formalism.

This section draws on the quantum field theory texts of Maggiore, Ryder, Hatfield, Gross and Peskin [19, 29, 20, 15, 18] to present a charged scalar model of nucleons. With the introduction of charge the simple scalar Lagrangian involving products of scalar fields is replaced with a Lagrangian involving complex scalar fields to describe the protons, anti-protons, neutrons and anti-neutrons, and scalar fields to describe the exchange particles, the three pions. We shall develop the theory to the extent possible without engaging in the isospin formalism, which involves products of isospin vectors and matrices to couple the fields of the interacting particles. Our intent in modeling nucleon interactions using the charged scalar field is not to include electric interactions, but simply to include both particles and anti-particles in order to resolve the issue of interpreting s-channel diagrams

of meson exchanges.

3.1   Complex Scalar Fields of Free Charged Particles

The fields of charged scalar particles are described by the complex scalar field. The theory of the complex scalar field is very similar to the theory of the scalar field given in section 2. However unlike the scalar field, the complex scalar field is able to describe particles having positive and negative energy states. Particles with negative energy states are interpreted as anti-particles with positive energy. The complex scalar field ψ is assembled from two real scalar field components ψ_1 and ψ_2

$$\begin{aligned}
\psi &= \frac{\psi_1 + i\psi_2}{\sqrt{2}} \\
\overline{\psi} &= \frac{\psi_1 - i\psi_2}{\sqrt{2}}
\end{aligned} \tag{79}$$

Since ψ and $\overline{\psi}$ are linear combinations of real scalar fields, they automatically satisfy the Klein Gordon equation. ψ is chosen to be the particle field, and $\overline{\psi}$ the anti-particle field.

For protons, the complex scalar field describes a particle and anti-particle having equal and opposite electric charge, whereas for neutrons, the particle and anti-particle both have zero charge. For both protons and neutrons, particle and anti-particle fields are distinguished by having different sets of creation and destruction operators.

The complex field is expressed as a Fourier expansion of plane waves in which the coefficients a_p, $a_p^\dagger$ are the creation and annihilation operators for the particle, and the coefficients b_p, $b_p^\dagger$ are the creation and annihilation operators for the anti-particle. The particle field $\psi(x)$ is

$$\psi(x) = \int \frac{d^3p}{(2\pi)^3 \sqrt{2E_\mathbf{p}}} (a_\mathbf{p} e^{-ipx} + b_\mathbf{p}^\dagger e^{+ipx}) \tag{80}$$

and the anti-particle field $\overline{\psi}(x)$ is

$$\overline{\psi}(x) = \int \frac{d^3p}{(2\pi)^3 \sqrt{2E_\mathbf{p}}} (a_\mathbf{p}^\dagger e^{+ipx} + b_\mathbf{p} e^{-ipx}) \tag{81}$$

The creation and annihilation operators obey the commutation relations

$$[a_{\mathbf{p}}, a_{\mathbf{q}}^{\dagger}] \;=\; [b_{\mathbf{p}}, b_{\mathbf{q}}^{\dagger}] \;=\; (2\pi)^3 \delta^3(\mathbf{p} - \mathbf{q}) \tag{82}$$

The vacuum state $|0\rangle$ of the particle and anti-particle Fock space is defined by

$$a_{\mathbf{p}}|0\rangle \;=\; b_{\mathbf{p}}|0\rangle \;=\; 0 \tag{83}$$

and the Fock space is built by the creation operators acting repeatedly on the vacuum state

$$a_{\mathbf{p}}^{\dagger}|0\rangle \;=\; \frac{1}{\sqrt{2E_{\mathbf{p}}}}|\mathbf{p}\rangle$$

$$b_{\mathbf{q}}^{\dagger}|0\rangle \;=\; \frac{1}{\sqrt{2E_{\mathbf{q}}}}|\mathbf{q}\rangle \tag{84}$$

The normal ordered Hamiltonian density is given by

$$:\mathcal{H}: \;=\; \int \frac{d^3p}{(2\pi)^3} E_{\mathbf{p}}(a_{\mathbf{p}}^{\dagger}a_{\mathbf{p}} + b_{\mathbf{p}}^{\dagger}b_{\mathbf{p}}) \tag{85}$$

The $U(1)$ charge is conserved and is given in terms of the creation and annihilation operators, and in terms of the particle number operator N_a and anti-particle number operator N_b by

$$\begin{aligned} Q_{U(1)} \;&=\; \int \frac{d^3p}{(2\pi)^3}((a_{\mathbf{p}}^{\dagger}a_{\mathbf{p}} - b_{\mathbf{p}}^{\dagger}b_{\mathbf{p}}) \\ &=\; \int \frac{d^3p}{(2\pi)^3}(N_a - N_b) \\ N_a \;&=\; a_{\mathbf{p}}^{\dagger}a_{\mathbf{p}} \\ N_b \;&=\; b_{\mathbf{p}}^{\dagger}b_{\mathbf{p}} \end{aligned} \tag{86}$$

showing that the total charge of a system of particles is simply the number of field quanta (particles) created by $a_{\mathbf{p}}^{\dagger}$ minus the number of field quanta (anti-particles) created by $b_{\mathbf{p}}^{\dagger}$, integrated over all momenta. The states $a_{\mathbf{p}}|0\rangle$ represent particles of momentum $\mathbf{p}$ and charge $+1$, while the states $b_{\mathbf{p}}|0\rangle$ represent anti-particles of momentum $\mathbf{p}$ and charge -1. The formulation of the complex scalar field contrasts with that of the scalar field, where the requirement that the scalar field be real forces $a_{\mathbf{p}} \equiv b_{\mathbf{p}}$, so that the scalar particle is its own anti-particle.

3.2 Interaction Lagrangian for Nucleons

For the complex scalar formulation of the nucleon-pion interaction, the interaction Lagrangian is written by analogy with Yukawa's spinor formulation ([15], eq. 9.92)

$$\mathcal{L}_I \;=\; -ig_p\overline{\psi}_p\psi_p\gamma^5\phi_0 - ig_n\overline{\psi}_n\gamma^5\psi_n\phi_0 - ig_+\overline{\psi}_n\gamma^5\psi_p\phi_+^\dagger - ig_+\overline{\psi}_p\gamma^5\psi_n\phi_+ \tag{87}$$

where ψ_p and ψ_n are the Dirac spinors for the proton and neutron. In our formulation we shall use complex scalar fields instead of spinor fields, and omit the γ^5 bilinear covariant. Thus the interaction Lagrangian for two nucleons, a proton and neutron, interacting through the exchange of neutral and charged pseudo-scalar pions takes the form

$$\mathcal{L}_I \;=\; -ig_p\overline{\psi}_p\psi_p\phi_0 - ig_n\overline{\psi}_n\psi_n\phi_0 - ig_+\overline{\psi}_n\psi_p\phi_+^\dagger - ig_+\overline{\psi}_p\psi_n\phi_+ \tag{88}$$

where ψ_p is the proton field, ψ_n is the neutron field, and the ϕ_i are the pion fields; ϕ_0 for the π^0, ϕ_+ for the π^+, and $\phi_- = \phi_+^\dagger$ for the π^-. $\mathcal{L}_I$ is Hermitian, and the coupling constants g_p, g_n and g_+ are real. The coupling constants are related by

$$g_p \;=\; -g_n \;=\; \frac{g_+}{\sqrt{2}} \;=\; g \tag{89}$$

In this relation, the minus sign of g_n and the factor of $\sqrt{2}$ on g_+ are determined by requiring invariance of the spinor-based Lagrangian (87) under isospin rotations ([15] pgs. 265-268). In terms of g the Lagrangian (88) becomes

$$\mathcal{L}_I \;=\; -ig\overline{\psi}_p\psi_p\phi_0 + ig\overline{\psi}_n\psi_n\phi_0 - i\sqrt{2}g\overline{\psi}_n\psi_p\phi_+^\dagger - i\sqrt{2}g\overline{\psi}_p\psi_n\phi_+ \tag{90}$$

Using the isospin formalism, $\mathcal{L}_I$ can also be written

$$\mathcal{L}_I \;=\; -ig\overline{\psi}\tau\psi \cdot \phi \tag{91}$$

where ψ is the two-component nucleon field in isospin space

$$\psi \;=\; \begin{pmatrix} \psi_p \\ \psi_n \end{pmatrix} \tag{92}$$

τ is the Pauli spin matrix

$$\tau = (\tau_1, \tau_2, \tau_3) \tag{93}$$

$$\tau_1 = \begin{pmatrix} 0 & 1 \\ 1 & 0 \end{pmatrix} \tag{94}$$

$$\tau_2 = \begin{pmatrix} 0 & -i \\ i & 0 \end{pmatrix} \tag{95}$$

$$\tau_2 = \begin{pmatrix} 1 & 0 \\ 0 & -1 \end{pmatrix} \tag{96}$$

and ϕ is the three-component pion field in isospin space

$$\phi = \begin{pmatrix} \phi_1 \\ \phi_2 \\ \phi_3 \end{pmatrix} \tag{97}$$

$$\phi_1 = \frac{1}{\sqrt{2}}(\phi_+ + \phi_+^\dagger)$$
$$\phi_2 = \frac{i}{\sqrt{2}}(\phi_+ - \phi_+^\dagger)$$
$$\phi_3 = \phi_0 \tag{98}$$

We shall work with the first Lagrangian (90) to develop 2nd order diagrams, and leave the isospin formulation for future work involving the Δ baryon.

3.3   Contractions

Wick contractions and external (Peskin) contractions for complex scalar fields are different from contractions for scalar fields (see section 2.1.6). Whereas a scalar field $\phi(x_1)$ at x_1 contracts with a like field $\phi(x_2)$ at x_2, a complex scalar field $\psi(x_1)$ contracts with an adjoint field $\overline{\psi}(x_2)$

$$\langle 0 | \psi(x_1)\overline{\psi}(x_2) | 0 \rangle = D_F(x_1 - x_2) \tag{99}$$

to produce the Feynman propagator. For external contractions, a scalar field ϕ can contract with a particle on the left (final state) or on the right (initial state), but a complex scalar

field ψ can contract with a particle on the right or an anti-particle on the left, while the field $\overline{\psi}$ can contract with a particle on the left and an anti-particle on the right. Thus for an initial state particle $|\mathbf{p}\rangle$

$$\underline{\psi(x)|\mathbf{p}\rangle} = \mathbf{e}^{-\mathbf{i}\mathbf{p}\cdot\mathbf{x}}|\mathbf{0}\rangle \tag{100}$$

and for an initial state anti-particle $|\mathbf{q}\rangle$

$$\underline{\overline{\psi}(x)|\mathbf{q}\rangle} = \mathbf{e}^{-\mathbf{i}\mathbf{q}\cdot\mathbf{x}}|\mathbf{0}\rangle \tag{101}$$

For a final state particle $\langle\mathbf{p}|$

$$\langle\mathbf{p}|\underline{\overline{\psi}(\mathbf{x})} = \langle\mathbf{0}|\mathbf{e}^{+\mathbf{i}\mathbf{p}\cdot\mathbf{x}} \tag{102}$$

and for a final state anti-particle $\langle\mathbf{q}|$

$$\langle\mathbf{q}|\underline{\psi(\mathbf{x})} = \langle\mathbf{0}|\mathbf{e}^{+\mathbf{i}\mathbf{q}\cdot\mathbf{x}} \tag{103}$$

In the next section the contractions are applied to terms in the S-matrix to generate Feynman diagrams.

3.4   2nd Order Diagrams

The 2nd order Feynman diagrams for the elastic proton-proton reaction $p + p \rightarrow p + p$ are derived from S_2, the 2nd order term in the expansion of the S-matrix (32)

$$S_2 \;=\; \frac{(-i)^2}{2!} \int d^4x_1 d^4x_2 T\left[\mathcal{H}_{\mathcal{I}}(x_1)\mathcal{H}_{\mathcal{I}}(x_2)\right] \tag{104}$$

Setting the Hamiltonian $\mathcal{H} = -\mathcal{L}$ with the Lagrangian (90), the product of Hamiltonians in S_2 contains sixteen terms

$$
\begin{aligned}
\mathcal{H}(x_1)\mathcal{H}(x_2) \;=\; & (ig\overline{\psi}_p\psi_p\phi_0 - ig\overline{\psi}_n\psi_n\phi_0 + i\sqrt{2}g\overline{\psi}_n\psi_p\phi_+^\dagger + i\sqrt{2}g\overline{\psi}_p\psi_n\phi_+)_1 \;\times \\
& (ig\overline{\psi}_p\psi_p\phi_0 - ig\overline{\psi}_n\psi_n\phi_0 + i\sqrt{2}g\overline{\psi}_n\psi_p\phi_+^\dagger + i\sqrt{2}g\overline{\psi}_p\psi_n\phi_+)_2 \\
\;=\; & -g^2(\overline{\psi}_p\psi_p\phi_0)_1(\overline{\psi}_p\psi_p\phi_0)_2 - g^2(\overline{\psi}_n\psi_n\phi_0)_1(\overline{\psi}_n\psi_n\phi_0)_2 \\
& +14 \; more \; terms
\end{aligned} \tag{105}
$$

Since the reaction of interest involves two protons p in both the initial and final states, only proton fields ψ_p are involved so only the first of the sixteen terms contributes to the reaction amplitude. Writing the initial state $|p_1\,p_2\rangle$ in terms of the momenta p_1 and p_2 of initial state particles 1 and 2, and the final state $\langle p_3\,p_4|$ in terms of the momenta p_3 and p_4 of final state particles 3 and 4, and performing contractions leads to four fully contracted terms

$$\langle p_3\,p_4|\,\overline{\psi}_p\,\psi_p\,\phi_0\quad\overline{\psi}_p\,\psi_p\,\phi_0\,|p_1\,p_2\rangle \tag{106}$$

$$\langle p_3\,p_4|\,\overline{\psi}_p\,\psi_p\,\phi_0\quad\overline{\psi}_p\,\psi_p\,\phi_0\,|p_1\,p_2\rangle \tag{107}$$

$$\langle p_3\,p_4|\,\overline{\psi}_p\,\psi_p\,\phi_0\quad\overline{\psi}_p\,\psi_p\,\phi_0\,|p_1\,p_2\rangle \tag{108}$$

$$\langle p_3\,p_4|\,\overline{\psi}_p\,\psi_p\,\phi_0\quad\overline{\psi}_p\,\psi_p\,\phi_0\,|p_1\,p_2\rangle \tag{109}$$

The first and fourth terms are identical (p_1 shares a vertex with p_3), and the second and fourth terms are identical (p_1 shares a vertex with p_4). The factor $1/2!$ in S_2 cancels the duplicity, leaving two distinct terms, the first and second, which correspond to the direct t-channel and exchange u-channel diagrams shown in figure 3.a. The second term in (105) yields contracted terms and diagrams for the neutron-neutron reaction $n + n \rightarrow n + n$ that are identical to those for the proton-proton reaction, replacing proton fields ψ_p with neutron fields ψ_n and line labels p with n.

3.5 The Δ Baryon in the Complex Scalar Model

The Δ baryon has spin 3/2 and isospin 3/2, and carries charges of -1, 0, 1 and 2. In the spinor formalism, the four Δ particles are represented by the four component Rarita-Schwinger field ψ_μ, and the three exchange pions π^0, π^+ and π^- by the iso-vector pion field π. As in section 3.2, the complex scalar Lagrangian is written by analogy with the spinor

Lagrangian, replacing the spinor fields with complex scalar fields, and the iso-vector pion field with a pseudo-scalar field. In doing so, we must specify terms for the interactions of the two nucleons and the four Δ particles. Let us consider the simpler case having only two particles, the proton p and the Δ^+, and having the Lagrangian

$$\mathcal{L}_I \quad = \quad -ig_{pp}\bar{\psi}_p\psi_p\phi_0 - ig_{p\Delta}\bar{\Delta}^+\psi_p\phi_0 - ig_{p\Delta}\bar{\psi}_p\Delta^+\phi_0 \tag{110}$$

This Lagrangian is Hermitian, and the three interaction terms suffice for a description of the reaction $p + p \to p + \Delta^+$. Inserting the Hamiltonian $\mathcal{H} = \mathcal{L}_I$ into S_2 produces nine terms

$$
\begin{aligned}
\mathcal{H}(x_1)\mathcal{H}(x_2) \quad = \quad & (-ig_{pp}\overline{\psi}_p\psi_p\phi_0 - ig_{p\Delta}\overline{\Delta}^+\psi_p\phi_0 - ig_{p\Delta}\overline{\psi}_p\Delta^+\phi_0)_1 \times \\
& (-ig_{pp}\overline{\psi}_p\psi_p\phi_0 - ig_{p\Delta}\overline{\Delta}^+\psi_p\phi_0 - ig_{p\Delta}\overline{\psi}_p\Delta^+\phi_0)_2 \\
= \quad & -g_{pp}g_{p\Delta}(\overline{\Delta}^+\psi_p\phi_0)_1(\overline{\psi}_p\psi_p\phi_0)_2 \\
& -g_{pp}g_{p\Delta}(\overline{\psi}_p\psi_p\phi_0)_1(\overline{\Delta}^+\psi_p\phi_0)_2 \\
& +7\ more\ terms
\end{aligned}
\tag{111}
$$

where each term is a product of six fields. For the reaction $p + p \to p + \Delta^+$, each of the two terms shown can be fully contracted in two ways

$$\langle\, p_3\, p_4 |\ \overline{\Delta}^+\ \psi_p\ \phi_0\quad \overline{\psi}_p\ \psi_p\ \phi_0\ | p_1\, p_2\rangle \tag{112}$$

and

$$\langle\, p_3\, p_4 |\ \overline{\Delta}^+\ \psi_p\ \phi_0\quad \overline{\psi}_p\ \psi_p\ \phi_0\ | p_1\, p_2\rangle \tag{113}$$

producing the t-channel and u-channel diagrams, respectively, shown in figure 3.b, which may be compared to the diagrams produced by the scalar model and shown in figure 2.

For the reaction $\bar{p} + p \to \bar{p}\Delta^+$ each of the terms shown in (111) can be contracted in one way

$$\langle\, p_3\, p_4 |\ \overline{\Delta}^+\ \psi_p\ \phi_0\quad \overline{\psi}_p\ \psi_p\ \phi_0\ | p_1\, p_2\rangle \tag{114}$$

producing the s-channel diagram shown in figure 3.c.
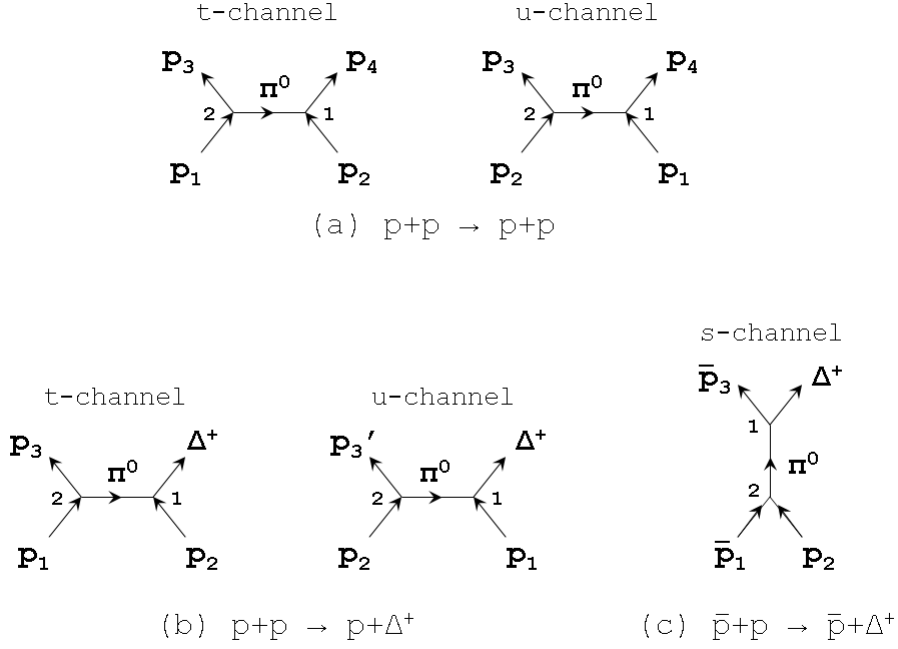
Figure 3: 2nd Order Diagrams of the Charged Scalar Model.

A comparison of the diagrams in figures 3 and 2 shows that for the reaction $p+p \rightarrow p+\Delta^+$ the complex scalar and scalar models are consistent. The complex scalar model gives two diagrams, the t and u channels, since the s channel does not contribute to the reaction. The scalar model also gives only the t and u channel diagrams *when we regard the s-channel diagram as corresponding to the different reaction* $p + \overline{p} \rightarrow \overline{p} + \Delta^+$.

4 Generalized Bethe-Salpeter Equation (GBSE) in Ladder Approximation

In [1] the 2nd order scalar one pion exchange (OPE) model is used to determine pion production cross sections. However, for nucleon interactions, 4th and higher order terms are significant. To improve upon the 2nd order results, this section takes up the Bethe-Salpeter equation (BSE), which sums over all orders of ladder diagrams. The BSE is formulated using the scalar model, and generalized to handle inelastic processes in the ladder approximation.

The BSE [15, 26] may be used to determine the amplitude of an elastic scattering process, given certain assumptions ([15] Chapter 12). The primary assumption is that the "ladder" diagrams dominate over other types of diagrams, in particular loop and cross diagrams. In the ladder approximation, the BSE sums over all ladder diagrams to give a compact integral equation expressing the process amplitude $\mathcal{M}$ in terms of itself. The sum is carried out to all orders in coupling constant g. In the series of ladder diagrams the rungs and spans are all identical in form. Take, for example, a simple model based on the two-vertex Lagrangian

$$\mathcal{L} \;=\; -g_{AAC}AAC - g_{BBC}BBC \tag{115}$$

with coupling constants g_{AAC} and g_{BBC} and scalar fields A, B and C. This Lagrangian suffices to give a simple yet meaningful description of the elastic scattering of two scalar particles A and B, which interact through the exchange of scalar particle C. The interaction is described symbolically by $A + B \to A + B$. A single ladder span sandwiched between two rungs is represented by a box diagram (figure 5), and is constructed from the two available types of vertices AAC and BBC, and the two coupling constants. The box is 4th order, having four vertices. The homogeneity of the ladders enables the infinite series to be summed and the BSE to take the compact form ([15] eq. 12.40)

$$\mathcal{M}(p,p';P) \;=\; U(p,p';P) - i \int \frac{d^4k}{(2\pi)^4} U(p,k;P)G(p,k;P)\mathcal{M}(k,p';P) \tag{116}$$

where the amplitude $\mathcal{M}$ appears both on the left-hand side and under the integral, and where $p = p_1$ is the 4-momentum of one of the initial state particles, $p' = p_3$ is the 4-

momentum of one of the final state particles, $P = p_1 + p_2 = p_3 + p_4$ is the total interaction 4-momentum, and k, the integration variable, is the 4-momentum of one of the propagating particles in the propagator G.

The BSE (116) is depicted in figure 4 as a graphical equation. The kernel U and propagator G are given by

$$U(p, p'; P) = \frac{g^2}{(p - p')^2 - m_C^2} \tag{117}$$

$$U(p, k_A; P) = \frac{g^2}{(p - k_A)^2 - m_C^2} \tag{118}$$

$$G(p, k_A; P) = \frac{1}{(k_A^2 - m_A^2)[(P - k_A)^2 - m_B^2]} \tag{119}$$

where m_A, m_B and m_C are the masses of particles A, B and C, and k_A is the 4-momenta of internal particle A. Integration occurs over k_A. Note that the coupling factor g^2 is associated with a rung (the kernel), despite the fact that the rung does not completely define the two vertices to which it is attached; vertices are defined by the conjunction of rungs and spans. However, the association succeeds for two reasons: 1) all pairs of vertices have the same coupling factor $g_{AAC}g_{BBC}$, and 2) there is a one-to-one correspondence between rungs and pairs of vertices.

The kernel consists of all irreducible diagrams [15], but in practice is often approximated by a single 2nd order diagram. For our discussion, the kernel is either a single 2nd order diagram representing one meson exchange, or a sum of 2nd order diagrams, one for each type of meson considered.

The amplitude may be substituted iteratively into itself to recreate the ladder expansion

$$\mathcal{M} = U - i \int \frac{d^4 k}{(2\pi)^4} U G U + (-i)^2 \int \frac{d^4 k_1}{(2\pi)^4} \frac{d^4 k_2}{(2\pi)^4} U G U G U + \dots$$

$$\mathcal{M} = U + U G \mathcal{M} = U + U G U + U G U G U + \dots \tag{120}$$

In the last line, the notation is simplified by hiding the integral operators. This equation corresponds to the ladder expansion shown in figure 4. The second term on the right hand side corresponds to figure 5, while the last term corresponds to the 6th order diagram

The BSE applies to elastic reactions   A + B → A + B

Closed Form
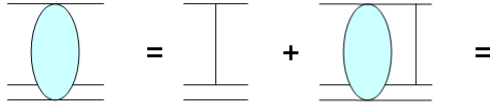
Ladder Expansion
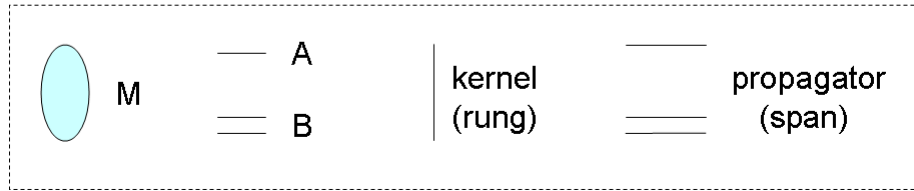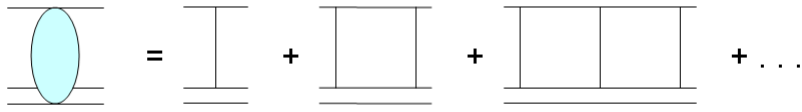
Figure 4: The BSE in Graphical Form.

shown in figure 6. Application of the BSE is restricted to scattering processes for which homogeneous ladders may be constructed. For ϕ^3 type Langrangians ([15] chap. 12) such as (115), in which three fields interact at a space-time point, inelastic processes not only require a Lagrangian having more than one type of vertex, but will necessarily involve inhomogeneous ladders with multiple types of rungs and spans. For the inelastic reaction $A + A \rightarrow A + B$ the Lagrangian must include at least two vertices

$$\mathcal{L} \;=\; -g_{AB}ABC - g_{AA}AAC \tag{121}$$

but most generally will have three vertices

$$\mathcal{L} \;=\; -g_{AB}ABC - g_{AA}AAC - g_{BB}BBC \tag{122}$$

The following discussion is based on the three-vertex Lagrangian (122). Figure 1 lists the most general sets of kernels and propagators for four different Lagrangians.
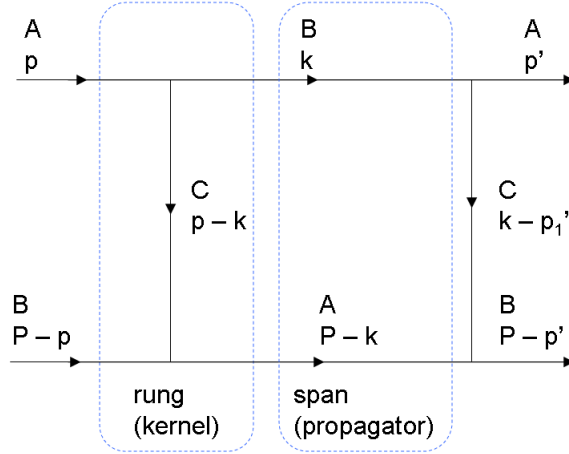
Figure 5: Box diagram, with two rungs (kernels) and one span (propagator).
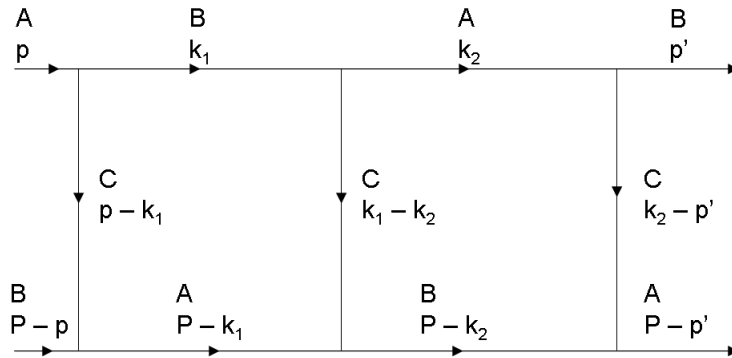
Figure 6: A 2-box diagram, with three rungs (kernels) and two spans (propagators).

The BSE (116) must now be generalized to handle ladders consisting of several types of rungs and spans. This will be done for two cases: 1) a single type of rung, called a C-rung,

and 2) multiple types of rungs. A C-rung involves the exchange of a C particle. Since the conjunction of rungs and spans determines coupling at the vertices, and since there are multiple types of rungs and spans, the coupling at each rung is no longer the simple factor g^2, but is determined by coupling matrices. These matrices are defined in the following subsections.

4.1 Restriction to C-rungs

If the contribution to the amplitude $\mathcal{M}$ from ladders constructed using C-rungs dominate over other ladders, we may restrict our considerations to C-rungs. The ladders will consist of four types of spans (the other 5 propagators are omitted, since they involve A or B exchange), constructed from vertices ABC, AAC and BBC, and coupling constants g_{AB}, g_{AA}, and g_{BB}.

4.2 A GBSE in the Ladder Approximation

The BSE (116) applies to the elastic reaction $A+B \rightarrow A+B$, and in the expansion generates homogeneous ladders constructed from the one type of propagator $G = G_B^A$ given by (119). Now consider the inelastic process $A + A \rightarrow A + B$. The first term of the expansion of the BSE is the 2nd order kernel U, with initial state $A+A = A+A$ and final state $A+B = A+B$. The next term in the expansion is the 4th order UGU, again with initial state AA and final state AB. But what shall we use for the intermediate virtual two-particle state represented by the propagator G? There are four possibilities, represented by the four propagators G_A^A, G_B^A, G_A^B and G_B^B given by (124) below. Thus, in our attempt to generalize the BSE to additionally describe inelastic processes such as $A+A \rightarrow A+B$, we are suddenly faced with inhomogeneous ladders consisting of four different types of propagators. The lowest order ladders that contain these propagators are 4th order and are depicted in figure 7. These ladders correspond to terms of the form UGU, which are formed in the first iteration of the expansion

$$\mathcal{M}' \;=\; U + UGU + UGUGM' \tag{123}$$

If we set the propagator G equal to the sum of the four possible propagators

$$
\begin{aligned}
G &= G_A^A + G_B^A + G_A^B + G_B^B = \sum_{i=1}^{4} G_i \\
G_1 &= G_A^A = \frac{\mathcal{G}_A^A}{(k_{A_1}^2 - m_A^2)(k_{A_2}^2 - m_A^2)} = \frac{\mathcal{G}_A^A}{\mathcal{D}_A^A} \\
G_2 &= G_B^A = \frac{\mathcal{G}_B^A}{(k_A^2 - m_A^2)(k_B^2 - m_B^2)} = \frac{\mathcal{G}_B^A}{\mathcal{D}_B^A} \\
G_3 &= G_A^B = \frac{\mathcal{G}_A^B}{(k_B^2 - m_B^2)(k_A^2 - m_A^2)} = \frac{\mathcal{G}_A^B}{\mathcal{D}_A^B} \\
G_4 &= G_B^B = \frac{\mathcal{G}_B^B}{(k_{B_1}^2 - m_B^2)(k_{B_2}^2 - m_B^2)} = \frac{\mathcal{G}_B^B}{\mathcal{D}_B^B}
\end{aligned} \tag{124}
$$

we are able to produce the complete set of four 4th order UGU ladders in the first iteration. In the second iteration

$$
\mathcal{M}' = U + UGU + UGUGU + UGUGUG\mathcal{M}' \tag{125}
$$

6th order terms $UGUGU \propto G^2$ are proportional to the square of G, which produces all possible products of two propagators $G_i G_j$. Clearly, for terms of order $2n$, G^n will produce all possible products of n propagators $G_{i_1} G_{i_2} \times ... G_{i_n}$. Thus, the sum of the G_i given by (124) enables us to construct ladders containing all possible sequences of propagators. However, we no longer have a fixed coupling factor $g_{AAC}\, g_{BBC}$ for each pair of vertices (that is, for each rung). Instead, in general the types of vertices change from rung to rung, and we are led to introduce coupling matrices in the kernel U and propagators G_i, such that the products of these matrices generate, rung by rung, the required coupling factors. The introduction of matrices further requires that the amplitude itself be a matrix. We shall label the amplitude matrix $\mathcal{M}'$.

We are now ready to propose a form of the GBSE that involves matrices U, G and $\mathcal{M}'$, but an important question remains. Is the series of ladders produced by the proposed GBSE equivalent to the series of ladders generated by the Dyson S-matrix? We defer the proof of the equivalence until later (section 4.17), first gaining some familiarity with the

48

proposed GBSE and the amplitude matrix $\mathcal{M}'$. The proof given in section 4.17 is for the case of ladders constructed with C-rungs.

With the restriction to C-rungs, a form of the generalized BSE (GBSE) that accommodates multiple types of propagators is

$$\mathcal{M}_{jl}^{ik} = \widetilde{\mathbf{u}}_j^i \, \mathcal{M}' \, \mathbf{v}_l^k \tag{126}$$

$$\mathcal{M}' = U + \int_k UG\mathcal{M}' \tag{127}$$

$$\int_k = -i \int \frac{d^4k}{(2\pi)^4} \tag{128}$$

where $\mathcal{M}_{jl}^{ik}$ is the amplitude of the process $i + j \rightarrow k + l$, and $\mathcal{M}'$ is a matrix that contains the amplitudes of a family of reactions related by a common set of kernels and propagators. The matrix $\mathcal{M}'$ is introduced to help articulate the mechanism by which vertex coupling factors are generated. As the GBSE formalism is developed in the following sections, $\mathcal{M}'$ becomes the centerpiece in a discussion of a different kind of coupling, the coupling between the amplitudes of different reactions.

If the family of reactions consists of a single elastic reaction, then the matrix $\mathcal{M}'$ reduces to a single element. In this case there will be only one type of propagator, and the GBSE given by (127) reduces to the BSE given by (116).

Returning to the discussion at hand, in (127) the vectors $\widetilde{\mathbf{u}}_j^i$ and $\mathbf{v}_l^k$ specify the initial and final states, respectively, for initial state particles i, j and final state particles k, l, where each of the particle labels i, j, k and l can specify either particle A or B. The row vector $\widetilde{\mathbf{u}}_j^i$ and column vector $\mathbf{v}_l^k$ are defined below by (134) and (138), noting that $\widetilde{\mathbf{u}}_j^i = \text{Transpose } \mathbf{u}_j^i$. The kernel U

$$U = \frac{1}{q^2 - m_C^2} \tag{129}$$

can no longer carry the coupling factor, since the coupling will vary from vertex to vertex depending on the sequence of propagators appearing in the ladders. Furthermore, for each ladder, the coupling factors of the first and last pairs of vertices are determined in part

by the initial and final states. To determine the coupling factors we introduce coupling matrices $\mathcal{G}_j^i$ into the propagator G, which is now the sum of four different propagators given by (124) and corresponding to the four types of box diagrams shown in figure 7.
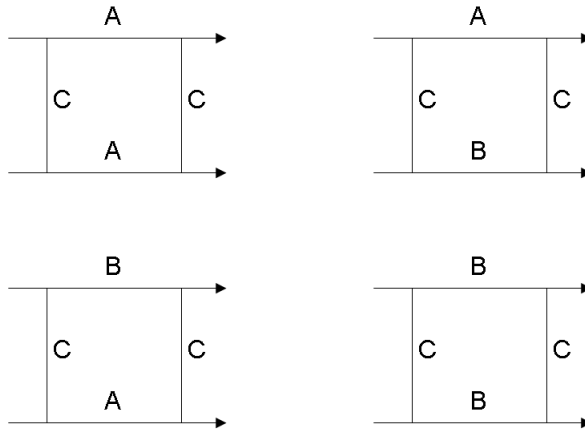
Figure 7: Four types of box diagrams and associated propagators.

The notation $\mathcal{D}_j^i$ used for the denominators in (124) provides for more concise expressions below. In the ladders, the coupling matrices $\mathcal{G}_j^i$ form products, operating on one another to determine the coupling factors of internal vertices, and operating on the initial and final state vectors $\widetilde{\mathbf{u}}$ and $\mathbf{v}$ to determine the coupling factors of the vertices connected to the external lines. The coupling matrices are dyadics formed by the tensor product of two vectors

$$\mathcal{G}_j^i \;\; = \;\; \mathbf{v}_j^i \otimes \widetilde{\mathbf{u}}_j^i \tag{130}$$

The tilde ~ indicates the transpose. For the four types of propagators, the vectors $\mathbf{u}_j^i$ are

defined in terms of the coupling constants, each vector presenting four coupling possibilities

$$\mathbf{u}_A^A \;=\; (g_{AA}^2, g_{AA}g_{AB}, g_{AB}g_{AA}, g_{AB}^2) \tag{131}$$

$$\mathbf{u}_B^A \;=\; (g_{AA}g_{AB}, g_{AA}g_{BB}, g_{AB}^2, g_{AB}g_{BB}) \tag{132}$$

$$\mathbf{u}_A^B \;=\; (g_{AA}g_{AB}, g_{AB}^2, g_{AA}g_{BB}, g_{AB}g_{BB}) \tag{133}$$

$$\mathbf{u}_B^B \;=\; (g_{AB}^2, g_{AB}g_{BB}, g_{BB}g_{AB}, g_{BB}^2) \tag{134}$$

The vectors $\mathbf{v}_j^i$ act as column selectors

$$\mathbf{v}_A^A \;=\; (1, 0, 0, 0) \tag{135}$$

$$\mathbf{v}_B^A \;=\; (0, 1, 0, 0) \tag{136}$$

$$\mathbf{v}_A^B \;=\; (0, 0, 1, 0) \tag{137}$$

$$\mathbf{v}_B^B \;=\; (0, 0, 0, 1) \tag{138}$$

Carrying out the tensor products, the coupling matrices are

$$\mathcal{G}_A^A \;=\; \mathbf{v}_A^A \otimes \widetilde{\mathbf{u}}_A^A = \begin{pmatrix} g_{AA}^2 & g_{AA}g_{AB} & g_{AB}g_{AA} & g_{AB}^2 \\ 0 & 0 & 0 & 0 \\ 0 & 0 & 0 & 0 \\ 0 & 0 & 0 & 0 \end{pmatrix} \tag{139}$$

$$\mathcal{G}_B^A \;=\; \mathbf{v}_B^A \otimes \widetilde{\mathbf{u}}_B^A = \begin{pmatrix} 0 & 0 & 0 & 0 \\ g_{AA}g_{AB} & g_{AA}g_{BB} & g_{AB}^2 & g_{AB}g_{BB} \\ 0 & 0 & 0 & 0 \\ 0 & 0 & 0 & 0 \end{pmatrix} \tag{140}$$

$$\mathcal{G}_A^B \;=\; \mathbf{v}_A^B \otimes \widetilde{\mathbf{u}}_A^B = \begin{pmatrix} 0 & 0 & 0 & 0 \\ 0 & 0 & 0 & 0 \\ g_{AB}g_{AA} & g_{AB}^2 & g_{BB}g_{AA} & g_{AB}g_{BB} \\ 0 & 0 & 0 & 0 \end{pmatrix} \tag{141}$$

$$\mathcal{G}_B^B \;=\; \mathbf{v}_B^B \otimes \widetilde{\mathbf{u}}_B^B = \begin{pmatrix} 0 & 0 & 0 & 0 \\ 0 & 0 & 0 & 0 \\ 0 & 0 & 0 & 0 \\ g_{AB}^2 & g_{AB}g_{BB} & g_{BB}g_{AB} & g_{BB}^2 \end{pmatrix} \tag{142}$$

In the ladders, products of propagators are formed. Adjacent propagators define a pair of vertices. In the products, the coupling matrices of adjacent propagators act on each other, the $\mathbf{v}$ of a propagator acting on the $\widetilde{\mathbf{u}}$ of the preceding propagator to select the correct coupling factor for the pair of vertices. This operation is illustrated below for the inelastic process $A + A \rightarrow A + B$.

The GBSE (127) is expanded by substituting $\mathcal{M}'$ into itself iteratively to obtain the series of all possible terms of the form $G^n U^{n+1}$. The second order term

$$G^2 U^3 \;\; = \;\; U^3 (G_A^A + G_B^A + G_A^B + G_B^B)(G_A^A + G_B^A + G_A^B + G_B^B) \tag{143}$$

contains sixteen propagator products $G_j^i G_l^k$, each of which describes a two-span, three-rung ladder. As an example of the operation of the coupling matrices $\mathcal{G}_j^i$, take the term containing propagators $G_B^A G_B^B$. Bracketing the term with the initial and final state vectors

$$\widetilde{\mathbf{u}}_A^A G_B^A G_B^B \mathbf{v}_B^A \;\; = \;\; \widetilde{\mathbf{u}}_A^A \frac{\mathcal{G}_B^A}{\mathcal{D}_B^A} \frac{\mathcal{G}_B^B}{\mathcal{D}_B^B} \mathbf{v}_B^A \tag{144}$$

and evaluating the coupling factor gives

$$\widetilde{\mathbf{u}}_A^A \mathcal{G}_B^A \mathcal{G}_B^B \mathbf{v}_B^A \;\; = \;\; g_{AA} \, g_{AB}^3 \, g_{BB}^2 \tag{145}$$

which can be read directly from the corresponding diagram in figure 8.

4.3   Multiple Types of Rungs

The preceding section dealt with ladders restricted to a single type of rung, the C-rung. If such a restriction cannot be made (for example, if box diagrams formed with other types of rungs make comparable contributions to the amplitude), all types of rungs must be considered. For the Lagrangian (122) three types of rungs are possible (figure 9). For the inelastic reaction $A + A \rightarrow A + B$ there will also be five types of spans, the four listed in (124) and the fifth:

$$G_C^C \;\; = \;\; \frac{\mathcal{G}_C^C}{(k_{C_1}^2 - m_C^2)(k_{C_2}^2 - m_C^2)} = \frac{\mathcal{G}_C^C}{\mathcal{D}_C^C} \tag{146}$$
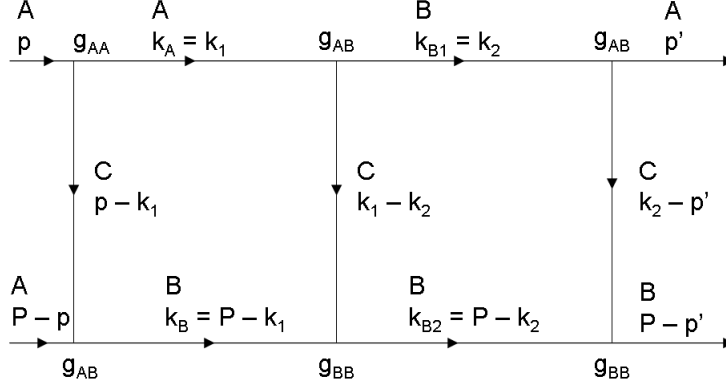
Figure 8: A 2-box ladder with coupling labeled at the vertices.

The combined propagator becomes

$$G = G_A^A + G_B^A + G_A^B + G_B^B + G_C^C \tag{147}$$

$$\tag{148}$$

The coupling matrices are now defined in a slightly different manner than was used in the preceding section. It is easy to show that the new method reduces to the former for the case of one type of rung (the C-rung). As before, the $\mathcal{G}_j^i$ matrices are defined in terms of the vectors $\mathbf{u}_j^i$ and $\mathbf{v}_j^i$, but now the vectors have five dimensions and the $\mathbf{u}_j^i$ are identical to the $\mathbf{v}_j^i$

$$\mathbf{u}_A^A = \mathbf{v}_A^A = (1,0,0,0,0) \tag{149}$$

$$\mathbf{u}_B^A = \mathbf{v}_B^A = (0,1,0,0,0) \tag{150}$$

$$\mathbf{u}_A^B = \mathbf{v}_A^B = (0,0,1,0,0) \tag{151}$$

$$\mathbf{u}_B^B = \mathbf{v}_B^B = (0,0,0,1,0) \tag{152}$$

$$\mathbf{u}_C^C = \mathbf{v}_C^C = (0,0,0,0,1) \tag{153}$$

53

The $\mathbf{u}^i_j$ define the internal lines of the propagators, but no longer carry the associated coupling factors. Instead, the coupling factors are placed in a new set of matrices $\mathcal{U}^k$, and the $\mathcal{U}^k$ become fastened to the kernels

$$U_k \;\; = \;\; \frac{\mathcal{U}_k}{q_k^2 - m_k^2} \tag{154}$$

where $k = A, B, C$ labels the type of kernel, and q_k and m_k are the momentum and mass of the exchange particle. In section 4.5, $\mathcal{U}_C$ is constructed for a one kernel system.

Kernels (rungs)

A   B   C

Propagators (spans)

A   A   B

A   B   A

B   C

B   C
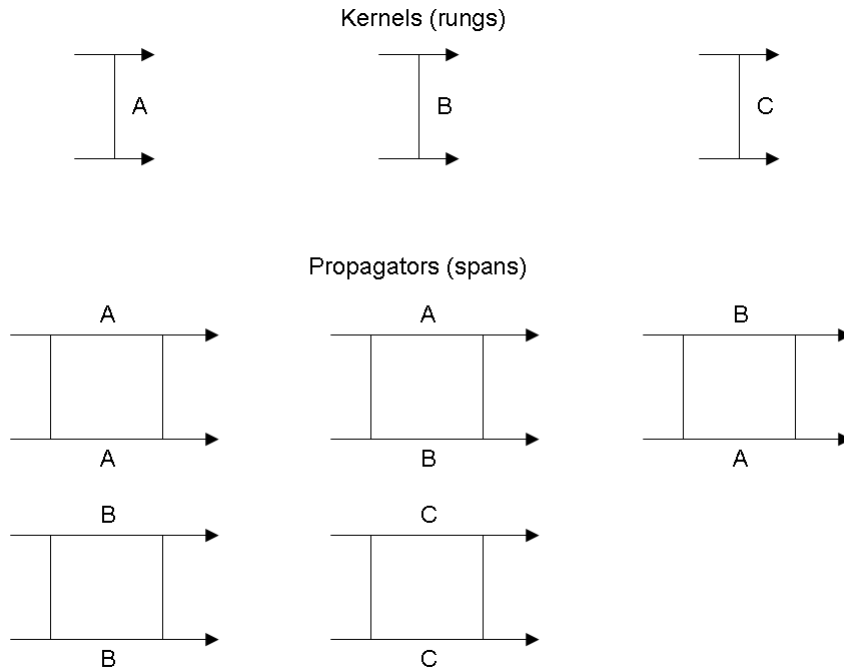
Figure 9: Multiple rungs and spans.

4.4 Form of the GBSE for Multiple Exchange Particles

This section proposes a form of the GBSE for a model that involves more than one type of exchange particle. A proof of the equivalence of the ladder series of this GBSE and the S-matrix is given in section 4.18.

Consider a Lagrangian of the form

$$
\mathcal{L} = \sum_{i=1}^{N_U} \mathcal{L}_i
$$
$$
\mathcal{L}_i = -g_{AAi}AAC_i - g_{ABi}ABC_i - g_{BBi}BBC_i \equiv -AAC_i - ABC_i - BBC_i \quad (155)
$$

which describes interactions between two types of particles A and B, involving N_U different types of exchange particles C_i. In general, some of the coupling constants g_{XYi} may be zero, signifying that the corresponding interaction vertex is not included (see section 4.10 for an example involving six different exchange mesons). Since each type of exchange particle represents an independent reaction channel, the reaction amplitudes are additive and the kernel U is the sum of N_U kernels

$$
U = \sum_{i=1}^{4} U_i
$$
$$
U_i = \frac{\mathcal{U}_i}{(q_i^2 - m_i^2)} \quad (156)
$$

one for each exchange particle. Each U_i contains its own unique coupling matrix $\mathcal{U}_i$ where q_i and m_i are the momentum and mass of the exchange particle C_i. For the set of two particles A and B there are four possible initial reaction states and therefore four types of propagators. The propagator G is the sum of the four propagators previously defined by (124) for the case of a single kernel

$$
G = \sum_{i=1}^{4} G_i = \sum_{i=1}^{4} \frac{\mathcal{G}_i}{\mathcal{D}_i} \quad (157)
$$

Given U and G above, the GBSE retains the form

$$
\mathcal{M}_{rs} = \widetilde{\mathbf{u}}_r \, \mathcal{M}' \, \mathbf{v}_s
$$
$$
\mathcal{M}' = U + \int_k UG\mathcal{M}' \quad (158)
$$

A proof of the equivalence of the ladder series generated by (158) and the S-matrix is given in section 4.18. In (158), $\widetilde{\mathbf{u}}_r$ and $\mathbf{v}_s$ are 4-dimensional vectors that specify the initial state r and final state s, respectively. The coupling matrices $\mathcal{U}_i$ and $\mathcal{G}_j$ are constructed so as to

reproduce only the vertices found in the Lagrangian. As mentioned previously, $\mathcal{M}'$ can also be formulated to include terms for exchange diagrams. Exchange diagrams are discussed in section 4.12.

4.5 Building the Coupling Matrices

In the expansion of the GBSE, the coupling matrices form products during ladder formation to produce coupling factors for the vertices. The Lagrangian defines the set of allowed vertices. The vertices determine the types of ladders that can be formed. The coupling matrices must be constructed so that only those sequences of kernels and propagators (rungs and spans) that form *allowed vertices* produce non-zero coupling factors for the vertices.

For our example we use the 2-vertex Lagrangian

$$\mathcal{L} \;\; = \;\; -g_{AAC}AAC - g_{ABC}ABC \tag{159}$$

which has vertices AAC and ABC and defines the set of three kernels and nine propagators shown in figure 1. We restrict our example to a single kernel, the C-kernel. In the expansion of the GBSE, 4th order diagrams (also called box diagrams or 2-rung ladders) are produced. Four such ladders are shown in the figure 10. The top two ladders consist of allowed vertices, but the bottom two ladders contain a BBC vertex, which does not appear in the Lagrangian. The product of the coupling matrices must exclude the latter ladders by generating a coupling factor of zero for the prohibited vertices.

The coupling matrices are derived for the given Lagrangian. The method is easily generalized for arbitrary Lagrangian.

Two vertices are formed in the product of two propagators and one kernel, producing a product of coupling matrices $\mathcal{G}_i$ and $\mathcal{U}_k$

$$G_i U_k G_j \;\; \propto \;\; \mathcal{G}_i \mathcal{U}_k \mathcal{G}_j \tag{160}$$

Propagator coupling matrices $\mathcal{G}_i$ are formed from tensor products of the vectors $\mathbf{u}$ and $\widetilde{\mathbf{v}}$

$$\mathcal{G}_i \;\; = \;\; \mathbf{u}_i \otimes \widetilde{\mathbf{v}}_j \tag{161}$$

56
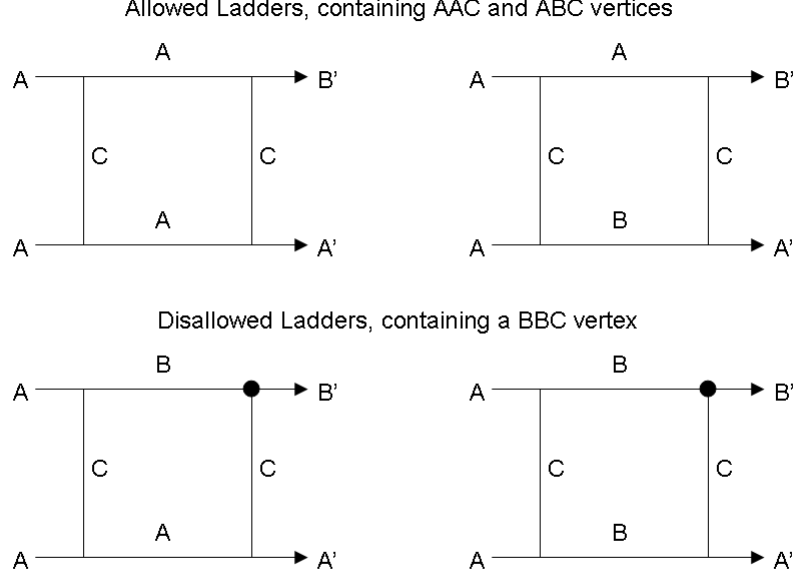
Figure 10: Exclusion of Ladders with disallowed vertices.

Substituting (161) into (160) gives

$$
\begin{aligned}
\mathcal{G}_i \mathcal{U}_k \mathcal{G}_j &= \mathbf{u}_i \otimes \widetilde{\mathbf{v}}_i \mathcal{U}_k \mathbf{u}_j \otimes \widetilde{\mathbf{v}}_j \\
&= \mathbf{u}_i (\mathcal{U}_k)_{ij} \widetilde{\mathbf{v}}_j
\end{aligned}
\tag{162}
$$

which defines the matrix element

$$
(\mathcal{U}_k)_{ij} \equiv \widetilde{\mathbf{v}}_i \mathcal{U}_k \mathbf{u}_j
\tag{163}
$$

We can use (163) to generate the matrices $\mathcal{U}_k$. Our procedure involves the following steps:

1) From the Lagrangian, list the allowed vertices, kernels and propagators. For the chosen Lagrangian, there are two vertices, AAC and ABC, three kernels and nine propagators (see figure 1).

2) Apply desired restrictions. In our case, we choose to use only one kernel, the C-kernel U_C, which contains coupling matrix $\mathcal{U}_C$. As a result, only four of the propagators may be

used, G_A^A, G_A^B, G_B^A and G_B^B. The other five propagators, when combined with the C-type kernel, produce unwanted vertices of the form CCX. The four propagators contain the four coupling matrices $\mathcal{G}_A^A$, $\mathcal{G}_A^B$, $\mathcal{G}_B^A$ and $\mathcal{G}_B^B$.

3) The number of propagators $N_G = 4$ determines the dimensions of the vectors and coupling matrices. Vectors $\mathbf{u}_i^j$ and $\mathbf{v}_i^j$ have dimension N_G, and coupling matrices $\mathcal{U}_C$ and $\mathcal{G}_i^j$ have dimensions $N_G \times N_G$.

4) Define the vectors $\mathbf{u}_i^j$ and $\mathbf{v}_i^j$. These vectors act on $\mathcal{U}_C$ as row and column selectors, so their definitions are arbitrary. We choose the following:

$$\mathbf{u}_A^A = \mathbf{v}_A^A = (1,0,0,0) \tag{164}$$

$$\mathbf{u}_B^A = \mathbf{v}_B^A = (0,1,0,0) \tag{165}$$

$$\mathbf{u}_A^B = \mathbf{v}_A^B = (0,0,1,0) \tag{166}$$

$$\mathbf{u}_B^B = \mathbf{v}_B^B = (0,0,0,1) \tag{167}$$

5. The coupling matrices $\mathcal{G}_i^j$ are tensor products of the vectors

$$\mathcal{G}_A^A = \mathbf{v}_A^A \otimes \widetilde{\mathbf{u}}_A^A = \begin{pmatrix} 1 & 0 & 0 & 0 \\ 0 & 0 & 0 & 0 \\ 0 & 0 & 0 & 0 \\ 0 & 0 & 0 & 0 \end{pmatrix} \tag{168}$$

$$\mathcal{G}_B^A = \mathbf{v}_B^A \otimes \widetilde{\mathbf{u}}_B^A = \begin{pmatrix} 0 & 0 & 0 & 0 \\ 0 & 1 & 0 & 0 \\ 0 & 0 & 0 & 0 \\ 0 & 0 & 0 & 0 \end{pmatrix} \tag{169}$$

$$\mathcal{G}_A^B = \mathbf{v}_A^B \otimes \widetilde{\mathbf{u}}_A^B = \begin{pmatrix} 0 & 0 & 0 & 0 \\ 0 & 0 & 0 & 0 \\ 0 & 0 & 1 & 0 \\ 0 & 0 & 0 & 0 \end{pmatrix} \tag{170}$$

$$\mathcal{G}_B^B = \mathbf{v}_B^B \otimes \widetilde{\mathbf{u}}_B^B = \begin{pmatrix} 0 & 0 & 0 & 0 \\ 0 & 0 & 0 & 0 \\ 0 & 0 & 0 & 0 \\ 0 & 0 & 0 & 1 \end{pmatrix} \tag{171}$$

6. Use (163) to calculate the elements of coupling matrix $\mathcal{U}_C$. First, we simplify the notation by setting

$$g_{AAC} = g_1 \tag{172}$$

$$g_{ABC} = g_2 \tag{173}$$

$$\mathcal{G}_A^A = \mathcal{G}_1 \tag{174}$$

$$\mathcal{G}_A^B = \mathcal{G}_2 \tag{175}$$

$$\mathcal{G}_B^A = \mathcal{G}_3 \tag{176}$$

$$\mathcal{G}_B^B = \mathcal{G}_4 \tag{177}$$

We calculate several matrix elements explicitly (refer to figure 10). The product $\mathcal{G}_1 \mathcal{U}_C \mathcal{G}_1$ produces two AAC vertices, each with coupling constant g_1. Therefore

$$(\mathcal{U}_C)_{11} = g_1^2 \tag{178}$$

The product $\mathcal{G}_1 \mathcal{U}_C \mathcal{G}_2$ produces vertices AAC and ABC, with coupling constants g_1 and g_2, respectively. Therefore

$$(\mathcal{U}_C)_{23} = g_1 g_2 \tag{179}$$

The product $\mathcal{G}_3 \mathcal{U}_C \mathcal{G}_3$ produces the prohibited vertex BBC. Therefore

$$(\mathcal{U}_C)_{33} = 0 \tag{180}$$

Repeating this process for all sixteen elements, the complete matrix is

$$\mathcal{U}_C = \begin{pmatrix} g_1^2 & g_1 g_2 & g_1 g_2 & g_2^2 \\ g_1 g_2 & 0 & g_2^2 & 0 \\ g_1 g_2 & g_2^2 & 0 & 0 \\ g_2^2 & 0 & 0 & 0 \end{pmatrix} \tag{181}$$

4.6 Generation of Fourth-Order Diagrams

In the ladder approximation ([15] chap. 12), the GBSE sums over all orders of ladder diagrams. The 2nd order diagrams, each with a single internal line, represent the exchange

of a single virtual particle. Next in line are the 4th order diagrams, also called box diagrams, which have 4 internal lines, representing the exchange of 4 virtual particles, 2 of which are often considered to be on-shell or nearly so ([15]). For the Lagrangian

$$
\begin{aligned}
\mathcal{L} &= -g_{AAC}A_1(x)A_2(x)C(x) - g_{ABC}A(x)B(x)C(x) - g_{BBC}B_1(x)B_2(x)C(x) \\
&= -g_{AA}AAC - g_{AB}ABC - g_{BB}BBC
\end{aligned}
\tag{182}
$$

the GBSE, in its most general form, will have the 3 kernels and 9 propagators shown in figure 1, where all three types of particles A, B and C appear in the kernels as exchange particles. In practice, usually only one of the particles, C, is treated as an exchange particle. This eliminates two kernels. Further, for the inelastic reaction $A + A \rightarrow A + B$ only four of the nine propagators generate allowed vertices: G_A^A, G_A^B, G_B^A and G_B^B. This situation was discussed in the preceding subsections.

In the expansion of the GBSE, ladders of all orders are formed from products of the basic building blocks, the kernels and propagators. To be exact, the GBSE must generate all types of ladder diagrams, each with the correct multiplicity of diagrams, produced by the Dyson S-matrix. The next section describes program *FindFeynmanDiagrams*, which generates all diagrams of the S-matrix up to 4th order for a specified reaction. *FindFeynmanDiagrams* validates the GBSE to 4th order.

4.7   Program FindFeynmanDiagrams

To verify the GBSE to 4th order, we generate all 4th order diagrams from the S_4 term of the scattering matrix, and determine the multiplicities of each type of diagram. This is done using program *FindFeynmanDiagrams* for the reaction $N + N \rightarrow N + \Delta$, which in our general notation is $A + A \rightarrow A + B$. *FindFeynmanDiagrams* generates the types of diagrams shown in figure 11. See section 4.8 for a listing of *FindFeynmanDiagrams*. The diagrams are equivalent to those of Gross [15] figure 12.1. Descriptive names have been assigned and the shapes chosen to emphasize identifying features. These are discussed below. The box diagrams are further subdivided by propagator type. These are shown in figure 7.

The multiplicities of the 4th order diagrams are generated by *FindFeynmanDiagrams* and
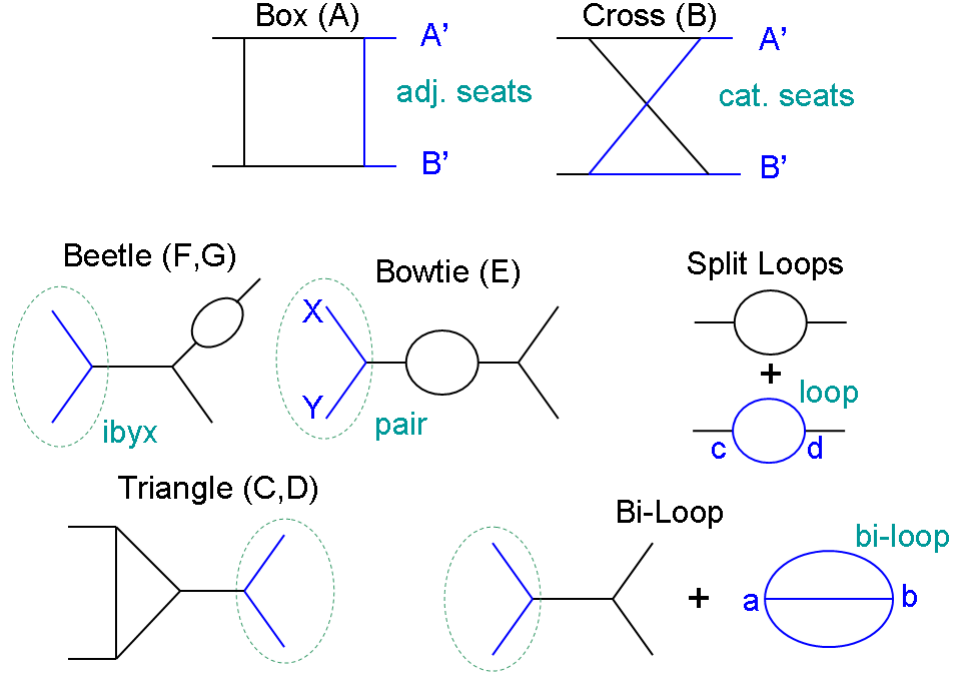
Figure 11: Geometrical Types of 4th Order Diagrams.

written to file "results.txt". This file is listed at the end of section 4.8.

4.8   The *FindFeynmanDiagrams* Algorithm

FindFeynmanDiagrams uses Wick/Peskin contraction (see section 2.1.6) to determine all diagrams arising from S_4, the 4th order term in the scattering matrix

$$S_4 = \frac{(-i)^4}{4!} \int d^4x_1 d^4x_2 d^4x_3 d^4x_4 T\{\mathcal{H}_1 \mathcal{H}_2 \mathcal{H}_3 \mathcal{H}_4\} \tag{183}$$

$$\mathcal{H}_i = -\mathcal{L}_i = g_{ABC} A(x_i) B(x_i) C(x_i) + g(AAC) A^1(x_i) A^2(x_i) C(x_i) +$$

$$+ g(BBC) B^1(x_i) B^2(x_i) C(x_i) \tag{184}$$

where the subscripts 1 through 4 on the interaction Hamiltonians identify the vertices x_1 through x_4 at which the Hamiltonians are respectively evaluated. T is the time ordering

operator which operates on the products of fields appearing in the terms. The products of fields are produced by the products of Hamiltonians. *FindFeynmanDiagrams* expands the product of four Hamiltonians to produce 81 terms

$$
\begin{aligned}
\mathcal{H}_1\,\mathcal{H}_2\,\mathcal{H}_3\,\mathcal{H}_4 \;=\;& \mathcal{H}(x_1)\,\mathcal{H}(x_2)\,\mathcal{H}(x_3)\,\mathcal{H}(x_4) \\
=\;& (-ig_{ABC})^4 A(x_1)B(x_1)C(x_1)\;A(x_2)B(x_2)C(x_2)\;\times \\
& A(x_3)B(x_3)C(x_3)A(x_4)B(x_4)C(x_4)\;+80\;more\;terms \quad (185)
\end{aligned}
$$

in which each term is the product of 12 fields. Of the 81 terms, only 36 of the terms contribute to the amplitude of the process $A + A \to A + B$. The 36 terms (listed below) are found by pairing internal fields with external state particles (field A with external particle A, etc), then counting the remaining fields. If there are an even number of A fields, B fields and C fields, the term contributes to the process. This method ensures that all external particles contract with a field, and that the remaining fields contract in pairs to form propagators. The list below uses a compact notation (taking one term as an example)

$$
\begin{aligned}
& g_{ABC}\,g_{AAC}^3 A(x_1)B(x_1)C(x_1)\;A_1(x_2)A_2(x_2)C(x_2)\;\times \\
& A_1(x_3)A_2(x_3)C(x_3)\;A_1(x_4)A_2(x_4)C(x_4) \\
=\;& (ABC)_1(AAC)_2(AAC)_3(AAC)_4 \quad\quad\quad\quad\quad\quad (186)
\end{aligned}
$$

This notation hides the coupling constants as well as the dependence of the fields on the 4-space coordinates x_i, but retains the coordinate subscripts to distinguish the vertices. The notation also drops the field subscripts, with the understanding that $AAC =$

$A_1(x)\, A_2(x)\, C(x)$. The 36 contributing terms are

$$(ABC)_1(ABC)_2(ABC)_3(AAC)_4 + (ABC)_1(ABC)_2(AAC)_3(ABC)_4 +$$

$$(ABC)_1(AAC)_2(ABC)_3(ABC)_4 + (AAC)_1(ABC)_2(ABC)_3(ABC)_4 +$$

$$(ABC)_1(AAC)_2(AAC)_3(AAC)_4 + (AAC)_1(ABC)_2(AAC)_3(AAC)_4 +$$

$$(AAC)_1(AAC)_2(ABC)_3(AAC)_4 + (AAC)_1(AAC)_2(AAC)_3(ABC)_4 +$$

$$(ABC)_1(ABC)_2(ABC)_3(BBC)_4 + (ABC)_1(ABC)_2(BBC)_3(ABC)_4 +$$

$$(ABC)_1(BBC)_2(ABC)_3(ABC)_4 + (BBC)_1(ABC)_2(ABC)_3(ABC)_4 +$$

$$(AAC)_1(ABC)_2(BBC)_3(AAC)_4 + (ABC)_1(AAC)_2(AAC)_3(BBC)_4 +$$

$$(ABC)_1(AAC)_2(BBC)_3(AAC)_4 + (ABC)_1(BBC)_2(AAC)_3(AAC)_4 +$$

$$(AAC)_1(ABC)_2(AAC)_3(BBC)_4 + (AAC)_1(AAC)_2(ABC)_3(BBC)_4 +$$

$$(AAC)_1(AAC)_2(BBC)_3(ABC)_4 + (AAC)_1(BBC)_2(ABC)_3(AAC)_4 +$$

$$(AAC)_1(BBC)_2(AAC)_3(ABC)_4 + (BBC)_1(ABC)_2(AAC)_3(AAC)_4 +$$

$$(BBC)_1(AAC)_2(ABC)_3(AAC)_4 + (BBC)_1(AAC)_2(AAC)_3(ABC)_4 +$$

$$(ABC)_1(AAC)_2(BBC)_3(BBC)_4 + (ABC)_1(BBC)_2(AAC)_3(BBC)_4 +$$

$$(ABC)_1(BBC)_2(BBC)_3(AAC)_4 + (AAC)_1(ABC)_2(BBC)_3(BBC)_4 +$$

$$(AAC)_1(BBC)_2(ABC)_3(BBC)_4 + (AAC)_1(BBC)_2(BBC)_3(ABC)_4 +$$

$$(BBC)_1(ABC)_2(AAC)_3(BBC)_4 + (BBC)_1(ABC)_2(BBC)_3(AAC)_4 +$$

$$(BBC)_1(AAC)_2(ABC)_3(BBC)_4 + (BBC)_1(AAC)_2(BBC)_3(ABC)_4 +$$

$$(BBC)_1(BBC)_2(ABC)_3(AAC)_4 + (BBC)_1(BBC)_2(AAC)_3(ABC)_4 \qquad (187)$$

Table 1: Features of 4th Order Diagrams.

Feature	Description
Pair	An Ibyx with either two initial or two final state lines
Ibyx	Two external lines share a vertex
Loop	Two vertices that share two internal lines
Bi-loop	Two vertices that share three internal lines
Seat	In a box diagram, final state vertices sit adjacent or catecorner

For each of the 36 terms, *FindFeynmanDiagrams* determines all diagrams resulting from the term by finding all ways that contractions can be made. To create a diagram, external contractions are made first. These determine which external lines attach to which vertices. Internal contractions are then made until no fields remain un-contracted. The internal contractions determine the internal lines between vertices. The resulting diagram is classified and counted by type, and printed to a file in symbolic form. The procedure of Wick/Peskin contraction takes care of normal ordering automatically.

A diagram is classified by finding the identifying features in the diagram. The identifying features are *pairs, ibyxs, loops, bi-loops and seats*. The features are defined in the table 1, and shown in figure 11. An *ibyx* is a vertex having two external lines. The lines can be either initial or final state particles. A *pair* is an ibyx in which the two external lines are both initial state particles, or both final state particles. In the figure, X and Y are both initial state particles, so the ibyx is also a pair. A *loop* is a pair of vertices that share two internal lines (vertices c,d in the figure). A *bi-loop* is a pair of vertices that share three internal lines (vertices a,b in the figure). The *seat* distinguishes box and cross diagrams. If the two final state particles (A' and B' in the figure) are separated by one internal line, they have adjacent seats, and the diagram is a box. If the two final state particles are separated by two internal lines, they have catecorner seats, and the diagram is a cross. *FindFeynmanDiagrams* uses the features to classify the diagram as one of the types shown in figure 11. Gross [15] figure 12.1 also shows the types of 4th order diagrams.

Figure 11 matches the diagrams to those of Gross (Gross labels the diagrams A through G). Gross omits the split diagrams. Gross shapes the diagrams to emphasize the box shape and deviations from the box shape. In figure 11 the diagrams are shaped to emphasize the identifying features. Of particular interest for the GBSE discussion are the four types of box diagrams which involve C exchange, and their multiplicities. These diagrams correspond to the four types of propagators (see figure 7).

FindFeynmanDiagrams prints a summary of the results of generating all possible diagrams. The file is listed in section 6.1. The summary gives the total number of diagrams, the number of diagrams for each type of diagram (figure 11), and the number of diagrams for each of five types of boxes. *FindFeynmanDiagrams* verifies that the numbers sum to the total, and that the numbers of box diagrams are integrally divisible by 4!.

4.8.1   Multiplicity of the "AA" Box Diagrams

To further verify the veracity of *FindFeynmanDiagrams*, we count "by hand" the number of box diagrams in which the propagator is G_A^A. *FindFeynmanDiagrams* gives

$$\text{number of AA boxes} = 48/24 = 2$$

The hand count is depicted in figure 12. Before proceeding with the count, we note that for box diagrams, only one external particle can connect to each or the four vertices. Furthermore, the two final state particles must share an internal C line, and the two initial state particles must share an internal C line. The G_A^A box diagram has one ABC vertex and three AAC vertices. Of the 36 contributing terms (see preceding section), four terms have the correct set of vertices. In the diagram, the vertices are labeled a, b, c and d. For the selected term (dotted rectangle), in steps (2) through (5) the vertices are labeled 1 through 4. Once all contractions have been made, the diagram vertices {a,b,c,d} will map to the term vertices {1,2,3,4}. For the following five calculation steps (1) through (5), refer to the figure.

1. For each of the four terms, the external final state particle B' contracts in one way

only to the ABC vertex. *This gives a factor of 4 in the total number of diagrams.*

2. In the first term, with B' contracted to vertex 1, A' can contract three ways, once to each of the AAC vertices. Having established the vertices of the final state particles, the B' at vertex 1, and the A' at vertex 2, the two internal C lines become fixed. *This gives a factor of 3.*

3. Initial state particle A_1 can contract two ways, once to each of the two remaining vertices. *This gives a factor of 2. Accumulating factors gives $4 \times 3 \times 2 = 24 = 4!$, the number of time orderings. This factor gets canceled by the S_4 factor of $1/4!$.*

4. The remaining initial state particle A_2 can contract in one way only, to the one remaining vertex.

5. An internal A contraction can be formed in two ways, from the ABC vertex to either of the two vertices occupied by the initial state particles. This internal line generates the direct and exchange box diagrams. *This gives a factor of 2.*

Having completed the contractions, the diagram vertices {a,b,c,d} map to the term vertices {1,2,3,4}, respectively. Multiplying the factors produced in steps i) through v) gives $4 \times 3 \times 2 \times 2 = 48$ diagrams, the same number of diagrams determined by *FindFeynmanDiagrams*. The multiplicity of 2 for AA box diagrams counts the direct and exchange diagrams, both of which appear since there are two identical initial state particles A_1 and A_2.

Concerning time ordering, note that the final state particle B' can contract in 4 ways (once for each of four terms). For each term, the B' occupies one vertex, so the final state particle A' can contract 3 ways, once for each of the three remaining vertices. For each contraction of A', the initial state particle A_1 contracts 2 ways, one for each of the remaining two vertices. The combined factor of $4 \times 3 \times 2 = 24$ gives the number of arrangements of the external state particles (excluding exchanges). These 24 arrangements are identical, recalling that vertex labels are dummy labels. The labels may be reassigned to show the equivalence of any two arrangements. The 24 arrangements correspond to the $4! = 24$

duplicates produced by time ordering. The factor of 24 is canceled by the factor $1/4!$ appearing in S_4, leaving $48/24 = 2$ unique AA box diagrams.

Multiplicity derives in part from duplicate terms. For example the two terms

$$(ABC)_1(AAC)_2(AAC)_3(AAC)_4$$

and

$$(AAC)_1(ABC)_2(AAC)_3(AAC)_4$$

are in fact identical. This is seen by recognizing that the indices 1 through 4 are dummy labels and may be reassigned. Swapping indices 1 and 2 in the second term shows that it is equivalent to the first term. As discussed above, these multiplicities arise precisely because of the multiplicities resulting from time ordering. The operator T generates 4! orderings *for each of the 36 terms*, a multiplicity that is canceled by the factor $1/4!$ in S_4.

4.9 Matrix Solutions of the GBSE

Numerical solutions of the BSE determine the complex-valued function $\mathcal{M}(p, p', P)$ at n points over a desired range of momentum p in the integral equation ([15] eq. 12.40)

$$\mathcal{M}(p, p'; P) = U(p, p'; P) + \int_k U(p, k; P)G(p, k; P)\mathcal{M}(k, p'; P) \qquad (188)$$

where $p = p_1$ is the 4-momentum of one of the initial state particles, $p' = p_3$ is the 4-momentum of one of the final state particles, $P = p_1 + p_2 = p_3 + p_4$ is the total interaction 4-momentum, and k, the integration variable, is the 4-momentum of one of the propagating particles in the propagator G.

For the GBSE, the numerical solution involves determining the complex-valued elements of the matrix $\mathcal{M}'(p, p'; P)$ over a range of momentum p in the integral equation

$$\mathcal{M}'(p, p'; P) = U(p, p'; P) + \int_k U(p, k; P)G(p, k; P)\mathcal{M}'(k, p'; P) \qquad (189)$$

where $\mathcal{M}'$ consists of a set $N_G \times N_G$ coupled functions. N_G is the number of propagators, which is equal to the number of initial states. The numerical task is considerably lightened

$\langle A'B' | \underline{\textbf{ABC}}\ \text{AAC}\ \text{AAC}\ \text{AAC} | A_1A_2 \rangle$

1) $\langle A'B' | \text{AAC}\ \underline{\textbf{ABC}}\ \text{AAC}\ \text{AAC} | A_1A_2 \rangle$

$\langle A'B' | \text{AAC}\ \text{AAC}\ \underline{\textbf{ABC}}\ \text{AAC} | A_1A_2 \rangle$

$\langle A'B' | \text{AAC}\ \text{AAC}\ \text{AAC}\ \underline{\textbf{ABC}} | A_1A_2 \rangle$

2) $\langle A'B' | (ABC)_1\ (AAC)_2\ (AAC)_3\ (AAC)_4 | A_1A_2 \rangle$

3) $\langle A'B' | (ABC)_1\ (AAC)_2\ (AAC)_3\ (AAC)_4 | A_1A_2 \rangle$

4) $\langle A'B' | (ABC)_1\ (AAC)_2\ (AAC)_3\ (AAC)_4 | A_1A_2 \rangle$

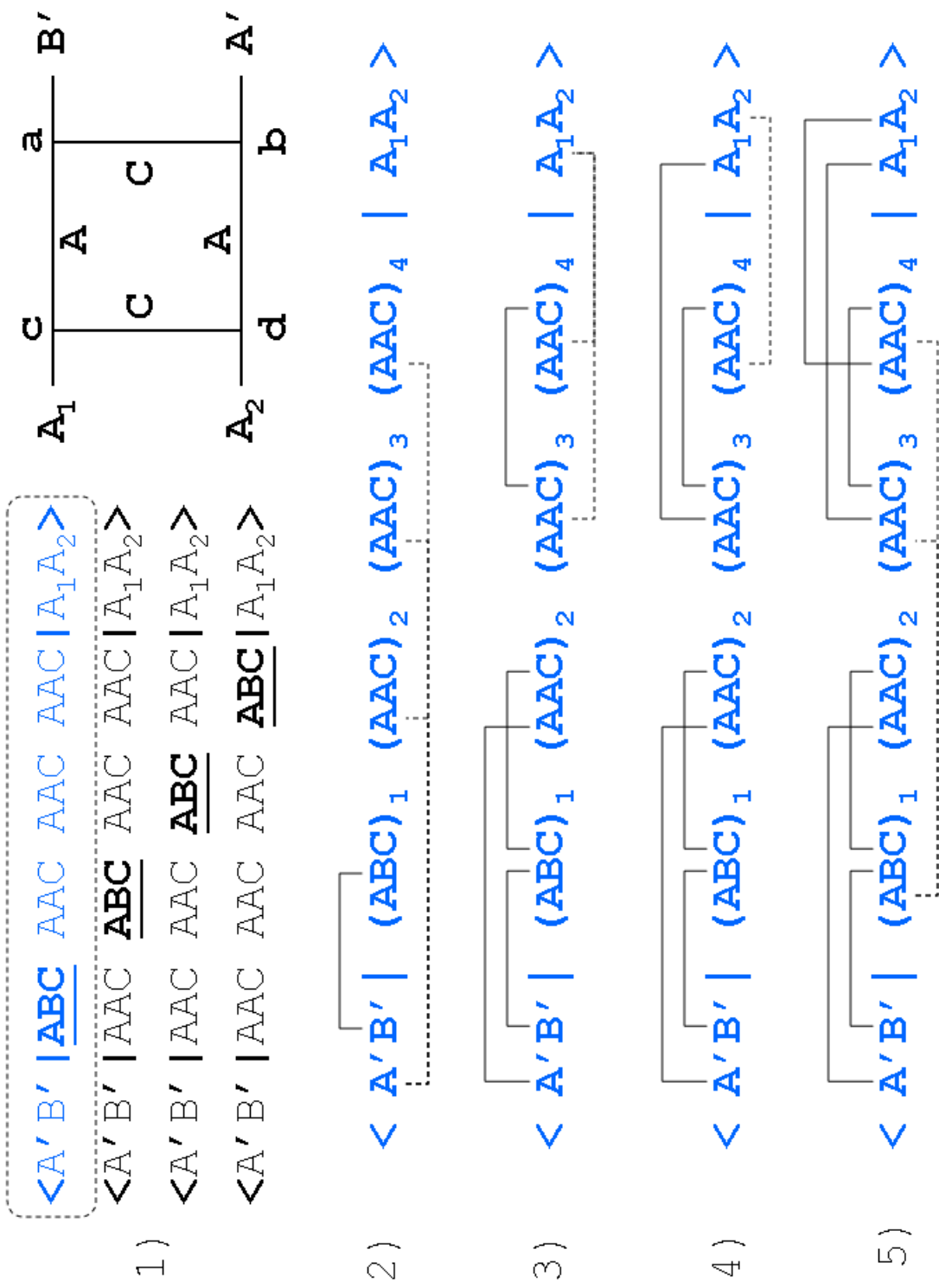5) $\langle A'B' | (ABC)_1\ (AAC)_2\ (AAC)_3\ (AAC)_4 | A_1A_2 \rangle$

Figure 12: An AA Box Diagram by Wick Contraction.

by the fact that many of the functions are equivalent under "exchange" equivalence and/or "time reversal" equivalence (these forms of equivalence are defined in section 4.11). The family of functions corresponds to a family of interaction processes that are related by shared sets of kernels and propagators. Once a solution has been found for $\mathcal{M}'$, the amplitude of an individual process is obtained by specifying the initial and final state vectors $\mathbf{x}_r$ and $\mathbf{y}_s$

$$\mathcal{M}_{rs} = \widetilde{\mathbf{u}}_r \mathcal{M}' \mathbf{v}_s \tag{190}$$

The characteristics of $\mathcal{M}'$ are explored in the following sections, where we use a simpler notation. Hiding the integral sign in (189) gives

$$\mathcal{M}' \;\; = \;\; U + UG\mathcal{M}' \;\; = \;\; U + UGU + UGUGU + \ldots \tag{191}$$

In expansions of (191), integrations are understood in all terms containing products of $\mathcal{M}'$, G and U, with one integration for each G in a given term.

4.10   The Coupled BSE of Faassen and Tjon [2]

The Coupled BSE of Faassen and Tjon is introduced at this point to motivate the ensuing discussion of the detailed form of $\mathcal{M}'$. Faassen and Tjon (FT) [2, 33, 34] use coupled Bethe-Salpeter equations (CBSE) to describe the inelastic process $N + N \rightarrow N + \Delta$. In this section we discuss the CBSE and show how it can be derived from the GBSE by applying the restrictions imposed by FT on their model.

FT treats the nucleon and Δ baryon fields as spinors, as reflected in their Lagrangian. We, however, treat all particles as scalars, consequently our Lagrangian differs from theirs, as do our kernels and propagators. Despite the differences, both treatments can be described by the same set of graphical and symbolic equations, in which the symbols represent the kernels and propagators. Fundamentally, in both treatments, these equations embody the same particle lines and interaction vertices that make up the ladder diagrams.

The CBSE takes the form of three coupled BSE equations, the first for $N+N$ production, the second for $N+\Delta$ production and the third for $\Delta+\Delta$ production. The CBSE is depicted

in figure 13 in the form of graphical equations, which correspond to the symbolic equations

$$
\begin{aligned}
\mathcal{M}'_{11} &= V_1 + \mathcal{M}'_{11}H_1V_1 + \mathcal{M}'_{13}H_3V_3 + \mathcal{M}'_{14}H_4V_4 \\
\mathcal{M}'_{13} &= V_3 + \mathcal{M}'_{12}H_2V_4 + \mathcal{M}'_{11}H_1V_3 \\
\mathcal{M}'_{14} &= V_4 + \mathcal{M}'_{11}H_1V_4
\end{aligned}
\tag{192}
$$

The V_i and H_j introduced here are forms of the kernels and propagators which contain the coupling constants rather than the coupling matrices

$$
\begin{aligned}
V_1 &= \frac{g_{AA}^2}{p_C^2 - m_C^2} \\
V_2 &= V_3 = \frac{g_{AA}g_{AB}}{p_C^2 - m_C^2} \\
V_4 &= \frac{g_{AB}^2}{p_C^2 - m_C^2} \\
H_1 &= \frac{1}{(p_A^2 - m_A^2)(q_A^2 - m_A^2)} \\
H_2 &= \frac{1}{(p_A^2 - m_A^2)(q_B^2 - m_B^2)} \\
H_3 &= \frac{1}{(p_B^2 - m_B^2)(q_A^2 - m_A^2)} \\
H_4 &= \frac{1}{(p_B^2 - m_B^2)(q_B^2 - m_B^2)}
\end{aligned}
\tag{193}
$$

V_2 and V_3 are equivalent, but both are specified so that there is a one-to-one association between the V_i and U_i. There is also a one-to-one association between the H_i and G_i. Equation (192) places $\mathcal{M}'$ *to the left of* H and V to be consistent with figure 13, which retains the order of kernels and propagators used by FT. See the end of this section and end of section 4.14 for further discussion of the left-to-right order of $\mathcal{M}'$, H and V.

In the CBSE, $N + N$ may be produced through the exchange of any of the six mesons π, ρ, η, ϵ, δ and ω, while the Δ is produced only through the exchange of the two mesons π and ρ. Thus in (192), V_1 is a sum of six kernels while V_2, V_3 and V_4 are each a sum of

two kernels

$$
\begin{aligned}
V_1 &= V_{1\pi} + V_{1\rho} + V_{1\eta} + V_{1\epsilon} + V_{1\delta} + V_{1\omega} \\
V_2 &= V_{2\pi} + V_{2\rho} \\
V_3 &= V_{3\pi} + V_{3\rho} \\
V_4 &= V_{4\pi} + V_{4\rho}
\end{aligned}
\tag{194}
$$

FT excludes the $\Delta\Delta = BB$ vertex from their Lagrangian. We apply these features of the CBSE in the next section to formulate a GBSE that is equivalent to the CBSE.
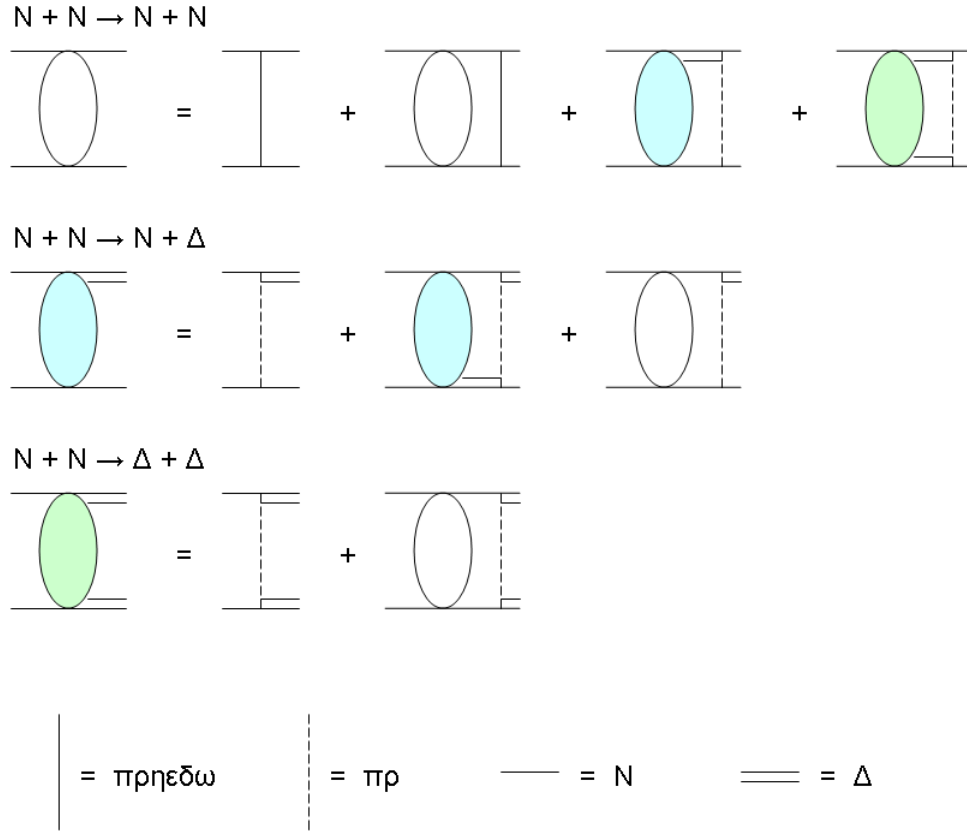

Figure 13: The Coupled BSE (adapted from Faassen and Tjon [2]).

In adapting figure 13 from FT, we keep the left to right order of the rungs $\mathcal{M}$ (fat rung) and V (thin rung) despite the fact that we have used the reverse order in previous sections

of our GBSE discussion. Here, $\mathcal{M}'$ precedes H precedes V, whereas in previous sections U precedes G precedes $\mathcal{M}'$. We further note that the order used in previous sections is the same as used in the textbook of Gross [15] and many other BSE articles, both older and newer than FT, to cite two [7, 35]. Nevertheless, the order used in the figure is consistent with the order of the symbols V_i, H_j and $\mathcal{M}'$ in the CBSE equations above. The text and papers cited are also self-consistent, keeping the same order of rungs in both the graphical and symbolic forms of the BSE, although this consistency does not matter. Interestingly, FT is not self-consistent, but in their formulation it also does not matter. In the GBSE formulation, one might expect that order does matter. The G_i are diagonal, and $U_j = \widetilde{U_j}$ is symmetric, but $\mathcal{M}' = time\ reversed\ \widetilde{\mathcal{M}}'$ is not symmetric, so in fact order does matter. However, changing the left-to-right order of $\mathcal{M}'$, H_j and V_i from $V_i H_j \mathcal{M}'$ to $\mathcal{M}' H_j V_i$ simply produces another equally valid set of coupled equations *involving the time-reversed elements of $\mathcal{M}'$*, e.g., $\mathcal{M}'_{21}$ is replaced by $\mathcal{M}'_{12}$. The order is discussed further in section 4.14.

4.10.1   2nd Order Content of the CBSE

The 2nd order content of the CBSE is analyzed using the GBSE formalism. The 2nd order diagrams embedded in the CBSE are identified and used to populate $\mathcal{M}'$ *to second order*. In the process, the coupling matrices $\mathcal{U}_i$ and $\mathcal{G}_j$ are evaluated. The goal is to express the CBSE in matrix form, and incorporate the same restrictions imposed by FT (mentioned in the previous section).

Since the set of propagators $\mathcal{G}_i$ is the same as that in section 4.5, the coupling matrices $\mathcal{G}_i$ are the same (repeated here for convenience)

$$\mathcal{G}_A^A \;=\; \mathbf{v}_A^A \otimes \widetilde{\mathbf{u}}_A^A = \begin{pmatrix} 1 & 0 & 0 & 0 \\ 0 & 0 & 0 & 0 \\ 0 & 0 & 0 & 0 \\ 0 & 0 & 0 & 0 \end{pmatrix} \tag{195}$$

$$\mathcal{G}_B^A \;=\; \mathbf{v}_B^A \otimes \widetilde{\mathbf{u}}_B^A = \begin{pmatrix} 0 & 0 & 0 & 0 \\ 0 & 1 & 0 & 0 \\ 0 & 0 & 0 & 0 \\ 0 & 0 & 0 & 0 \end{pmatrix} \tag{196}$$

72

$$\mathcal{G}_A^B = \mathbf{v}_A^B \otimes \widetilde{\mathbf{u}}_A^B = \begin{pmatrix} 0 & 0 & 0 & 0 \\ 0 & 0 & 0 & 0 \\ 0 & 0 & 1 & 0 \\ 0 & 0 & 0 & 0 \end{pmatrix} \tag{197}$$

$$\mathcal{G}_B^B = \mathbf{v}_B^B \otimes \widetilde{\mathbf{u}}_B^B = \begin{pmatrix} 0 & 0 & 0 & 0 \\ 0 & 0 & 0 & 0 \\ 0 & 0 & 0 & 0 \\ 0 & 0 & 0 & 1 \end{pmatrix} \tag{198}$$

Using the method of section 4.5, the $\mathcal{U}_k$ matrices are found by listing all possible GUG propagator-kernel-propagator combinations for each kernel, and using these to calculate the elements $(\mathcal{U}_k)_{ij}$. The GUGs define 2nd order diagrams (2ODs). Having derived $\mathcal{U}_\pi$ and $\mathcal{U}_\eta$, $\mathcal{U}_\rho$ is then obtained from $\mathcal{U}_\pi$ simply by replacing π coupling constants $g_{xx\pi}$ with ρ coupling constants $g_{xx\rho}$, and $\mathcal{U}_\epsilon$, $\mathcal{U}_\delta$ and $\mathcal{U}_\omega$ are similarly obtained from $\mathcal{U}_\eta$.

The GUG combinations used in the CBSE are found by inspection of the rungs and spans in figure 13. For each rung U appearing in the graphical equations, the two lines entering the rung from the left define the first G, and the two lines exiting the rung from the right define the second G. In this manner, six GUGs can be read directly from the figure. However, the second graphical equation shown in the figure is coupled to itself "upside-down". The upside-down image amounts to a fourth equation, which contains two more GUGs, bringing the total to eight.

The eight $GUGs$ are shown in figure 14 along with eight $GUGs$ that do not appear in the CBSE. One contains ABC and AAC vertices, and seven contain a BBC vertex. $GUGs$ found in the CBSE correspond to non-zero elements in $\mathcal{M}'$ and $\mathcal{U}$. $GUGs$ not found in the CBSE correspond to zeros in $\mathcal{M}'$ and $\mathcal{U}$. Each GUG specifies a 2nd order diagram and a product of two coupling constants. The computed $\mathcal{U}_k$ are

$$\mathcal{U}_\pi = \begin{pmatrix} g_{AA}^2 & 0 & g_{AA}g_{AB} & g_{AB}^2 \\ g_{AA}g_{AB} & 0 & g_{AB}^2 & 0 \\ g_{AA}g_{AB} & g_{AB}^2 & 0 & 0 \\ g_{AB}^2 & 0 & 0 & 0 \end{pmatrix} \tag{199}$$
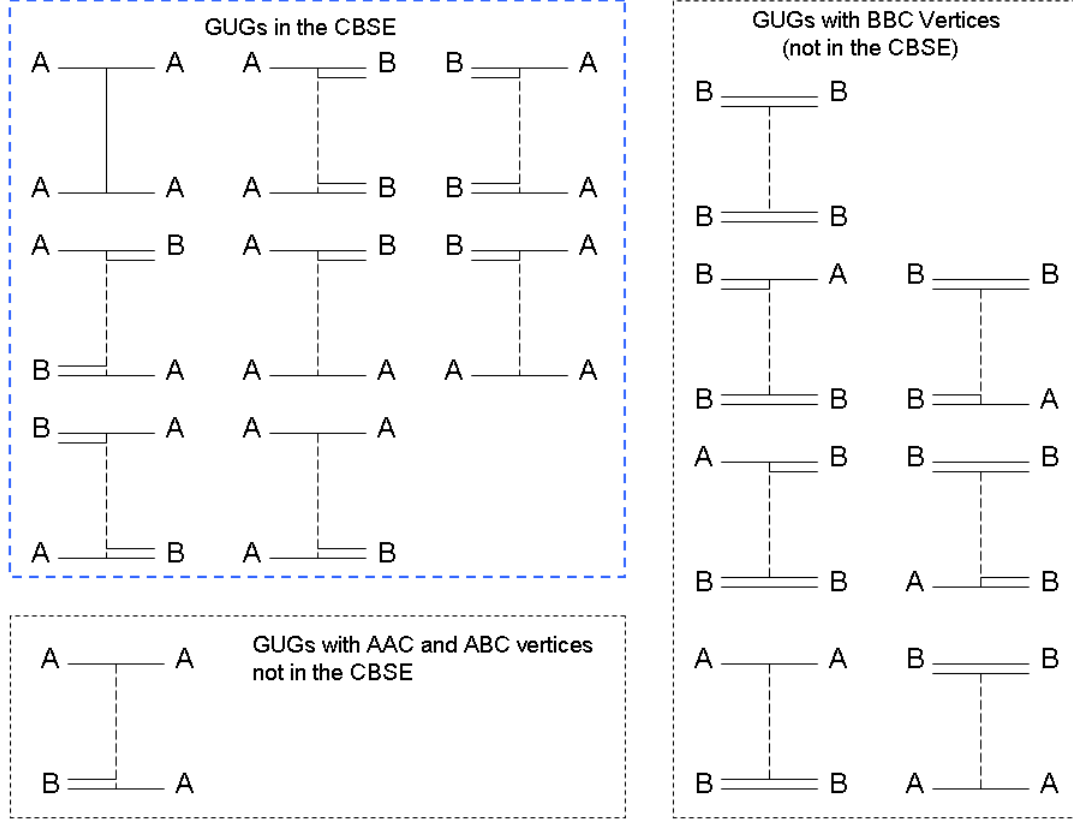
Figure 14: GUG Combinations involving AAC, ABC and BBC Vertices.

$$\mathcal{U}_\eta \;=\; \begin{pmatrix} g_{AA}^2 & 0 & 0 & 0 \\ 0 & 0 & 0 & 0 \\ 0 & 0 & 0 & 0 \\ 0 & 0 & 0 & 0 \end{pmatrix} \tag{200}$$

In $\mathcal{U}_\pi$, the subscript $C = \pi$ is implied in all the coupling constants (e.g., $g_{AA} = g_{AAC} = g_{NN\pi}$) and in $\mathcal{U}_\eta$ the subscript η is implied. The null value of $\mathcal{U}_{12}$ is a first indication that the CBSE lacks a coupling channel. A fuller explanation is given in section 4.14. In the next section, we show how the $\mathcal{U}_k$ can be read directly from $\mathcal{M}'$ approximated to second order.

4.11 2nd Order $\mathcal{M}'$

As mentioned in the preceding sections, $\mathcal{M}'$ embodies a coupled set of $N_G \times N_G$ equations (N_G is the number of propagators G_i), each equation giving the amplitude of one of $N_G \times N_G$ interaction processes. The family of interaction processes are related by sharing the sets of kernels U_i and propagators G_j. The set of equations are coupled, and their solutions are obtained simultaneously. The solution of $\mathcal{M}'$ is precisely the simultaneous solution of the set of equations. Each element $\mathcal{M}'_{ij}$ gives the amplitude of the process defined by initial and final state vectors $\mathbf{x_i}$ and y_j. Although $\mathcal{M}'$ contains $N_G \times N_G$ elements, $\mathcal{M}'$ contains groups of equivalent elements, so that the number of unique equations, thus the number of unique processes, is significantly smaller. These characteristics of $\mathcal{M}'$ are explored below.

The first term in (127), namely U, defines $\mathcal{M}'$ to second order. From (127) and (163), we see that the element U_{ij} and the element $\mathcal{M}'_{ij}$ to second order, are both given by

$$U_{ij} \;\; = \;\; 2nd\,order\;\mathcal{M}'_{ij} \;\; = \;\; \widetilde{\mathbf{u}}_i U \mathbf{v}_j \tag{201}$$

Figure 16 shows $\mathcal{M}'$ to 2nd order for the 3-vertex interaction Hamiltonian $\mathcal{H}_I = AAC + ABC + BBC$, and for a model in which the only exchange particle is the C particle. Each element $\mathcal{M}_{ij}$ is the amplitude of a particular process. For example, given an initial state vector $\mathbf{u}_1 = \widetilde{\mathbf{u}}_A^A$ and final state vector $\mathbf{v}_1 = \mathbf{v}_A^A$ (see equation (167) for the definitions of $\widetilde{\mathbf{u}}_A^A$) and $\mathbf{v}_A^A$, we find that the amplitude, to 2nd order, for the process $A + A \rightarrow A + A$ is

$$\mathcal{M}(A + A \rightarrow A + A) \;\; = \;\; \widetilde{\mathbf{u}}_1 \mathcal{M}' \mathbf{v}_1 \;\; = \;\; \mathcal{M}'_{11} \tag{202}$$

In the formalism of the GBSE developed thus far, exchange diagrams are not included. When it is known in advance that either the initial or final state is composed of two identical particles, the GBSE must sum twice the number of terms, the direct terms and the exchange terms. The latter are obtained from the former by exchanging the identical particles. In the formulation, this amounts to exchange the momenta p_1 and p_2 for identical initial state particles, and p'_1 and p'_2 for identical final state particles. Exchange amplitudes are discussed in section 4.12.

Figure 15: $\mathcal{M}'$ to 2nd Order for the CBSE.

Figure 16: $\mathcal{M}'$ to 2nd Order for $\mathcal{H}_I = AAC + ABC + BBC$.
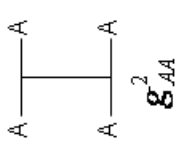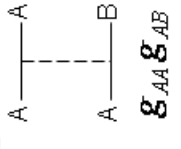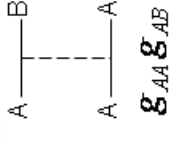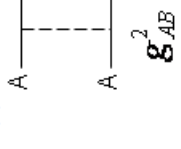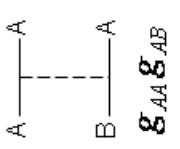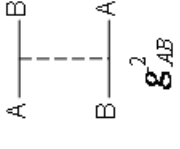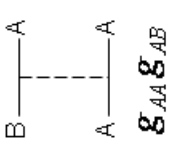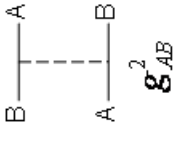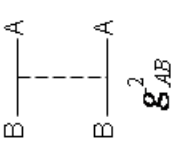
	$\langle AA\|$	$\langle AB\|$	$\langle BA\|$	$\langle BB\|$
$\|AA\rangle$	$\mathcal{M}'_{11}$ g^2_{AA}	$\mathcal{M}'_{12}$ $g_{AA}g_{AB}$	$\mathcal{M}'_{13}$ $g_{AA}g_{AB}$	$\mathcal{M}'_{14}$ g^2_{AB}
$\|AB\rangle$	$\mathcal{M}'_{21}$ $g_{AA}g_{AB}$	$\mathcal{M}'_{22}$ 0	$\mathcal{M}'_{23}$ g^2_{AB}	$\mathcal{M}'_{24}$ 0
$\|BA\rangle$	$\mathcal{M}'_{31}$ $g_{AA}g_{AB}$	$\mathcal{M}'_{32}$ g^2_{AB}	$\mathcal{M}'_{33}$ 0	$\mathcal{M}'_{34}$ 0
$\|BB\rangle$	$\mathcal{M}'_{41}$ g^2_{AB}	$\mathcal{M}'_{42}$ 0	$\mathcal{M}'_{43}$ 0	$\mathcal{M}'_{44}$ 0

Figure 17: $\mathcal{M}'$ to 2nd Order for $\mathcal{H}_I = AAC + ABC$.

Inspection of figure 16 reveals that many of the interaction amplitudes are "equivalent" for one of two reasons:

- The associated processes are identical under interchange of the initial (or final) state particles (for example, the reaction $A + B \rightarrow A + B$ is equivalent to the process $A + B \rightarrow B + A$).

- The processes are equivalent under time reversal ($A + A \rightarrow B + B$ is equivalent to $B + B \rightarrow A + A$).

Thus there are seven unique amplitudes

$$
\begin{aligned}
\mathcal{M}'_{11} & \\
\mathcal{M}'_{12} &= \tau\mathcal{M}'_{21} = \varepsilon\mathcal{M}'_{13} = \varepsilon\tau\mathcal{M}'_{31} \\
\mathcal{M}'_{14} &= \tau\mathcal{M}'_{41} \\
\mathcal{M}'_{24} &= \tau\mathcal{M}'_{42} = \varepsilon\mathcal{M}'_{34} = \varepsilon\tau\mathcal{M}'_{43} \\
\mathcal{M}'_{22} &= \varepsilon\tau\mathcal{M}'_{33} \\
\mathcal{M}'_{32} &= \varepsilon\tau\mathcal{M}'_{23} \\
\mathcal{M}'_{44} &
\end{aligned}
\tag{203}
$$

and the problem of solving for $\mathcal{M}'$ amounts to solving seven simultaneous equations. The operators ε and τ signify exchange and time-reversal, respectively, and care must be taken in applying the "equivalence" in numerical solutions. Equation (203) is a shorthand for more explicit statements. The explicit statement for exchange equivalence is

$$
\mathcal{M}'_{12}(p_1, p_2, p_3, p_4) = \varepsilon\mathcal{M}'_{13} = \mathcal{M}'_{13}(p_2, p_1, p_3, p_4)
\tag{204}
$$

where the momenta of the initial state particles are exchanged. The explicit statement for equivalence under time reversal is

$$
\mathcal{M}'_{12}(p_1, p_2, p_3, p_4) = \tau\mathcal{M}'_{21} = \mathcal{M}'_{21}(p_3, p_4, p_1, p_2)
\tag{205}
$$

where initial and final state momenta are exchanged. Both operators act in

$$\mathcal{M}'_{12}(p_1, p_2, p_3, p_4) \;\; = \;\; \varepsilon\tau\mathcal{M}'_{31} \;\; = \;\; \mathcal{M}'_{31}(p_4, p_3, p_1, p_2) \tag{206}$$

If we choose to exclude the BBC vertex and work in the 2-vertex model, the 2nd order $\mathcal{M}'$ takes the form shown in Figure 17. The absence of the BBC vertex eliminates seven of the original sixteen processes, leaving only four unique processes

$$\mathcal{M}'_{11}$$

$$\mathcal{M}'_{12} \;\; = \;\; \tau\mathcal{M}'_{21} \;\; = \;\; \varepsilon\mathcal{M}'_{13} \;\; = \;\; \varepsilon\tau\mathcal{M}'_{31}$$

$$\mathcal{M}'_{14} \;\; = \;\; \tau\mathcal{M}'_{41}$$

$$\mathcal{M}'_{32} \;\; = \;\; \varepsilon\tau\mathcal{M}'_{23} \tag{207}$$

and the problem of solving for $\mathcal{M}'$ is reduced to one of solving four simultaneous equations.

By removing the BBC vertex we have in effect removed the seven $GUGs$ that contain a BBC vertex (see figure 14). If now we keep only those $GUGs$ that appear in the $CBSE$, the 2nd order $\mathcal{M}'$ takes the form shown in figure 15, having one less GUG than figure 17. It is readily seen that the CBSE cannot produce all ladder diagrams that are possible in the two vertex model. The missing GUG in the CBSE $\mathcal{M}'$ precludes the generation of ladders containing those GUGs.

The differences between the 2-vertex $\mathcal{M}'$ and the CBSE $\mathcal{M}'$ are shown by expanding each into a ladder series. The expansions are accomplished with the help of program $CalcGBSE$ (a complete listing is given in section 6.2). Denoting the two versions of the matrix element $\mathcal{M}'_{13}$ for the 2-vertex model and $\mathcal{M}'^{(CBSE)}_{13}$ for the CBSE, and expanding to 8th order we obtain two series of ladder diagrams for the reaction $A + A \rightarrow A + B$. To verify $\mathcal{M}'^{(CBSE)}_{13}$, a third sequence is obtained by substituting the three CBSE equations (192) iteratively into

themselves. This series is equivalent to $\mathcal{M}'^{(CBSE)}_{13}$. The two series, to 8th order are

$$
\begin{aligned}
\mathcal{M}'_{13} &= V_3 + iV_1H_1V_3 + iV_2H_2V_4 + V_1H_1V_1H_1V_3 - V_3H_3V_3H_1V_3 - \underline{2V_1H_1V_2H_2V_3} \\
&\quad -V_3H_3V_2H_2V_4 - V_4H_4V_4H_1V_3 - iV_1H_1V_1H_1V_1H_1V_3 - \underline{iV_2H_2V_2H_1V_2H_2V_4} \\
&\quad -\underline{3iV_1H_1V_2H_2V_2H_1V_3} - 2iV_2H_1V_3H_3V_3H_1V_3 - iV_2H_2V_4H_3V_4H_2V_4 \\
&\quad -\underline{4iV_1H_1V_3H_3V_4H_2V_4} - 2iV_1H_1V_4H_4V_4H_1V_3 - iV_4H_4V_4H_1V_2H_2V_4
\end{aligned}
$$

$$(208)$$

and

$$
\begin{aligned}
\mathcal{M}'^{(CBSE)}_{13} &= V_3 + iV_1H_1V_3 + iV_2H_2V_4 + V_1H_1V_1H_1V_3 - V_3H_3V_3H_1V_3 - \underline{V_1H_1V_2H_2V_3} \\
&\quad -V_3H_3V_2H_2V_4 - V_4H_4V_4H_1V_3 - iV_1H_1V_1H_1V_1H_1V_3 - \underline{0} \\
&\quad -\underline{iV_1H_1V_2H_2V_2H_1V_3} - 2iV_2H_1V_3H_3V_3H_1V_3 - iV_2H_2V_4H_3V_4H_2V_4 \\
&\quad -\underline{3iV_1H_1V_3H_3V_4H_2V_4} - 2iV_1H_1V_4H_4V_4H_1V_3 - iV_4H_4V_4H_1V_2H_2V_4
\end{aligned}
$$

$$(209)$$

The underlines mark the terms that are different between the two series. The CBSE is correct to 4th order, but is lacking one of six 6th order terms, and four of fifteen 8th order terms.

Despite lacking one GUG, $\mathcal{M}'^{(CBSE)}_{13}$ still contains four unique amplitudes

$$
\begin{aligned}
\mathcal{M}'_{11} & \\
\mathcal{M}'_{13} &= \tau\mathcal{M}_{31} = \varepsilon\tau\mathcal{M}_{12} \\
\mathcal{M}'_{14} &= \tau\mathcal{M}_{41} \\
\mathcal{M}'_{23} &= \varepsilon\tau\mathcal{M}_{32}
\end{aligned}
$$

$$(210)$$

implying that the solution of $\mathcal{M}'$ amounts to solving four simultaneous equations. But the CBSE consists of only three equations. How did the fourth equation enter into $\mathcal{M}'^{(CBSE)}$? The answer is that the 2nd equation of the CBSE, that is the 2nd equation in (192) and

in figure 13, is actually two equations combined. The second equation of (192) shows that $\mathcal{M}'_{13}$ is coupled to $\mathcal{M}'_{12}$. By this coupling, FT have in effect combined two equations in one. In figure 1 of FT (and in our figure 13), the second graphical equation shows that FT clearly treats $\mathcal{M}'_{12}$ as equivalent to $\mathcal{M}'_{13}$, but in our formalism $\mathcal{M}'_{12}$ is obtained from $\mathcal{M}'_{13}$ by exchange equivalence, in which the momenta p_1 and p_2 trade places. The implied fourth equation is therefore

$$\mathcal{M}'_{12} \;=\; \varepsilon \mathcal{M}'_{13} \;=\; V_2 + \mathcal{M}'_{13} H_3 V_4 + \mathcal{M}'_{11} H_1 V_2 \tag{211}$$

Section 4.14 further clarifies the structure of the CBSE. The next four sections continue to develop the GBSE formalism.

4.11.1 Evolution of the 2-vertex $\mathcal{M}'$ in Iteration

The evolution of $\mathcal{M}'$ in iteration illustrates how, with each iteration, the four unique elements in $\mathcal{M}'$ progressively emerge. *Mathematica* program *CalcGBSE* (listed in section 6.2) carries out the first ten iterations. In the first iteration of $\mathcal{M}'$ given by $\mathcal{M}' = U + UGM'$, $\mathcal{M}'$ contains nine coupled equations, in which nine amplitudes are coupled among themselves (the other seven amplitudes are absent from these equations). The nine equations can be read directly from the output of *CalcGBSE*

$$
\begin{aligned}
\mathcal{M}'_{11} &= V_1 + V_1 H_1 \mathcal{M}'_{11} + V_2 H_2 \mathcal{M}'_{21} + V_3 H_3 \mathcal{M}'_{31} + V_4 H_4 \mathcal{M}'_{41} \\
\mathcal{M}'_{12} &= V_2 + V_1 H_1 \mathcal{M}'_{12} + V_2 H_3 \mathcal{M}'_{32} \\
\mathcal{M}'_{13} &= V_3 + V_1 H_1 \mathcal{M}'_{13} + V_2 H_2 \mathcal{M}'_{23} \\
\mathcal{M}'_{14} &= V_4 + V_1 H_1 \mathcal{M}'_{14} \\
\mathcal{M}'_{21} &= V_2 + V_2 H_1 \mathcal{M}'_{11} + V_4 H_3 \mathcal{M}'_{31} \\
\mathcal{M}'_{23} &= V_4 + V_3 H_1 \mathcal{M}'_{13} \\
\mathcal{M}'_{31} &= V_3 + V_3 H_1 \mathcal{M}'_{11} + V_4 H_2 \mathcal{M}'_{21} \\
\mathcal{M}'_{32} &= V_4 + V_3 H_1 \mathcal{M}'_{12} \\
\mathcal{M}'_{41} &= V_4 + V_4 H_1 \mathcal{M}'_{11}
\end{aligned}
\tag{212}
$$

Figure 18 shows the graphical form of these equations.

The nine matrix elements in (212) give the amplitudes, respectively of the nine reactions

$$
\begin{aligned}
A + A &\rightarrow A + A \\
A + A &\rightarrow A + B \\
A + A &\rightarrow B + A \\
A + A &\rightarrow B + B \\
A + B &\rightarrow A + A \\
A + B &\rightarrow B + A \\
B + A &\rightarrow A + A \\
B + A &\rightarrow A + B \\
B + B &\rightarrow A + A
\end{aligned}
\tag{213}
$$

For simplicity, we let the V_i represent only pion exchange. The extension to the full array of mesons $\pi, \rho, \eta, \epsilon, \delta, \omega$ is a simple matter of summation over their kernels, keeping in mind that in our model the latter four mesons $\eta, \epsilon, \delta, \omega$ only participate in the reaction $A + A \rightarrow A + A$ (we choose to exclude them from reactions involving a B particle, following FT). Only the first terms of the nine elements in (214) below indicate the equality of elements in (207)

$$
\begin{aligned}
\mathcal{M}'_{11} &= g_{AA}^2 \\
\mathcal{M}'_{12} &= \mathcal{M}'_{21} = \mathcal{M}'_{13} = \mathcal{M}'_{31} = g_{AA}g_{AB} \\
\mathcal{M}'_{14} &= \mathcal{M}'_{41} = g_{AB}^2 \\
\mathcal{M}'_{32} &= \mathcal{M}'_{23} = g_{AB}^2
\end{aligned}
\tag{214}
$$

Thus in the first iteration the elements are equivalent to 2nd order in coupling constants (or vertices). In the second iteration, the equality expands to include terms up to 4th order, and in the third iteration, the equality expands still further to include terms up to 6th order. A printout of selected 3rd iteration terms is included in section 6.2, following the
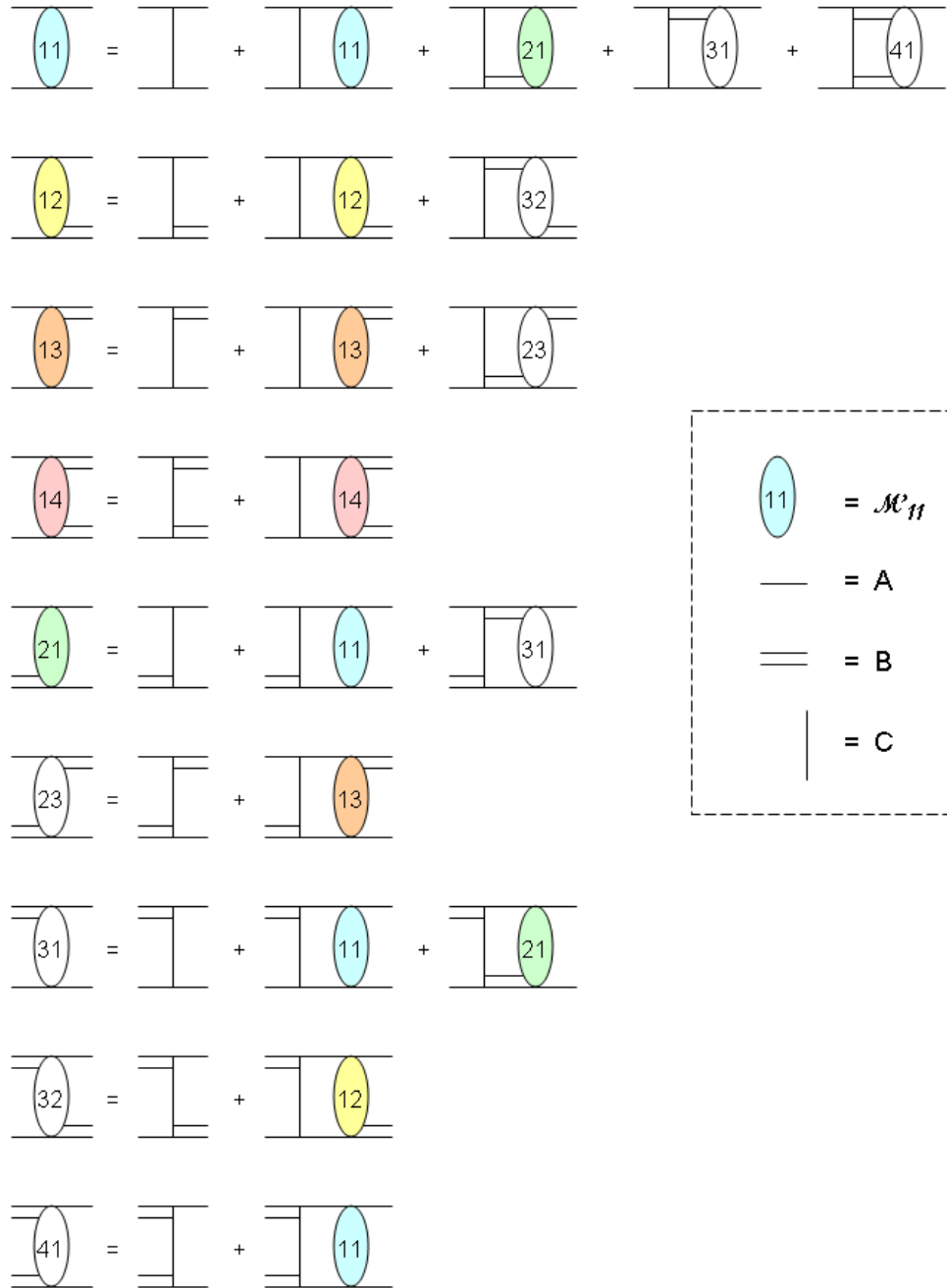
Figure 18: Graphical form of the nine equations (212).

code listing. The 10th iteration shows the equality of elements up to 20th order (listing not included in 6.2).

The preceding discussion of the nine equations implies that the solution of the 2-vertex $\mathcal{M}'$ involves solving the nine equations, a procedure that appears to be equivalent to solving a matrix containing nine elements

$$\mathcal{M}' = \begin{pmatrix} a & b & b & c \\ b & 0 & d & 0 \\ b & d & 0 & 0 \\ c & 0 & 0 & 0 \end{pmatrix} \tag{215}$$

where a, b, c and d are the four independent quantities to be determined. Similar statements can be made about the 3-vertex $\mathcal{M}'$ (the $AAC + ABC + BBC$ system). In this system, the solution of $\mathcal{M}'$ entails solving sixteen equations involving seven independent amplitudes, a procedure that is equivalent to solving a matrix of sixteen elements involving seven independent quantities a, b, c, d, e, f and g

$$\mathcal{M}' = \begin{pmatrix} a & b & b & c \\ b & e & d & f \\ b & d & e & f \\ c & f & f & g \end{pmatrix} \tag{216}$$

For the 3-vertex system, the statements are correct, but for the 2-vertex system, they statements are not correct, and the solution of the nine equations is not the complete solution of $\mathcal{M}'$. Before discussing the complete solution of $\mathcal{M}'$ in section 4.15, we shall first discuss separable systems in the nine equations.

4.11.2 Separable Systems in $\mathcal{M}'$

The solution of $\mathcal{M}'$ given by (212) involves nine equations that are separable into four independent groups of coupled equations. These can be reduced to a form in which only two of the original nine amplitudes are coupled. The other seven amplitudes can either be solved for individually, or expressed in terms of other amplitudes.

$\mathcal{M}'_{13}$ and $\mathcal{M}'_{23}$ form a semi-coupled system that is independent of the other seven

elements

$$\mathcal{M}'_{13} = V_3 + V_1 H_1 \mathcal{M}'_{13} + V_2 H_2 \mathcal{M}'_{23} \tag{217}$$

$$\mathcal{M}'_{23} = V_4 + V_3 H_1 \mathcal{M}'_{13} \tag{218}$$

$\mathcal{M}'_{23}$ is not a direct function of itself and may be eliminated by substituting it into $\mathcal{M}'_{13}$ to give

$$\mathcal{M}'_{13} = V_3 + V_2 H_2 V_4 + V_1 H_1 \mathcal{M}'_{13} + V_2 H_2 V_3 H_1 \mathcal{M}'_{13} \tag{219}$$

a single, uncoupled BSE for $\mathcal{M}'_{13}$ containing a double integral. This equation can be solved for $\mathcal{M}'_{13}$, which can be substituted back into (218) to give $\mathcal{M}'_{23}$.

$\mathcal{M}'_{12}$ and $\mathcal{M}'_{32}$ also form an independent semi-coupled system

$$\mathcal{M}'_{12} = V_2 + V_1 H_1 \mathcal{M}'_{12} + V_2 H_3 \mathcal{M}'_{32} \tag{220}$$

$$\mathcal{M}'_{32} = V_4 + V_3 H_1 \mathcal{M}'_{12} \tag{221}$$

Substituting $\mathcal{M}'_{32}$ into $\mathcal{M}'_{12}$ gives

$$\mathcal{M}'_{12} = V_2 + V_2 H_3 V_4 + V_1 H_1 \mathcal{M}'_{12} + V_2 H_3 V_3 H_1 \mathcal{M}'_{12} \tag{222}$$

a single, uncoupled BSE for $\mathcal{M}'_{12}$ containing a double integral. This equation can be solved for $\mathcal{M}'_{12}$, which can be substituted back into (221) to give $\mathcal{M}'_{32}$.

$\mathcal{M}'_{14}$ is a standalone system that does not couple to any other element in $\mathcal{M}'$

$$\mathcal{M}'_{14} = V_4 + V_1 H_1 \mathcal{M}'_{14} \tag{223}$$

This equation can be solved for $\mathcal{M}'_{14}$.

The remaining four elements $\mathcal{M}'_{11}$, $\mathcal{M}'_{21}$, $\mathcal{M}'_{31}$ and $\mathcal{M}'_{41}$ form a semi-coupled system

$$\mathcal{M}'_{11} = V_1 + V_1 H_1 \mathcal{M}'_{11} + V_2 H_2 \mathcal{M}'_{21} + V_3 H_3 \mathcal{M}'_{31} + V_4 H_4 \mathcal{M}'_{41} \tag{224}$$

$$\mathcal{M}'_{21} = V_2 + V_2 H_1 \mathcal{M}'_{11} + V_4 H_3 \mathcal{M}'_{31} \tag{225}$$

$$\mathcal{M}'_{31} = V_3 + V_3 H_1 \mathcal{M}'_{11} + V_4 H_2 \mathcal{M}'_{21} \tag{226}$$

$$\mathcal{M}'_{41} = V_4 + V_4 H_1 \mathcal{M}'_{11} \tag{227}$$

In this system $\mathcal{M}'_{31}$ and $\mathcal{M}'_{41}$ are not direct functions of themselves, so may be eliminated by substituting them into $\mathcal{M}'_{11}$ and $\mathcal{M}'_{21}$. The result is two fully coupled equations containing $\mathcal{M}'_{11}$ and $\mathcal{M}'_{21}$

$$\mathcal{M}'_{11} = V_1 + V_3 H_3 V_3 + V_4 H_4 V_4 + V_1 H_1 \mathcal{M}'_{11} + V_2 H_2 \mathcal{M}'_{21} + V_3 H_3 V_3 H_1 \mathcal{M}'_{11} +$$
$$V_3 H_3 V_4 H_2 \mathcal{M}'_{21} + V_4 H_4 V_4 H_1 \mathcal{M}'_{11} \tag{228}$$

$$\mathcal{M}'_{21} = V_2 + V_4 H_3 V_3 + V_2 H_1 \mathcal{M}'_{11} + V_4 H_3 V_3 H_1 \mathcal{M}'_{11} + V_4 H_3 V_4 H_2 \mathcal{M}'_{21} \tag{229}$$

The equations of the reduced system are

$$\mathcal{M}'_{11} = V_1 + V_3 H_3 V_3 + V_4 H_4 V_4 + V_1 H_1 \mathcal{M}'_{11} + V_2 H_2 \mathcal{M}'_{21} + V_3 H_3 V_3 H_1 \mathcal{M}'_{11} +$$
$$V_3 H_3 V_4 H_2 \mathcal{M}'_{21} + V_4 H_4 V_4 H_1 \mathcal{M}'_{11}$$

$$\mathcal{M}'_{21} = V_2 + V_4 H_3 V_3 + V_2 H_1 \mathcal{M}'_{11} + V_4 H_3 V_3 H_1 \mathcal{M}'_{11} + V_4 H_3 V_4 H_2 \mathcal{M}'_{21}$$

$$\mathcal{M}'_{12} = V_2 + V_2 H_3 V_4 + V_1 H_1 \mathcal{M}'_{12} + V_2 H_3 V_3 H_1 \mathcal{M}'_{12}$$

$$\mathcal{M}'_{13} = V_3 + V_2 H_2 V_4 + V_1 H_1 \mathcal{M}'_{13} + V_2 H_2 V_3 H_1 \mathcal{M}'_{13}$$

$$\mathcal{M}'_{14} = V_4 + V_1 H_1 \mathcal{M}'_{14}$$

$$\mathcal{M}'_{23} = V_4 + V_3 H_1 \mathcal{M}'_{13}$$

$$\mathcal{M}'_{32} = V_4 + V_3 H_1 \mathcal{M}'_{12}$$

$$\mathcal{M}'_{31} = V_3 + V_3 H_1 \mathcal{M}'_{11} + V_4 H_2 \mathcal{M}'_{21}$$

$$\mathcal{M}'_{41} = V_4 + V_4 H_1 \mathcal{M}'_{11} \tag{230}$$

Figure 19 depicts the equations in graphical form. There are still nine equations, but only the first five require numerical solution, yielding five amplitudes. The first two equations are coupled while the next three are independent. The remaining four amplitudes are expressed in terms of the first four.

If only one of the amplitudes, the amplitude of the reaction $A + A \to A + B$, is sought, the simplest approach is to solve one equation, either (222) or (219), both of which involve

Figure 19: The Reduced Equations of $\mathcal{M}'$.

a single amplitude coupled to itself. Of course, the exchange amplitude must be included to obtain the total amplitude of the reaction. Exchange amplitudes are discussed in the next section.

4.12   Total Amplitudes of Dual-channel Processes

To obtain the total amplitude of a process in which either the initial or final states (or both) have identical particles, exchange amplitudes must be included. The direct amplitudes of these "dual-channel" processes appear in the first column and first row of $\mathcal{M}'$, and are seven in number: $\mathcal{M}'_{11}$, $\mathcal{M}'_{12}$, $\mathcal{M}'_{13}$, $\mathcal{M}'_{14}$, $\mathcal{M}'_{21}$, $\mathcal{M}'_{31}$ and $\mathcal{M}'_{41}$. The remaining two amplitudes $\mathcal{M}'_{23}$ and $\mathcal{M}'_{32}$ do not represent dual-channel processes, and are total amplitudes.

$\mathcal{M}'$ as formulated contains only the direct amplitudes of the dual-channel processes. The exchange amplitudes are obtained from the direct amplitudes by exchanging the identical particles. In figure 20 the 2nd and 4th order direct and exchange diagrams are labeled with the 4-momenta of the internal and external lines

$$
\begin{aligned}
p &= p_1 \\
P - p &= p_2 \\
p' &= p_3 \\
P - p' &= p_4 \\
P &= p_1 + p_2 = p_3 + p_4
\end{aligned}
\tag{231}
$$

where p_1 and p_2 are the momenta of the initial state particles, p_3 and p_4 are the momenta of the final state particles, and P is the total momentum of the interaction. The functional forms of these diagrams are expressed in terms of direct and exchange kernels V and $\overline{V}$ and

the propagator H

$$V = \frac{1}{(p-k)^2 - m_C^2}$$

$$\overline{V} = \frac{1}{(P-p-k)^2 - m_C^2}$$

$$H = \frac{1}{(k^2 - m_k^2)[(P-k)^2 - m_q^2]}$$

where m_k and m_q are the masses of the upper and lower lines in the propagator. The coupling constants not shown. All direct $\mathcal{M}'_{ij}$ and exchange $\overline{\mathcal{M}}'_{ij}$ amplitudes are built from products of these basic components. The total amplitudes $\widehat{\mathcal{M}}'_{ij}$ of the dual-channel processes are simply the sums of the direct and exchange amplitudes

$$\widehat{\mathcal{M}}'_{ij} = \mathcal{M}'_{ij} + \overline{\mathcal{M}}'_{ij} \tag{232}$$

The exchange amplitudes of the seven dual-channel processes are

$$\overline{\mathcal{M}}'_{11} = \overline{V}_1 + \overline{V}_1 H_1 \mathcal{M}'_{11} + \overline{V}_2 H_2 \mathcal{M}'_{21} + \overline{V}_3 H_3 \mathcal{M}'_{31} + \overline{V}_4 H_4 \mathcal{M}'_{41}$$

$$\overline{\mathcal{M}}'_{12} = \overline{V}_2 + \overline{V}_1 H_1 \mathcal{M}'_{12} + \overline{V}_2 H_3 \mathcal{M}'_{32}$$

$$\overline{\mathcal{M}}'_{13} = \overline{V}_3 + \overline{V}_1 H_1 \mathcal{M}'_{13} + \overline{V}_2 H_2 \mathcal{M}'_{23}$$

$$\overline{\mathcal{M}}'_{14} = \overline{V}_4 + \overline{V}_1 H_1 \mathcal{M}'_{14}$$

$$\overline{\mathcal{M}}'_{21} = \overline{V}_2 + \overline{V}_2 H_1 \mathcal{M}'_{11} + \overline{V}_4 H_3 \mathcal{M}'_{31}$$

$$\overline{\mathcal{M}}'_{31} = \overline{V}_3 + \overline{V}_3 H_1 \mathcal{M}'_{11} + \overline{V}_4 H_2 \mathcal{M}'_{21}$$

$$\overline{\mathcal{M}}'_{41} = \overline{V}_4 + \overline{V}_4 H_1 \mathcal{M}'_{11} \tag{233}$$

These correspond to the direct amplitudes given in (212). Note that the direct amplitudes (212) are functions of themselves in products with the direct kernels, while the exchange amplitudes are functions of the direct amplitudes in products with the exchange kernels. We could have defined the amplitudes the other way around, with the exchange amplitudes as functions of themselves in products with the direct kernels, and the direct amplitudes as functions of the exchange amplitudes in products with the exchange kernels. In this second

form of the direct amplitudes, the two "flips" (exchanges) cancel to give back the direct amplitudes as functions of themselves.

$$p = p_1 \qquad P\text{-}p = p_2$$
$$p' = p_3 \qquad P\text{-}p' = p_4 \qquad P = p_1+p_2 = p_3+p_4$$
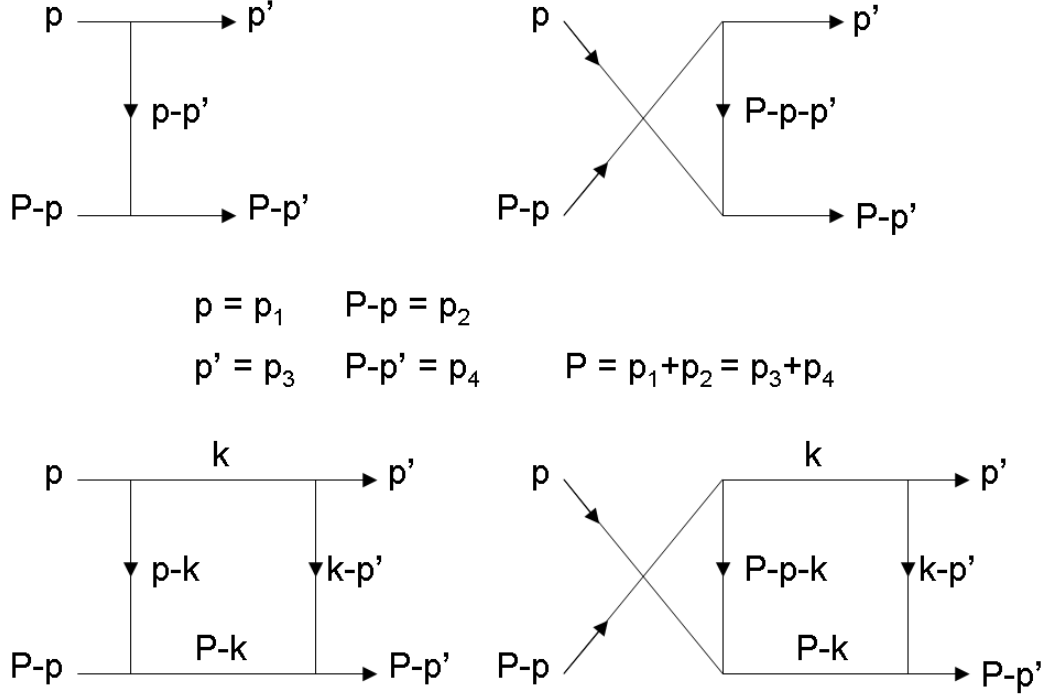
Figure 20: 2nd and 4th Order Direct and Exchange Diagrams.

4.13 Uniqueness of Amplitudes $\mathcal{M}'_{21}$, $\overline{\mathcal{M}}'_{21}$, $\mathcal{M}'_{31}$ and $\overline{\mathcal{M}}'_{31}$

In figure 18, which corresponds to equation (212), by turning the graphical equations upside down, it would appear that the exchange amplitude $\overline{\mathcal{M}}'_{21}$ is equivalent to the direct amplitude $\mathcal{M}'_{31}$, and that the exchange amplitude $\overline{\mathcal{M}}'_{31}$ is equivalent to the direct amplitude $\mathcal{M}'_{21}$. This is true under exchange equivalence (see section 4.11) for amplitudes that appear on the *left-hand side* of the equal sign, since these amplitudes are functions of p, p' and P

or equivalently p_1, p_2, p_3 and p_4, and by exchange equivalence

$$\mathcal{M'}_{21} = \varepsilon \mathcal{M'}_{31}$$
$$\mathcal{M'}_{31} = \varepsilon \mathcal{M'}_{21} \tag{234}$$

But for amplitudes appearing on the *right hand side* of the equal sign, the amplitudes appear under the integral $\int d^4k$, and are functions of p, k and P. Under exchange, a kernel $V(p-k)$ becomes $V(P-p-k)$, and vice versa. Since amplitudes are functions of kernels, amplitudes change form as well. If this were not the case, adding the direct and exchange amplitudes $\mathcal{M'}_{11}$ and $\overline{\mathcal{M}}'_{11}$ to obtain the total amplitude of the process $A + A \to A + A$ would result in double counting of box diagrams. The uniqueness of the four amplitudes can be shown by expanding the direct amplitude $\mathcal{M'}_{11}$ and exchange amplitude $\overline{\mathcal{M}}'_{11}$ to 4th order

$$
\begin{aligned}
\mathcal{M'}_{11} &= V_1 + V_1 H_1 \mathcal{M'}_{11} + V_2 H_2 V_2 + V_3 H_3 V_3 + \ldots \\
&= V_1 + i \int \frac{d^4k}{(2\pi)^4}(V_1 H_1 \mathcal{M'}_{11} + \underline{V_2 H_2 V_2} + \underline{V_3 H_3 V_3} + \ldots) \\
\overline{\mathcal{M}}'_{11} &= \overline{V}_1 + \overline{V}_1 H_1 \mathcal{M'}_{11} + \overline{V}_2 H_2 V_2 + \overline{V}_3 H_3 V_3 + \ldots \\
&= \overline{V}_1 + i \int \frac{d^4k}{(2\pi)^4}(\overline{V}_1 H_1 \mathcal{M'}_{11} + \underline{\overline{V}_2 H_2 V_2} + \underline{\overline{V}_3 H_3 V_3} + \ldots) \tag{235}
\end{aligned}
$$

and comparing the functional form of the last two terms (underlined) of both equations above. Figure 21 depicts the four box diagrams corresponding to the last two terms of both equations, showing the momenta of all lines. Two are direct and two are exchange box diagrams. Writing the functional form of the box diagrams in terms of the momenta, and as functions of k

$$
\begin{aligned}
(V_2 H_2 V_2)(k) &= \frac{g_{AA}g_{AB}}{(p-k)^2 - m_C^2} \frac{1}{(k^2 - m_A^2)[(P-k)^2 - m_B^2]} \frac{g_{AA}g_{AB}}{(k-p')^2 - m_C^2} \\
(\overline{V}_2 H_2 V_2)(k) &= \frac{g_{AA}g_{AB}}{(P-p-k)^2 - m_C^2} \frac{1}{(k^2 - m_A^2)[(P-k)^2 - m_B^2]} \frac{g_{AA}g_{AB}}{(k-p')^2 - m_C^2} \\
(V_3 H_3 V_3)(k) &= \frac{g_{AA}g_{AB}}{(p-k)^2 - m_C^2} \frac{1}{(k^2 - m_B^2)[(P-k)^2 - m_A^2]} \frac{g_{AA}g_{AB}}{(k-p')^2 - m_C^2} \\
(\overline{V}_3 H_3 V_3)(k) &= \frac{g_{AA}g_{AB}}{(P-p-k)^2 - m_C^2} \frac{1}{(k^2 - m_B^2)[(P-k)^2 - m_A^2]} \frac{g_{AA}g_{AB}}{(k-p')^2 - m_C^2}
\end{aligned}
$$
$$\tag{236}$$

shows that all of the box diagrams are functionally unique. The differences appear in the leftmost kernels where either $(p - k)$ or $(P - p - k)$ appears, and in the placement of the masses m_A and m_B in the propagators. In forming the total amplitude of $\mathcal{M}'_{11}$, there is no double counting of diagrams.
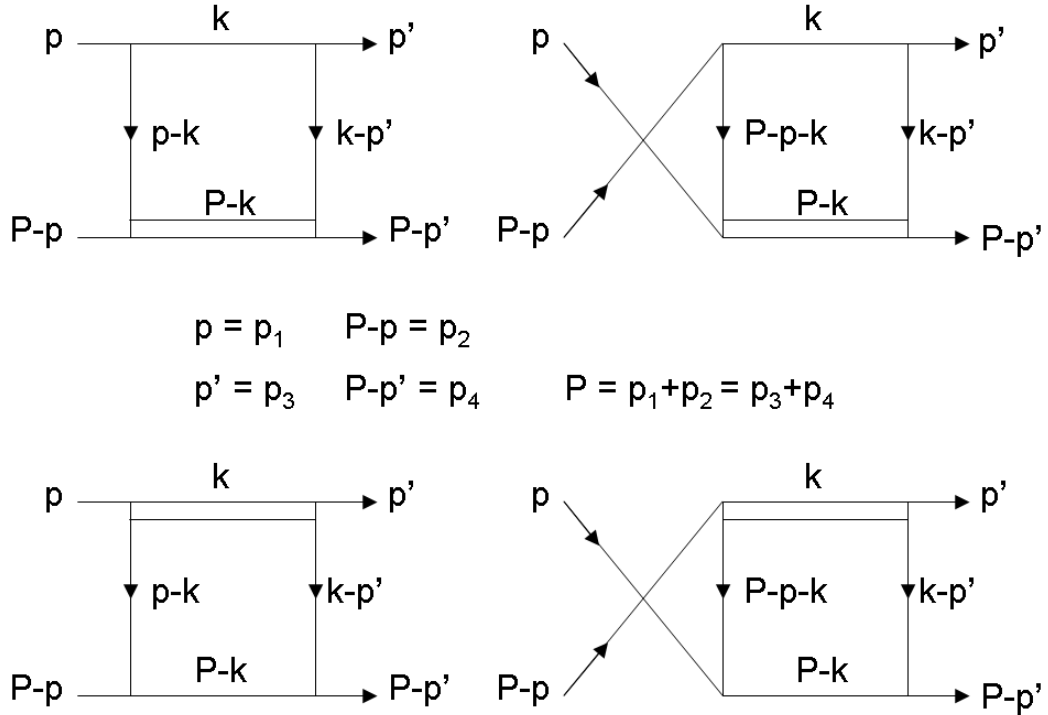
Figure 21: Direct and Exchange Box Diagrams.

4.14   Absence of $\mathcal{M}'_{12}$ Coupling in the CBSE

Since the amplitudes $\mathcal{M}'_{21}$ and $\mathcal{M}'_{31}$ are equivalent to the amplitudes $\mathcal{M}'_{12}$ and $\mathcal{M}'_{13}$ (by exchange and time reversal), they offer an alternate approach to determine the amplitude of the reaction $A + A \to A + B$. However, $\mathcal{M}'_{21}$ and $\mathcal{M}'_{31}$ are coupled to $\mathcal{M}'_{11}$, which is also coupled to $\mathcal{M}'_{41}$, so the reaction amplitude is found by simultaneous solution. Figure

22 shows the four semi-coupled equations at the top

$$
\begin{aligned}
\mathcal{M}'_{11} &= V_1 + V_1 H_1 \mathcal{M}'_{11} + V_2 H_2 \mathcal{M}'_{21} + V_3 H_3 \mathcal{M}'_{31} + V_4 H_4 \mathcal{M}'_{41} \\
\mathcal{M}'_{21} &= V_2 + V_2 H_1 \mathcal{M}'_{11} + V_4 H_3 \mathcal{M}'_{31} \\
\mathcal{M}'_{31} &= V_3 + V_3 H_1 \mathcal{M}'_{11} + V_4 H_2 \mathcal{M}'_{21} \\
\mathcal{M}'_{41} &= V_4 + V_4 H_1 \mathcal{M}'_{11}
\end{aligned}
\tag{237}
$$

and the time reversed versions at the bottom

$$
\begin{aligned}
\mathcal{M}'_{11} &= V_1 + \mathcal{M}'_{11} H_1 V_1 + \underline{\mathcal{M}'_{12} H_2 V_2} + \mathcal{M}'_{13} H_3 V_3 + \mathcal{M}'_{14} H_4 V_4 \\
\mathcal{M}'_{12} &= V_2 + \mathcal{M}'_{11} H_1 V_2 + \mathcal{M}'_{13} H_3 V_4 \\
\mathcal{M}'_{13} &= V_3 + \mathcal{M}'_{11} H_1 V_3 + \mathcal{M}'_{12} H_2 V_4 \\
\mathcal{M}'_{14} &= V_4 + \mathcal{M}'_{11} H_1 V_4
\end{aligned}
\tag{238}
$$

If $\mathcal{M}'_{12}$ is omitted from the time reversed equations (including the underlined term above and the component in the green dashed box in figure 22), the equations become the CBSE (compare figure 13 and equation (192)). Note that in time reversal, the amplitudes $\mathcal{M}'_{ij}$ on both the left and right hand sides are replaced by their time-reversed counterparts, that is, $\mathcal{M}'_{21} \rightarrow \mathcal{M}'_{12}$, $\mathcal{M}'_{31} \rightarrow \mathcal{M}'_{13}$ and $\mathcal{M}'_{41} \rightarrow \mathcal{M}'_{14}$. Going from (237) to (238) the order of V, H and $\mathcal{M}'_{ij}$ has been reversed to correspond to the order in the figure.

The time reversed equations can also be obtained by defining the GBSE in the alternate form

$$
\mathcal{M}' = U + \mathcal{M}' G U
\tag{239}
$$

in which the order of U, G and $\mathcal{M}'$ is the reverse of the order in (191).

From figure 22 it is clear that the CBSE lacks $\mathcal{M}'_{12}$ coupling in $\mathcal{M}'_{11}$, and is therefore a subset of the solution for the amplitude of the reaction $A + A \rightarrow A + B$ offered by (237).

The four semi-coupled equations of 2nd order $\mathcal{M}'$

The time-reversed equations. Remove the red-boxed component to obtain the CBSE.

Fassen and Tjon couple $\mathcal{M}'_{12}$ to $\mathcal{M}'_{13}$ implicitly defining the fourth equation by exchange equivalence

$$\mathcal{M}'_{12} = \varepsilon \, \mathcal{M}'_{13}$$

Figure 22: The CBSE as a subset of the time-reversed four coupled equations.

4.15 The Complete Solution of $\mathcal{M}'$

At the end of section 4.11.2, an approach was discussed to obtain the amplitude of the reaction $A + A \rightarrow A + B$ from element $\mathcal{M}'_{12}$. Another approach is to solve (229), which determines element $\mathcal{M}'_{21}$. This equation is coupled to (228), so to obtain the desired amplitude the two equations must be solved simultaneously. A comparison of the two approaches reveals that the latter contains the propagator H_4 (BB propagation), while the former does not. This demonstrates that the two solutions are not equivalent, since one solution generates ladders containing H_4, while the other does not. But the amplitudes $\mathcal{M}'_{12}$ and $\mathcal{M}'_{21}$ must be equivalent since both describe the same reaction under time reversal. The deficiency in the solutions given by sets of coupled equations such as (212) is that these sets of equations are drawn from the 2nd order $\mathcal{M}'$, which is a subset of $\mathcal{M}'$. In the 2nd order $\mathcal{M}'$, seven of the elements are zero. However, as program *CalcGBSE* demonstrates, already by the first iteration, these seven elements begin to acquire 4th order content, and feed it back to the other nine elements, so that by the 2nd iteration, 6th order terms containing H_4 appear in the elements $\mathcal{M}'_{12}$ and $\mathcal{M}'_{21}$. Clearly, the complete solution of $\mathcal{M}'$ involves solving for all sixteen elements of $\mathcal{M}'$ simultaneously, seven of which are unique since the

equivalence relations (203) still apply. The solution may be written as sixteen equations

$$
\begin{aligned}
\mathcal{M}'_{11} &= V_1 + V_1 H_1 \mathcal{M}'_{11} + V_2 H_2 \mathcal{M}'_{21} + V_3 H_3 \mathcal{M}'_{31} + V_4 H_4 \mathcal{M}'_{41} \\
\mathcal{M}'_{12} &= V_2 + V_1 H_1 \mathcal{M}'_{12} + V_2 H_2 \mathcal{M}'_{22} + V_3 H_3 \mathcal{M}'_{32} + V_4 H_4 \mathcal{M}'_{42} \\
\mathcal{M}'_{13} &= V_3 + V_1 H_1 \mathcal{M}'_{13} + V_2 H_2 \mathcal{M}'_{23} + V_3 H_3 \mathcal{M}'_{33} + V_4 H_4 \mathcal{M}'_{43} \\
\mathcal{M}'_{14} &= V_4 + V_1 H_1 \mathcal{M}'_{14} + V_2 H_2 \mathcal{M}'_{24} + V_3 H_3 \mathcal{M}'_{34} + V_4 H_4 \mathcal{M}'_{44} \\
\mathcal{M}'_{21} &= V_2 + V_2 H_1 \mathcal{M}'_{11} + V_4 H_3 \mathcal{M}'_{31} \\
\mathcal{M}'_{22} &= V_2 H_1 \mathcal{M}'_{12} + V_4 H_3 \mathcal{M}'_{13} \\
\mathcal{M}'_{23} &= V_4 + V_3 H_1 \mathcal{M}'_{13} + V_4 H_3 \mathcal{M}'_{33} \\
\mathcal{M}'_{24} &= V_2 H_1 \mathcal{M}'_{14} + V_4 H_3 \mathcal{M}'_{34} \\
\mathcal{M}'_{31} &= V_3 + V_3 H_1 \mathcal{M}'_{11} + V_4 H_2 \mathcal{M}'_{21} \\
\mathcal{M}'_{32} &= V_4 + V_3 H_1 \mathcal{M}'_{12} + V_4 H_2 \mathcal{M}'_{22} \\
\mathcal{M}'_{33} &= V_3 H_1 \mathcal{M}'_{13} + V_4 H_2 \mathcal{M}'_{23} \\
\mathcal{M}'_{34} &= V_2 H_1 \mathcal{M}'_{14} + V_4 H_2 \mathcal{M}'_{24} \\
\mathcal{M}'_{41} &= V_4 + V_4 H_1 \mathcal{M}'_{11} \\
\mathcal{M}'_{42} &= V_4 H_1 \mathcal{M}'_{12} \\
\mathcal{M}'_{43} &= V_3 H_1 \mathcal{M}'_{13} \\
\mathcal{M}'_{44} &= V_4 H_1 \mathcal{M}'_{14} \tag{240}
\end{aligned}
$$

which can be reduced in the same manner as for the nine equations of section 4.11.2. The sixteen equations were found using program *fullMprime.nb*, which is listed in section 6.3. The solutions drawn from the 2nd order $\mathcal{M}'$ and forming subsets of the sixteen coupled equations are approximate solutions, accurate to 4th order.

4.16 The 3-Vertex Scalar Model

At energies above the $\Delta 1600$ threshold, the BBC vertex appears and the double pion propagator G_C^C becomes active, opening a new channel through which interactions can

97

proceed. The 3-vertex Hamiltonian

$$\mathcal{H}_I \;=\; AAC + ABC + BBC$$

describes the interactions. Faassen and Tjon [2] disregard the $\Delta\Delta$ vertex due to uncertainties about its form. Nevertheless, this vertex begins to contribute at 2nd order for interaction energies above the $\Delta1600$ threshold. In *The Review of Particle Physics* ([36], pages 998-1018) Baryon Particle Listings, the decay process $\Delta \to \Delta + \pi$ is indicated for all of the Δ baryons except the lightest, the $\Delta1232$ baryon. This decay is described by the BBC vertex.

By continuing to restrict the model to C-kernels (pion exchange), the number of propagators remains at 4 (G_A^A, G_A^B, G_B^A and G_B^B) and $\mathcal{M}'$ remains a 4×4 matrix. However, with the inclusion of the BBC vertex, all sixteen elements of the 2nd order $\mathcal{M}'$ become populated. $\mathcal{M}'$ generates sixteen equations involving the sixteen amplitudes $\mathcal{M}'_{ij}$, which consist of seven unique amplitudes given by (203)

$$
\begin{aligned}
\mathcal{M}_{11} & \\
\mathcal{M}_{12} &= \mathcal{M}_{21} = \mathcal{M}_{13} = \mathcal{M}_{31} \\
\mathcal{M}_{14} &= \mathcal{M}_{41} \\
\mathcal{M}_{24} &= \mathcal{M}_{42} = \mathcal{M}_{34} = \mathcal{M}_{43} \\
\mathcal{M}_{22} &= \mathcal{M}_{33} \\
\mathcal{M}_{32} &= \mathcal{M}_{23} \\
\mathcal{M}_{44} &
\end{aligned}
\tag{241}
$$

By including the two kernels U_A and U_B, five more propagators G_A^C, G_C^A, G_B^C, G_C^B and G_C^C come into play, bringing the number of propagators to nine. In this model $\mathcal{M}'$ becomes a 9×9 matrix, but only 24 of the elements in the 2nd order $\mathcal{M}'$ are non-zero. The remaining elements become non-zero only by including the vertices $AAB = NN\Delta$, $BBA = \Delta\Delta N$, $ACC = N\pi\pi$ and $BCC = \Delta\pi\pi$, but these vertices are ruled out since they do not conserve

baryon number.

With the three vertices and three kernels, the 2nd order $\mathcal{M}'$ depicted in figure 23 generates 24 equations involving 24 amplitudes $\mathcal{M}'_{ij}$ consisting of 11 unique amplitudes, seven given by (241), and four more that accompany the introduction of the BBC vertex and A and B kernels

$$
\begin{aligned}
\mathcal{M}_{65} &= \mathcal{M}_{56} \\
\mathcal{M}_{71} &= \mathcal{M}_{17} \\
\mathcal{M}_{74} &= \mathcal{M}_{47} \\
\mathcal{M}_{87} &= \mathcal{M}_{78}
\end{aligned}
$$

The complete 3-vertex $\mathcal{M}'$ generates 81 equations involving 81 amplitudes, 27 of which are unique, about five times as many elements as the 2-vertex $\mathcal{M}'$, but only about four times as many unique elements. In figure 23, the elements of the 2-vertex $\mathcal{M}'$ are highlighted yellow. The elements added by the inclusion of the BBC vertex are highlighted green. The elements added by the inclusion of the A and B kernels are highlighted blue. Note how the restriction to C-kernels reduces $\mathcal{M}'$ to a 4×4 matrix.

In the scalar model of nucleon interactions, the A and B kernels represent nucleon and Δ baryon exchange particles, which lend *nucleon* and Δ *baryon* degrees of freedom to the model (see section 1.5 for a brief discussion of degrees of freedom). For the moment, we lump these two degrees of freedom together and call them *baryon* degrees of freedom. For the inelastic reaction $A + A \rightarrow A + B$ ($N + N \rightarrow N + \Delta$), *the baryon degrees of freedom begin to contribute at 6th order*, as demonstrated by program *3VertexMprime*. The program is listed in section 6.4, along with its output file. Since the meson and isobar degrees of freedom begin to contribute at 2nd order, the baryon degrees of freedom are clearly dominated by the former. We should emphasize that this observation is made from the standpoint of the scalar model.

Figure 23: 2nd Order $\mathcal{M}'$ in the 3-Vertex Model.

100

4.17 Equivalence of $\mathcal{M}'$ and S in the 2-vertex Model

In the GBSE, $\mathcal{M}'$ sums ladder diagrams of all orders $2n$, $n = 1, 2, \ldots$, beginning with the 2nd order one-rung ladders. The S-matrix, on the other hand, sums diagrams of all types, not just ladders, to all orders. To show the equivalence of $\mathcal{M}'$ and S, we must first extract the ladder diagrams from S, then show that $\mathcal{M}'$ and S produce equivalent series' of ladder diagrams. Before proceeding with the proof, we first establish a simple criterion for equivalence, and devise a notation with which to compare the two series.

4.17.1 Coupling Content of $\mathcal{M}'$

At the end of section 4.9 we introduced a simplified notation for $\mathcal{M}'$ by hiding the integrations in (189) to obtain (191)

$$\mathcal{M}' = U + UG\mathcal{M}' = U + UGU + UGUGU + \ldots = \sum_{n=1}^{\infty} U^n G^{n-1} \qquad (242)$$

In the 2-vertex model, restricting our considerations to C-rungs, U is defined by

$$U = \frac{\mathcal{U}}{q_C^2 - m_C^2} \qquad (243)$$

where the coupling matrix $\mathcal{U}$ is given by

$$\mathcal{U} = \begin{pmatrix} g_{AA}^2 & g_{AA}g_{AB} & g_{AA}g_{AB} & g_{AB}^2 \\ g_{AA}g_{AB} & 0 & g_{AB}^2 & 0 \\ g_{AA}g_{AB} & g_{AB}^2 & 0 & 0 \\ g_{AB}^2 & 0 & 0 & 0 \end{pmatrix} \qquad (244)$$

Also, G is given by

$$\begin{aligned} G &= G_1 + G_2 + G_3 + G_4 \\ &= \begin{pmatrix} 1/D_1 & 0 & 0 & 0 \\ 0 & 1/D_2 & 0 & 0 \\ 0 & 0 & 1/D_3 & 0 \\ 0 & 0 & 0 & 1/D_4 \end{pmatrix} \end{aligned} \qquad (245)$$

with propagator denominators

$$
\begin{aligned}
D_1 &= (k^2 - m_A^2)[(P-k)^2 - m_A^2] \\
D_2 &= (k^2 - m_A^2)[(P-k)^2 - m_B^2] \\
D_3 &= (k^2 - m_B^2)[(P-k)^2 - m_A^2] \\
D_4 &= (k^2 - m_B^2)[(P-k)^2 - m_B^2]
\end{aligned}
\tag{246}
$$

If we hide the denominator in U so that $U = \mathcal{U}$, and hide the denominators in G so that $G = I$ is the unit 4×4 matrix, we obtain an even more economical shorthand notation, with which (242) becomes

$$
\mathcal{M}' = \mathcal{U} + \mathcal{U}^2 + \mathcal{U}^3 + \ldots = \sum_{n=1}^{\infty} \mathcal{U}^n
\tag{247}
$$

Equation (247) states that the ladder content of $\mathcal{M}'$ is defined by the coupling content of $\mathcal{U}$. As we shall see, with coupling in hand, the ladders can be recreated, along with the hidden integrations and denominators. The denominators, although vital components of $\mathcal{M}'$, are nevertheless redundant with regard to definition of the ladder content. We shall use coupling content as the measure of ladder content for comparing $\mathcal{M}'$ and S.

In wielding the shorthand notation of (247) one must not blindly compute products of coupling factors, which in and of themselves do not specify the order in which vertices appear in the ladders. The shorthand $\mathcal{U}^n$ explicitly determines products of coupling factors, but implicitly determines the concatenation of one-rung, C-exchange, t-channel diagrams into n-rung ladder diagrams whose spans form two-particle propagators. Each of the one-rung ladders is completely specified by an element of $\mathcal{U}$, a two-vertex coupling factor. With this understanding, coupling content in the form of $\mathcal{U}^n$ equates to ladder content.

4.17.2 Ladder and Coupling Content of S

To demonstrate the equivalence of $\mathcal{M}'$ and S, the vertex coupling factors of the ladder diagrams must be extracted from S and compared to the coupling content of $\mathcal{M}'$ given by (247). Since $\mathcal{M}'$ in (247) generates "direct" ladder diagrams, it is sufficient to extract

only the direct ladders from S. If the series of direct ladders generated by $\mathcal{M}'$ and S are equivalent, the series of exchange ladders will also be equivalent since the exchange diagrams mirror the direct diagrams.

We begin by determining the vertex coupling content of S_2, the 2nd order term of S. The coupling content of S_2 takes the form of a 4×4 matrix of which the sixteen elements define the coupling for sixteen different reactions. S_2 generates the first ladders in the series, the one rung ladders. The one rung ladders are 2nd order, C-exchange, t-channel diagrams. Having determined the coupling of the one-rung ladders, we proceed to the two-rung ladders generated by S_4. These ladders are 4th order diagrams, also known as box diagrams. The two-rung ladders are shown to be formed by the conjunction of two one-rung ladders, where the final state of the first matches the initial state of the second, so that when joined an H propagator is formed. The coupling content of S_4 is shown to be equivalent to the matrix product of the coupling content of two S_2 matrices. Having extended the analysis from 2nd to 4th order, the way becomes immediately clear for extension to all orders of ladder diagrams, and the equivalence of $\mathcal{M}'$ and S is quickly shown.

The 2-vertex model is based on the Hamiltonian

$$\mathcal{H} \;=\; g_{AA}\,AAC + g_{AB}\,ABC \;=\; AAC + ABC \tag{248}$$

using a shorthand on right hand side that hides the coupling constants. Equation (248) defines two vertices AAC and ABC. Each vertex is labeled by the fields that interact at the vertex. The S-matrix term S_2 contains a time-ordered product of two Hamiltonians

$$\begin{aligned}
S_2 \;&=\; (-i)^2 \int d^4x_1 d^4x_2 \frac{T}{2!}\{\mathcal{H}(x_1)\mathcal{H}(x_2)\} \\
&=\; (-i)^2 \int d^4x_1 d^4x_2 \frac{T}{2!}\{(AAC + ABC)_1(AAC + ABC)_2\}
\end{aligned} \tag{249}$$

Simplifying the notation in a manner similar to that introduced for $\mathcal{M}'$ in section 4.9, we hide the integral

$$(-i)^2 \int d^4x_1 d^4x_2 \tag{250}$$

103

and write

$$S_2 \;=\; \frac{T}{2!}\{\mathcal{H}(x_1)\mathcal{H}(x_2)\} \;=\; \frac{T}{2!}\{\mathcal{H}^2\} \tag{251}$$

S_2 is a matrix, each element of which defines a set of 2nd order diagrams. This was shown in section 2.4.2 for the reaction $A + A \rightarrow A + B$, where, using the reduced notation of (251), the matrix element

$$\langle AB|S_2|AA \rangle \;=\; \langle AB|\frac{T}{2!}\{(AAC + ABC)_1(AAC + ABC)_2\}|AA \rangle \tag{252}$$

yielded three fully contracted terms corresponding to the three diagrams shown in figure 2, the s, t and u channel diagrams. S_2 is seen to be a 4×4 matrix whose elements give diagrams of all types for the sixteen reactions of the 2-vertex model.

Let us now define Q as the subset of S that includes only the ladder diagrams

$$Q \;=\; S, \text{ ladders only}$$

$$Q_2 \;=\; S_2, \text{ one-rung ladders only}$$

$$Q_{2n} \;=\; S_{2n}, \text{ n-rung ladders only}$$

$$Q \;=\; Q_2 + Q_4 + \ldots \;=\; \sum_{n=1}^{\infty} Q_n \tag{253}$$

Further, define box bracket vectors $\big[\,f\,\big|$ and $\big|\,i\,\big]$ and coupling matrix $\mathcal{F}$ such that the element

$$\mathcal{F}_{if} \;=\; \big[\,f\,\big|\,S_2\,\big|\,i\,\big] \tag{254}$$

equals the 2-vertex coupling factor of a one-rung ladder, specifically the 2nd order, C-exchange, t-channel diagram with initial state i and final state f. Both i and f range over the values $\{1, 2, 3, 4\}$. The four initial state vectors are

$$\big|\,1\,\big] \;=\; \big|\,AA\,\big]$$

$$\big|\,2\,\big] \;=\; \big|\,AB\,\big]$$

$$\big|\,3\,\big] \;=\; \big|\,BA\,\big]$$

$$\big|\,4\,\big] \;=\; \big|\,BB\,\big] \tag{255}$$

As an example using the box brackets, we calculate the element $\mathcal{F}_{if}$ for the reaction $A+A \rightarrow A+B$. The initial and final state vectors are $\left|1\right] = \left|AA\right]$ and $\left[2\right| = \left[AB\right|$, respectively. Then

$$
\begin{aligned}
\mathcal{F}_{12} &= \left[2\left|\frac{T}{2!}S_2\right|1\right] = \left[AB\left|\frac{T}{2!}S_2\right|AA\right] \\
&= \left[AB\left|\frac{T}{2!}\{\mathcal{H}^2\}\right|AA\right] \\
&= \left[AB\left|\frac{T}{2!}\{(AAC+ABC)_1(AAC+ABC)_2\}\right|AA\right] \\
\mathcal{F}_{12} &= \left[AB\left|\frac{T}{2!}\{(AAC)_1(ABC)_2 + (ABC)_1(AAC)_2\}\right|AA\right] \quad\quad (256)
\end{aligned}
$$

where we have dropped the terms $(ABC)_1(ABC)_2$ and $(AAC)_1(AAC)_2$ since these do not fully contract with the given initial and final states and therefore do not contribute. Applying the usual Wick/Peskin contractions gives six fully contracted terms, two each for the s, t and u-channel diagrams. But the box brackets are defined to extract the coupling factor for only the t-channel diagrams, so we drop the s and u channel diagrams, leaving the two identical t-channel diagrams. The duplicity is removed by the factor of $1/2!$, leaving the coupling factor for a single t-channel diagram

$$
\mathcal{F}_{12} = g_{AA}g_{AB} \quad\quad (257)
$$

Using the method of the preceding example, the other fifteen elements of $\mathcal{F}$ are found, with the result

$$
\mathcal{F} = \mathcal{U} = \begin{pmatrix} g_{AA}^2 & g_{AA}g_{AB} & g_{AA}g_{AB} & g_{AB}^2 \\ g_{AA}g_{AB} & 0 & g_{AB}^2 & 0 \\ g_{AA}g_{AB} & g_{AB}^2 & 0 & 0 \\ g_{AB}^2 & 0 & 0 & 0 \end{pmatrix} \quad\quad (258)
$$

The $\mathcal{F}$ matrix is precisely the $\mathcal{U}$ coupling matrix of the GBSE, which should come as no surprise, having seen in previous sections that $\mathcal{U}$ can be read directly from the 2nd order $\mathcal{M}'$ (see figure 17), the latter being equivalent to Q_2 in ladder content. Analogous to (247), we may write Q_2 simply as

$$
Q_2 = \mathcal{F} \quad\quad (259)
$$

which states that the one-rung ladder content of Q_2 is defined by the coupling content of $\mathcal{F}$. For example the coupling factor

$$\left[\, AB \,\middle|\, Q_2 \,\middle|\, AA \,\right] \;=\; \left[\, AB \,\middle|\, \mathcal{F} \,\middle|\, \mathcal{AA} \,\right] \;=\; g_{AA}g_{AB} \tag{260}$$

defines the two-vertex, C-exchange, t-channel diagram with initial state particles A_1 and A_2 and final state particles A_3 and B_4. Being a t-channel diagram, particles A_1 and A_3 share a vertex, and particles A_2 and B_4 share the other vertex.

Having determined the coupling content of Q_2 we proceed to Q_4

$$
\begin{aligned}
S_4 \quad &= \quad \frac{T}{4!}\{\mathcal{H}_1\mathcal{H}_2\mathcal{H}_3\mathcal{H}_4\} \;=\; \frac{1}{24} \times \{ \\
(1st) \quad &\mathcal{H}_1\mathcal{H}_2\mathcal{H}_3\mathcal{H}_4 + \\
(2nd) \quad &\mathcal{H}_1\mathcal{H}_2\mathcal{H}_4\mathcal{H}_3 + \\
&\mathcal{H}_1\mathcal{H}_3\mathcal{H}_2\mathcal{H}_4 + \mathcal{H}_1\mathcal{H}_4\mathcal{H}_2\mathcal{H}_3 + \\
&\mathcal{H}_1\mathcal{H}_3\mathcal{H}_4\mathcal{H}_2 + \mathcal{H}_1\mathcal{H}_4\mathcal{H}_3\mathcal{H}_2 + \\
(7th) \quad &\mathcal{H}_2\mathcal{H}_1\mathcal{H}_3\mathcal{H}_4 + \\
(8th) \quad &\mathcal{H}_2\mathcal{H}_1\mathcal{H}_4\mathcal{H}_3 + \\
&\mathcal{H}_3\mathcal{H}_1\mathcal{H}_2\mathcal{H}_4 + \mathcal{H}_4\mathcal{H}_1\mathcal{H}_2\mathcal{H}_3 + \\
&\mathcal{H}_3\mathcal{H}_1\mathcal{H}_4\mathcal{H}_2 + \mathcal{H}_4\mathcal{H}_1\mathcal{H}_3\mathcal{H}_2 + \\
&\mathcal{H}_2\mathcal{H}_3\mathcal{H}_1\mathcal{H}_4 + \mathcal{H}_2\mathcal{H}_4\mathcal{H}_1\mathcal{H}_3 + \\
&\mathcal{H}_3\mathcal{H}_2\mathcal{H}_1\mathcal{H}_4 + \mathcal{H}_4\mathcal{H}_2\mathcal{H}_1\mathcal{H}_3 + \\
&\mathcal{H}_3\mathcal{H}_4\mathcal{H}_1\mathcal{H}_2 + \mathcal{H}_4\mathcal{H}_3\mathcal{H}_1\mathcal{H}_2 + \\
&\mathcal{H}_2\mathcal{H}_3\mathcal{H}_4\mathcal{H}_1 + \mathcal{H}_2\mathcal{H}_4\mathcal{H}_3\mathcal{H}_1 + \\
&\mathcal{H}_3\mathcal{H}_2\mathcal{H}_4\mathcal{H}_1 + \mathcal{H}_4\mathcal{H}_2\mathcal{H}_3\mathcal{H}_1 + \\
&\mathcal{H}_3\mathcal{H}_4\mathcal{H}_2\mathcal{H}_1 + \mathcal{H}_4\mathcal{H}_3\mathcal{H}_2\mathcal{H}_1\}
\end{aligned} \tag{261}
$$

T operates on $\{\mathcal{H}_1\mathcal{H}_2\mathcal{H}_3\mathcal{H}_4\}$ to produce the 24 different time ordered products shown above, where the right-to-left order of indices indicates order in time. However, since the integrals

in the S-matrix

$$\int_{-\infty}^{+\infty} d^4x_1 \int_{-\infty}^{+\infty} d^4x_2 \int_{-\infty}^{+\infty} d^4x_3 \int_{-\infty}^{+\infty} d^4x_4 \tag{262}$$

range over time $-\infty < t < \infty$, the diagrams produced by any one of the time ordered products are equivalent to those of any other product, the only difference being in the assignment of dummy labels 1, 2, 3 and 4 to the vertices in the diagrams. Collectively, the 24 time ordered products produce 24 identical sets of diagrams. The factor of $1/24$ in S_4 cancels the multiplicity, leaving one set of diagrams. Now consider the expansion of time ordered products

$$\begin{aligned}
\frac{T}{2!}\{\mathcal{H}^2\}\frac{T}{2!}\{\mathcal{H}^2\} &= \frac{1}{4} \times \{ \\
&\mathcal{H}_1\mathcal{H}_2\mathcal{H}_3\mathcal{H}_4 + \\
&\mathcal{H}_1\mathcal{H}_2\mathcal{H}_4\mathcal{H}_3 + \\
&\mathcal{H}_2\mathcal{H}_1\mathcal{H}_3\mathcal{H}_4 + \\
&\mathcal{H}_2\mathcal{H}_1\mathcal{H}_4\mathcal{H}_3 \}
\end{aligned} \tag{263}$$

The four time ordered products are identical to the 1st, 2nd, 7th and 8th time ordered products appearing in the preceding equation. The four time ordered products produce four equivalent sets of diagrams. The factor of $1/4$ cancels the multiplicity, leaving one set of diagrams. We may therefore write

$$\frac{T}{4!}\{\mathcal{H}^4\} = \frac{T}{2!}\{\mathcal{H}^2\}\frac{T}{2!}\{\mathcal{H}^2\} \tag{264}$$

The left hand side produces 24 equivalent sets of diagrams, divided by 24. The right hand side produces four equivalent sets of diagrams, divided by 4. Both sides produce the same set of diagrams, so we may write

$$\left[\,f\,|\,S_4\,|\,i\,\right] = \left[\,f\,|\,\frac{T}{2!}\{\mathcal{H}^2\}\frac{T}{2!}\{\mathcal{H}^2\}\,|\,i\,\right] \tag{265}$$

To evaluate (265) we employ the ortho-normality and completeness relations

$$\left[\,f\,|\,i\,\right] = \delta_{if} \tag{266}$$

107

and

$$I \;=\; \sum_{k=1}^{4} |k] [k| \tag{267}$$

where I is the unit 4×4 matrix. Inserting I into (265)

$$
\begin{aligned}
[f|S_4|i] &= [f|\frac{T}{2!}\{\mathcal{H}^2\}\,(I)\,\frac{T}{2!}\{\mathcal{H}^2\}|i] \\
&= [f|\frac{T}{2!}\{\mathcal{H}^2\}\left(\sum_{k=1}^{4}|k][k|\right)\frac{T}{2!}\{\mathcal{H}^2\}|i] \\
&= \sum_{k=1}^{4}\frac{T}{2!}\{[f|\mathcal{H}^2|k]\}\frac{T}{2!}\{[k|\mathcal{H}^2|i]\}
\end{aligned}
\tag{268}
$$

and comparing to the second line of (256) we see that

$$
\begin{aligned}
\frac{T}{2!}\{[f|\mathcal{H}^2|k]\} &= \mathcal{F}_{kf} \\
\frac{T}{2!}\{[k|\mathcal{H}^2|i]\} &= \mathcal{F}_{ik}
\end{aligned}
\tag{269}
$$

so that $[f|S_4|i]$ becomes

$$[f|S_4|i] \;=\; \sum_{k=1}^{4}\mathcal{F}_{kf}\,\mathcal{F}_{ik} \;=\; (Q_4)_{if} \tag{270}$$

which is the definition of the matrix product

$$Q_4 \;=\; \mathcal{F}\mathcal{F} \;=\; \mathcal{F}^2 \tag{271}$$

As previously defined, Q_4 consists of the ladder diagrams of S_4. Equation (271) states that the ladder content of Q_4 is defined by the coupling content of $\mathcal{F}^2$. In (270) the coupling factor $\mathcal{F}_{kf}$ represents a one-rung ladder with initial state k, while the coupling factor $\mathcal{F}_{ik}$ represents a one-rung ladder with final state k. The product of the two factors represents a two-rung ladder formed by the conjunction of the one-rung ladders. The joining of the one-rung ladders is possible because the final state of one matches the initial state of the other. The joint forms the propagator H_k defined by state k.

The result (271) is easily generalized to

$$Q_{2n} \;=\; \mathcal{F}^n \tag{272}$$

since the same arguments used to show (264) may be used to show

$$\frac{T}{(2n)!}\{\mathcal{H}^{2n}\} = \left(\frac{T}{(2)!}\{\mathcal{H}^2\}\right)^n \tag{273}$$

Consequently

$$Q = Q_2 + Q_4 + \ldots = \sum_{n=1}^{\infty} Q_{2n} = \mathcal{F} + \mathcal{F}^2 + \ldots = \sum_{n=1}^{\infty} \mathcal{F}^n \tag{274}$$

Since by (258) $\mathcal{F} = \mathcal{U}$, the equivalence of $\mathcal{M}'$ and S is established by (247) and (253)

$$S, \text{ ladders only} = Q = \sum_{n=1}^{\infty} \mathcal{U}^n = \mathcal{M}' \tag{275}$$

The coupling content of $\mathcal{M}'$ is equivalent to that of Q, therefore the ladder content of $\mathcal{M}'$ is equivalent to that of S.

4.18 Equivalence of $\mathcal{M}'$ and S for Multiple Exchange Particles

In section 4.4 a form of the GBSE was given for case of N_U exchange particles C_i. In this section we prove the equivalence of the ladder series generated by the "multi-C" GBSE to that of the S-matrix. The proof follows the procedure of section 4.17 which dealt with the case of one type of exchange particle. We let coupling content represent the ladder content for both $\mathcal{M}'$ and S, then show that the two are equivalent in coupling content.

The multi-C GBSE is given by (158)

$$\mathcal{M}_{rs} = \widetilde{\mathbf{u}}_r \, \mathcal{M}' \, \mathbf{v}_s$$
$$\mathcal{M}' = U + \int_k UG\mathcal{M}' \tag{276}$$

where the kernel U is the sum of N_U kernels (156)

$$U = \sum_{i=1}^{N_U} U_i$$
$$U_i = \frac{\mathcal{U}_i}{q_i^2 - m_i^2} \tag{277}$$

For the 3-vertex Hamiltonian, the coupling matrices $\mathcal{U}_i$ are fully populated

$$\mathcal{U}_i = \begin{pmatrix} g_{AAi}^2 & g_{AAi}g_{ABi} & g_{AAi}g_{ABi} & g_{ABi}^2 \\ g_{AAi}g_{ABi} & g_{AAi}g_{BBi} & g_{ABi}^2 & g_{BBi}g_{ABi} \\ g_{AAi}g_{ABi} & g_{ABi}^2 & g_{AAi}g_{BBi} & g_{BBi}g_{ABi} \\ g_{ABi}^2 & g_{BBi}g_{ABi} & g_{BBi}g_{ABi} & g_{BBi}^2 \end{pmatrix} \tag{278}$$

The subscript i labels the coupling constants for vertices involving exchange particle C_i. The propagator G is given by (279)

$$\begin{aligned} G &= G_1 + G_2 + G_3 + G_4 \\ &= \begin{pmatrix} 1/D_1 & 0 & 0 & 0 \\ 0 & 1/D_2 & 0 & 0 \\ 0 & 0 & 1/D_3 & 0 \\ 0 & 0 & 0 & 1/D_4 \end{pmatrix} \end{aligned} \tag{279}$$

in which the denominators D_j are given by (246). Letting the coupling matrices $\mathcal{U}_i$ define the ladders (as done in section 4.17 for the case of a single kernel), we hide the integral operator in (276) and the denominators in the U_i and G_i, so that $U_i = \mathcal{U}_i$ and $G = I$, the unit 4×4 matrix. Then (276) becomes

$$\begin{aligned} \mathcal{M}' &= U + UG\mathcal{M}' = U + U\mathcal{M}' = U + U^2 + U^3 + \dots \\ &= \sum_{k=1}^{\infty} U^k = \sum_{k=1}^{\infty} \left(\sum_{i=1}^{N_U} \mathcal{U}_i \right)^k = \sum_{k=1}^{\infty} \mathcal{M}'_{2k} \\ \mathcal{M}'_{2k} &= \left(\sum_{i=1}^{N_U} \mathcal{U}_i \right)^k \end{aligned} \tag{280}$$

Equation (280) states that the ladder content of $\mathcal{M}'$ is defined by the coupling matrices $\mathcal{U}_i$. The 2nd order coupling content is given by

$$\mathcal{M}'_2 = \sum_{i=1}^{N_U} \mathcal{U}_i \tag{281}$$

the 4th order content by

$$\mathcal{M}'_4 = \left(\sum_{i=1}^{N_U} \mathcal{U}_i \right)^2 \tag{282}$$

and so forth.

We now determine the coupling content of S for ladders comprised of C-rungs, first evaluating S_2 and S_4, and generalizing to S_{2k}. From (155), the Hamiltonian is

$$\mathcal{H} = \sum_{i=1}^{N_U} \mathcal{H}_i$$
$$\mathcal{H}_i = g_{AAi}AAC_i + g_{ABi}ABC_i + g_{BBi}BBC_i \equiv AAC_i + ABC_i + BBC_i$$

$$(283)$$

Recycling the simplified notation of (251), the 2nd order term S_2 is

$$S_2 = \frac{T}{2!}\{\mathcal{H}^2\} = \frac{T}{2!}\{\left(\sum_{i=1}^{N_U}\mathcal{H}_i\right)^2\} = \frac{T}{2!}\{\left(\sum_{i=1}^{N_U}\mathcal{H}_i\right)\left(\sum_{j=1}^{N_U}\mathcal{H}_j\right)\}$$

$$= \frac{T}{2!}\{\sum_{i,j}^{N_U}\mathcal{H}_i\mathcal{H}_j\} \qquad (284)$$

For the Hamiltonian given by (283) the above product $\mathcal{H}_i\mathcal{H}_j$ produces terms containing the fields C_i and C_j. Take, for example, the term AAC_iABC_j

$$AA\overset{\lceil\quad\quad\rceil}{C_i\,AB}C_j \qquad (285)$$

Contracting the C fields produces a non-zero result only if $i = j$, when the two C fields represent the same type of meson. Consequently, (284) reduces to

$$S_2 = \frac{T}{2!}\{\sum_{i,j}^{N_U}\delta_{ij}\mathcal{H}_i\mathcal{H}_j\} = \frac{T}{2!}\{\sum_{i=1}^{N_U}\mathcal{H}_i^2\} = \sum_{i=1}^{N_U}S_{2i}$$

$$S_{2i} = \frac{T}{2!}\{\mathcal{H}_i^2\} \qquad (286)$$

Each term S_{2i} involves a single type of exchange particle C_i, and is therefore identical in form to the 2-vertex S_2 in (251). The box bracket notation used to transform (251) into (259) may be applied to (286) to show that

$$Q_{2i} = \mathcal{U}_i \qquad (287)$$

where Q_{2i} represents the 2nd order, C_i-rung ladder content of S_2. Gathering the N_U terms and comparing to (281) shows that

$$Q_2 = \sum_{i=1}^{N_U}\mathcal{U}_i = \mathcal{M}'_2 \qquad (288)$$

The coupling content of S_2 is equivalent to that of $\mathcal{M'}_2$, therefore the 2nd order ladder content is equivalent.

We proceed to evaluate the C-rung coupling content of S_4. Again using the simplified notation of (251), the 4nd order term S_4 is

$$S_4 \;=\; \frac{T}{4!}\{\mathcal{H}^4\} \;=\; \frac{T}{4!}\{\left(\sum_{i=1}^{N_U}\mathcal{H}_i\right)^4\} \;=\; \frac{T}{4!}\{\left(\sum_{i=1}^{N_U}\mathcal{H}_i\right)^2\left(\sum_{j=1}^{N_U}\mathcal{H}_j\right)^2\} \tag{289}$$

From (284) and (286) we have that

$$\left(\sum_{i=1}^{N_U}\mathcal{H}_i\right)^2 \;=\; \sum_{i=1}^{N_U}\mathcal{H}_i^2 \tag{290}$$

which upon substitution into (289) gives

$$S_4 \;=\; \frac{T}{4!}\{\sum_{i=1}^{N_U}\sum_{j=1}^{N_U}\mathcal{H}_i^2\mathcal{H}_j^2\} \;=\; \sum_{i=1}^{N_U}\sum_{j=1}^{N_U}\frac{T}{4!}\{\mathcal{H}_i^2\mathcal{H}_j^2\} \tag{291}$$

Following the same line of reasoning that led to (264), the set of 24 time ordered products divided by 24 on the left-hand side of

$$\frac{T}{4!}\{\mathcal{H}_i^2\mathcal{H}_j^2\} \;=\; \frac{T}{2!}\{\mathcal{H}_i^2\}\frac{T}{2!}\{\mathcal{H}_j^2\} \tag{292}$$

are equivalent to the 4 time ordered products divided by 4 on the right hand side. Now we apply the initial state $\lfloor r\rceil$ and final state $\lceil s\rfloor$ box bracket vectors to extract the coupling content of Q_4, which defines the ladder content of S_4. Inserting the completeness relation (267) gives

$$
\begin{aligned}
[s\,|\,Q_4\,|\,r] \;&=\; [s\,|\sum_{i=1}^{N_U}\sum_{j=1}^{N_U}\left[\frac{T}{2!}\{\mathcal{H}_i^2\}\left(\sum_{k=1}^{4}|k]\,[k|\right)\frac{T}{2!}\{\mathcal{H}_j^2\}\right]|\,r] \\
&=\; \sum_{i=1}^{N_U}\sum_{j=1}^{N_U}\sum_{k=1}^{4}[s\,|\frac{T}{2!}\{\mathcal{H}_i^2\}|\,k]\,[k\,|\frac{T}{2!}\{\mathcal{H}_j^2\}|\,r] \\
&=\; \sum_{i=1}^{N_U}\sum_{j=1}^{N_U}\sum_{k=1}^{4}(\mathcal{U}_i)_{sk}(\mathcal{U}_j)_{kr} \;=\; \sum_{i=1}^{N_U}\sum_{j=1}^{N_U}[s\,|\,\mathcal{U}_i\mathcal{U}_j\,|\,r]
\end{aligned} \tag{293}
$$

from which it is readily seen that

$$Q_4 = \sum_{i=1}^{N_U} \sum_{j=1}^{N_U} \mathcal{U}_i \mathcal{U}_j = \left(\sum_{i=1}^{N_U} \mathcal{U}_i \right)^2 = \mathcal{M'}_4 \tag{294}$$

By (282), the 4th order C-rung ladder content of $\mathcal{M'}$ is equivalent to that of S.

The result (294) is easily generalized to

$$Q_{2n} = \left(\sum_{i=1}^{N_U} \mathcal{U}_i \right)^n = \mathcal{M'}_{2n} \tag{295}$$

by recognizing that the conversion of time ordered products may be extended to order $2n$

$$\frac{T}{(2n)!} \{ \mathcal{H}_{i1}^2 \mathcal{H}_{i2}^2 \dots \mathcal{H}_{in}^2 \} = \frac{T}{2!} \{ \mathcal{H}_{i1}^2 \} \frac{T}{2!} \{ \mathcal{H}_{i2}^2 \} \dots \frac{T}{2!} \{ \mathcal{H}_{in}^2 \} \tag{296}$$

By summing (295) over all n and comparing to (280)

$$Q = \sum_{n=1}^{\infty} Q_{2n} = \sum_{n=1}^{\infty} \left(\sum_{i=1}^{N_U} \mathcal{U}_i \right)^n = \mathcal{M'} \tag{297}$$

we establish the equivalence of $\mathcal{M'}$ and S with respect to C-rung ladder content.

4.19   2nd Order $\mathcal{M'}$ and the S-Matrix

The nature of 2nd order $\mathcal{M'}$ as a collection of independent groups of coupled systems speaks to the nature of the S-matrix itself, being related to $\mathcal{M'}$ by (38)

$$\begin{aligned} S_{fi} &= \langle f|S|i \rangle \\ &= 1 + (2\pi)^4 \delta^4 (p_1 + p_2 - p_3 - p_4) i \mathcal{M}_{fi} \end{aligned}$$

A given interaction Lagrangian defines a set of vertices and lines (propagating particles), which in turn define a family of interaction processes. To 2nd order, the family of processes is separable into groups of coupled processes, so that solutions (amplitudes) of the S-matrix segregate into groups of coupled solutions. As shown in the preceding sections, some solutions are standalone, for example $\mathcal{M'}_{14}$, while other solutions participate in "cross-over" between groups: the coupled system consisting of $\mathcal{M'}_{12}$ and $\mathcal{M'}_{32}$, and the coupled system

consisting of $\mathcal{M}'_{11}$, $\mathcal{M}'_{21}$, $\mathcal{M}'_{31}$ and $\mathcal{M}'_{41}$ both give independent determinations of the amplitude of the process $A + A \rightarrow A + B$. A defining characteristic of the amplitudes within a "coupling" group is that they share a common final state. Invariance of amplitudes under time reversal tells us that the amplitudes can also be grouped by a common initial state. The two forms of the GBSE given by (127)

$$\mathcal{M}' = U + UG\mathcal{M}'$$

and by (239)

$$\mathcal{M}' = U + \mathcal{M}'GU$$

yield these two groupings of amplitudes.

4.20 Building the GBSE for Arbitrary Models

The GBSE is defined by its kernel U and propagator G, which contain the coupling matrices $\mathcal{U}_i$ and $\mathcal{G}_j$

$$U = \sum_i \frac{\mathcal{U}_i}{q_C^2 - m_C^2} \tag{298}$$

$$G = \sum_j \frac{\mathcal{G}_j}{D_j} \tag{299}$$

For an arbitrary particle interaction model, U and G are readily determined once the Lagrangian of the model is known. The Lagrangian defines a set of vertices. The vertices define the set of 2nd order diagrams (one rung ladders), which in turn define the 2nd order $\mathcal{M}'$ and the $\mathcal{U}$ coupling matrix. The set of initial states and final states that span the dual state space can be read from the one rung ladders. Restriction to particular types of kernels (rungs) can be imposed on $\mathcal{M}'$ and $\mathcal{U}$, eliminating rungs from particular elements of these matrices. Multiple exchange particles for particle reactions translate into sums of rungs for particular elements of the two matrices. The propagator G is found from $\mathcal{U}^2$, which forms all possible combinations of one-rung ladders into two-rung ladders. The denominators of

the G_i are read directly from the spans of the two-rung ladders. G is a diagonal matrix whose elements are the reciprocals of the denominators

$$(G)_{kk} \;\; = \;\; 1/D_k \tag{300}$$

This concludes the GBSE discussion. The next section discusses several follow-on research efforts for the continued development of the GBSE.

5 Future Work

The generalized Bethe-Salpeter equation (GBSE) developed in the present work is new, and introduces a systematic method for analyzing families of coupled reactions. The GBSE is formulated using scalar theory, and is applied primarily to a 3-particle, 2-vertex model. Formulations of the GBSE using complex scalar and spinor models immediately suggest themselves. Several other projects suggest themselves, ranging from validation of the scalar 2-vertex GBSE by numerical solution and comparison to experiment, to spinor field formulations based on many-particle, many-vertex Lagrangians. Four projects which further the development and application of the GBSE are briefly outlined below.

5.1 Numerical Solutions

Having formulated the GBSE to some detail using scalar theory, an important next step is validation. This can be achieved by carrying out numerical solutions of the scalar GBSE for particular reactions and comparing the results to experiment. One such application is the $N\Delta\pi$ system treated in the present work. Numerical techniques solve the BSE for the single function $\mathcal{M}$). These techniques may be adapted to solve the GBSE for the matrix of functions $\mathcal{M}'$. Of course, one need not solve for the complete $\mathcal{M}'$, but can seek an approximate solution for a particular reaction by solving a reduced set of coupled equations (see section 4.11.2). Since the introduction of the BSE by Bethe and Salpeter in 1951 [37], much effort has been devoted to developing techniques for numerical solution of the BSE [38, 39, 40, 41]. These techniques may be applied whole-cloth to the solution of the GBSE. In solving for the complete $\mathcal{M}'$, the techniques must be incorporated into a sparse matrix solution.

5.2 The 3-Vertex Model

The 3-vertex model, based on the Lagrangian $\mathcal{L} = AAC + ABC + BBC$, was discussed briefly in section 4.16. For the $N\Delta\pi$ system, the BBC vertex is the $\Delta\Delta\pi$ vertex. Faassen and Tjon

[2] omit this vertex, but inclusion of this vertex brings the isobar degree of freedom into full expression (see section 1.5). The scalar model, with its simple description of vertices, has the capacity to describe the $\Delta\Delta\pi$ interaction. In the 3-vertex model, $\mathcal{M}'$ is a 9×9 matrix, the solution of which involves 81 elements, 27 unique (many of the elements are equivalent under momentum exchange or time reversal, or both). For even more complex systems, one can expect the number of unique elements to increase, while $\mathcal{M}'$ becomes increasingly sparse.

5.3   The Complex Scalar Model

The GBSE may be formulated using complex scalar fields. Going from scalar to complex fields, the number of particles increases at least by a factor 2, while the number of reactions increases at least by a factor of 4, and the number of elements in $\mathcal{M}'$ increases at least by a factor of 16. As an example, the $N\Delta\pi$ system has 2 particles in the scalar model, the nucleon and the Δ baryon (not including the exchange pion), but has 12 particles in the complex scalar model: the proton, neutron, four Δ^i particles, and six corresponding anti-particles. The most general Lagrangian includes 21 interactions vertices, one for each pair of interacting particles pp, pn, $p\Delta^0$, ... nn, $n\Delta^0$... . There are $12 \times 12 = 144$ two-particle initial states, and the same number of final states. Thus $\mathcal{M}'$ is a 144×144 matrix. However many of the elements represent reactions that violate conservation of charge or baryon number, hence are zero. Since reactions involve charge transitions, numerical solutions will necessarily involve the isospin formalism. While the scalar model has only the neutral pion π^0, the complex scalar model also includes the charged pions π^- and π^+. The presence of additional exchange particles does not increase the size of $\mathcal{M}'$ in the 2-vertex model, but does increase the number of kernels.

5.4   The Spinor Model

The GBSE may be formulated using Dirac spinor fields. A review of BSE spinor studies is found in [42]. The number of particles will be the same as with the complex scalar

model, but reactions will additionally involve angular momentum transitions mediated by the exchange of vector mesons. The presence of vector mesons (in addition to the pseudo-scalar mesons found in the scalar and complex scalar theories) increases the number of kernels. Numerical solutions will involve the spin formalism. The GBSE is constructed in the same manner as is done for the scalar model (see section 4.20).

6 Appendix - Code Listings

This appendix lists C and Mathematica programs and output files used in the development of the GBSE.

6.1 Program *FindFeynmanDiagrams*

The .cpp source code file for program *FindFeynmanDiagrams* is listed below along with three output files *results.txt*, *terms.txt* and *diagrams.txt*. The *FindFeynmanDiagrams* procedure is described in section 4.8.

```
// Find Feynman Diagrams Keep Duplicates.cpp
// Generate the all 4th order Feynman diagrams for AAC+ABC+BBC Lagrangian.
// Author: Frank Dick, WPI, December 2006
// The method utilizes Wick contraction with external contractions (Peskin).

#include "stdafx.h"
// ABC' lagrangian = ABC + AAC + BBC, field types are A=1, B=2, C=3
int la[3][3]={{1,2,3},{1,1,3},{2,2,3}};

#define NOTUSED      -1
#define ADJACENT     1
#define AFIELD       1
#define BFIELD       2
#define CFIELD       3

#define NUMCOUPLE    3   // the number of fields coupled at a point
#define ORDER        4   // order of the diagrams
#define NUMTERMS     81  // equals NUMCOUPLE ^ ORDER

// initial and final states, ist = AA, fst = AB

// reaction AA to AA
/*
int ist[2] = {1,1};
int fst[2] = {1,1};
int numA = 4; // number of external A's
int numB = 0; // number of external B's
int numC = 0; // number of external C's
*/

// reaction AA to AB
```

```
int ist[2] = {1,1};
int fst[2] = {1,2};
int numA = 3; // number of external A's
int numB = 1; // number of external B's
int numC = 0; // number of external C's


// reaction AB to AB
/*
int ist[2] = {1,2};
int fst[2] = {1,2};
int numA = 2; // number of external A's
int numB = 2; // number of external B's
int numC = 0; // number of external C's
*/

// reaction AB to BA
/*
int ist[2] = {1,2};
int fst[2] = {2,1};
int numA = 2; // number of external A's
int numB = 2; // number of external B's
int numC = 0; // number of external C's
*/

// reaction AB to BB
/*
int ist[2] = {1,2};
int fst[2] = {2,2};
int numA = 1; // number of external A's
int numB = 3; // number of external B's
int numC = 0; // number of external C's
*/

// reaction AA to BB
/*
int ist[2] = {1,1};
int fst[2] = {2,2};
int numA = 2; // number of external A's
int numB = 2; // number of external B's
int numC = 0; // number of external C's
*/
```

```
// reaction BB to BB
/*
int ist[2] = {2,2};
int fst[2] = {2,2};
int numA = 0; // number of external A's
int numB = 4; // number of external B's
int numC = 0; // number of external C's
*/

int anum, // number of A fields in a term
    bnum, // number of B fields in a term
    cnum; // number of C fields in a term

int numcontracts;
int numdiagrams = 0;
int extconxdone = 0;

int goodcount;  // a count of the terms that match the external states

// 81 4th order terms, each with 12 fields plus the four external states
int term[NUMTERMS][16];  // unique terms
int numuniqueterms = 0;
int term0[NUMTERMS][17]; // raw terms, before duplicates are removed
int numterms = NUMTERMS;
// int termvert0[81][4]; // each term has 4 vertices
int termvert[NUMTERMS][4];

// field keeps track of contractions
int field[16]; // -1 (not connected) or num (connected to field num 0 thru 15)

// node indicates the vertex (1,2,3 or 4) at which a field resides
int node[12] = {1,1,1,2,2,2,3,3,3,4,4,4};

// counts of the various types of diagrams
int boxes = 0,
    beetles = 0,
    sbeetles = 0,
    bowties = 0,
    crosses = 0,
    triangles = 0,
    striangles = 0,
    split_loops = 0,
    biloops = 0,
```

```
    sbiloops = 0,
    others0 = 0,
    others1 = 0,
    others2 = 0,
    others3 = 0;

int boxprop[6],      // counts of five types of propagators
    crossprop[6];

#define AAPROP  1
#define ABPROP  2
#define BAPROP  3
#define BBPROP  4
#define CCPROP  5

int ibyxs0, ibyxs1, ibyxs2;

    FILE* fh;
    FILE* fh_terms;

void createterms(void);
int sameterm(int x, int y);
int  goodterm(int tnum);
void countfields(int t);
void contractext(int t, int f );
void contractintA(int t, int f );
void contractintB(int t, int f );
void contractintC(int t, int f );
void store( int t);
void findups(void);
int  samediag(int x, int y);
void classify(int t);
void printresults(void);
void printdiagram(int t);

struct diagram {
    int field[16],  // the contractions
        t,          // corresponding term
        type;       // a number 1,2,3... labeling each type of diagram
} tab[20000];

int _tmain(int argc, _TCHAR* argv[])
{
```

```c
    int t,j;

    fh_terms = fopen("terms_keep_dups.txt", "w+");
    fh = fopen( "diagrams.txt", "w+" );

    // create the 4th order terms
    createterms();

    // search for terms that contribute to the inelastic process <AA| ~ |AB>
    // for each good term, recursively form contractions, then classify the
    // resulting diagram
    goodcount = 0;

    for ( t = 0; t < NUMTERMS; t++ )
    {
        if (goodterm( t ))
        {
            for (j=0; j<16; j++)
                field[j] = NOTUSED; // clear the contraction record

            // numcontracts = 0;
            contractext(t, 12 ); // start with first external A state
            fprintf(fh,"\n");
        }
    }

    // findups();
    printresults();
    fclose(fh_terms);
    fclose( fh );
    return 0;
}

void createterms(void)
{
    int i,j,k,l,n,x,y;

    // create the terms
    for (i=0; i<3; i++)
        for (j=0; j<3; j++)
            for (k=0; k<3; k++)
                for (l=0; l<3; l++)
                {
```

```
                    n = l+3*(k+3*(j+3*i));
                    termvert[n][0]=i;
                    termvert[n][1]=j;
                    termvert[n][2]=k;
                    termvert[n][3]=l;

                    term[n][0]= la[i][0];
                    term[n][1]= la[i][1];
                    term[n][2]= la[i][2];

                    term[n][3]= la[j][0];
                    term[n][4]= la[j][1];
                    term[n][5]= la[j][2];

                    term[n][6]= la[k][0];
                    term[n][7]= la[k][1];
                    term[n][8]= la[k][2];

                    term[n][9]= la[l][0];
                    term[n][10]= la[l][1];
                    term[n][11]= la[l][2];

                    // initial state
                    term[n][12]= ist[0];
                    term[n][13]= ist[1];

                    // final state
                    term[n][14]= fst[0];
                    term[n][15]= fst[1];

                    // print the term
                    for(x=0; x<4; x++)
                    {
                        for(y=0; y<3; y++)
                            fprintf(fh_terms, "%c", (char) term[n][3*x+y]+64);
                        fprintf(fh_terms, " ");
                    }
                    fprintf(fh_terms, "\n");
                }

        fprintf(fh_terms, "\n\n\n");

} // end creatterms
```

```
int sameterm(int x, int y)
{
    int i;
    int nx0=0,
        nx1=0,
        nx2=0,
        ny0=0,
        ny1=0,
        ny2=0;

    for (i=0; i<4; i++) // count the vertex types for both terms
    {
        if( termvert[x][i] == 0 )
            ++nx0;
        else if( termvert[x][i] == 1 )
            ++nx1;
        else
            ++nx2;

        if( termvert[y][i] == 0 )
            ++ny0;
        else if( termvert[y][i] == 1 )
            ++ny1;
        else
            ++ny2;
    }
    if (nx0 == ny0 && nx1 == ny1 && nx2 == ny2 )
        return(1);
    else
        return(0);
}

int goodterm( int t )
{
    int f, x, y;

    anum = 0;
    bnum = 0;
    cnum = 0;

    // count the number of A, B and C fields in the term (excluding
    // external states)
```

```
    for (f=0; f<12; f++)
    {
        if (term[t][f] == AFIELD) // its an A
            ++anum;
        else if (term[t][f] == BFIELD) // its a B
            ++bnum;
        else if (term[t][f] == CFIELD) // its a C
            ++cnum;
    }

    // the term must match the external states
    if ( anum >= numA && (anum - numA) % 2 == 0 &&
         bnum >= numB && (bnum - numB) % 2 == 0 &&
         cnum >= numC && (cnum - numC) % 2 == 0 )
    {
        ++goodcount;
        // print the term
        fprintf(fh_terms, "  &=& ");
        for(x=0; x<4; x++)
        {
            fprintf(fh_terms, "(");
            for(y=0; y<3; y++)
                fprintf(fh_terms, "%c", (char) term[t][3*x+y]+64);
            fprintf(fh_terms, ")_%i ", x+1);
        }
        fprintf(fh_terms, "+ \\nonumber \\\\\n");

        return(1); // its a match
    }
    else
        return(0); // does not match external state
}

void countfields(int t)
{
    int j;

    // count the number of A's, B's and C's not yet contracted
    anum = 0;
    bnum = 0;
    cnum = 0;

    for (j=0; j<12; j++)
```

```
        {
            if( field[j] == NOTUSED )
                if (term[t][j] == AFIELD)
                    ++anum;
                else if (term[t][j] == BFIELD)
                    ++bnum;
                else if (term[t][j] == CFIELD)
                    ++cnum;
        }
    }


    void contractext( int t, int f )
    {
        int i,
            visited[5] = {0}; // tracks whether nodes 1 thru 4 have been visited

        for( i=0; i<12; i++)
        {
            if (i != f && term[t][i] == term[t][f] && field[i] == NOTUSED
                && !visited[node[i]])
//          if (i != f && term[t][i] == term[t][f] && field[i] == NOTUSED )
            {
                visited[node[i]] = 1;
                // form the contraction
                field[i] = f;
                field[f] = i;
                // ++numcontracts;

                if ( f == 15 )
                {
                    ++extconxdone;

                    // count the remaining uncontracted fields in the term
                    countfields(t);

                    // do internal contractions
                    contractintA(t,0); // do internal contractions, A fields first
                }
                else
                    contractext(t, f+1); // do another external contraction

                // back out and form a different external contraction
                field[i] = NOTUSED;
```

```
                field[f] = NOTUSED;
                // --numcontracts;
            }
        }
}

void contractintA(int t, int f )
{
    int i,j,
        visited[5] = {0}; // tracks whether nodes 1 thru 4 have been visited

    if(!anum)
        contractintB(t,0);
    else
        for( i=f; i<12; i++)
        {
            if (term[t][i] == AFIELD && field[i] == NOTUSED )
            {
                for(j=i+1; j<12; j++)
                {
                    if (field[j] == NOTUSED &&
                        term[t][i] == term[t][j] && node[i] != node[j]
                            && !visited[node[j]])
                    {
                        // form the contraction
                        visited[node[j]]=1;
                        field[i] = j;
                        field[j] = i;
                        anum -= 2;
                        if (anum > 0)
                            contractintA(t, i+1);
                        else
                            contractintB(t, 0);

                        // back out and prepare to do another
                        anum += 2;
                        field[i] = NOTUSED;
                        field[j] = NOTUSED;
                    }
                } // for j
            }
        } // for i
}
```

```
void contractintB(int t, int f )
{
    int i,j,
    visited[5] = {0}; // tracks whether nodes 1 thru 4 have been visited

    if(!bnum)
        contractintC(t,0);
    else
        for( i=f; i<12; i++)
        {
            if (term[t][i] == BFIELD && field[i] == NOTUSED )
            {
                for(j=i+1; j<12; j++)
                {
                    if (field[j] == NOTUSED &&
                        term[t][i] == term[t][j] && node[i] != node[j]
                            && !visited[node[j]])
                    {
                        // form the contraction
                        visited[node[j]]=1;
                        field[i] = j;
                        field[j] = i;

                        bnum -= 2;
                        if (bnum > 0)
                            contractintB(t, i+1);
                        else
                            contractintC(t, 0);

                        // back out and prepare to do another
                        bnum += 2;
                        field[i] = NOTUSED;
                        field[j] = NOTUSED;
                    }
                } // for j
            }
        } // for i
}

void contractintC(int t, int f )
{
    int i,j,
```

```
        visited[5] = {0}; // tracks whether nodes 1 thru 4 have been visited

        for( i=f; i<12; i++)
        {
            if (term[t][i] == CFIELD && field[i] == NOTUSED)
            {
                for(j=i+1; j<12; j++)
                {
                    if (field[j] == NOTUSED &&
                        term[t][i] == term[t][j] && node[i] != node[j]
                            && !visited[node[j]])
                    {   // form the contraction
                        visited[node[j]]=1;
                        field[i] = j;
                        field[j] = i;

                        cnum -= 2;
                        if (cnum > 0)
                            contractintC(t, i+1);
                        else
                        {   // all contracted, we have a Feynman diagram
                            ++numdiagrams;
                            store(t);
                            classify(t);
                        }

                        // back out and prepare to do another
                        cnum += 2;
                        field[i] = NOTUSED;
                        field[j] = NOTUSED;
                    }
                } // for j
            }
        } // for i
}
void store(int t)
{
    int i;

    tab[numdiagrams].t = t;
    for(i=0; i<16; i++)
        tab[numdiagrams-1].field[i] = field[i];
}
```

```c
void findups(void)
{
    int i, j,
        k = 1;  // start with type 1

    for(i=0; i<numdiagrams; i++)
    {
        if (! tab[i].type )
        {
            tab[i].type = k;
            for (j=i+1; j<numdiagrams; j++)
                if ( ! tab[i].type && samediag(i, j) )
                    tab[j].type = k;
            ++k;
        }
    }
}
int samediag(int x, int y)
{
    int i;

    if (tab[x].t != tab[y].t) // do diagrams have same term?
        return(0);

    // do diagrams have the same set of contractions?
    for( i=0; i<16; i++)
        if( tab[x].field[i] != tab[y].field[i] )
            return(0);
    return(1);
}

void classify(int t)
{
    // Determine the type of diagram (box, beetle, bowtie, triangle, cross,
    // split, other). Upon entry field[t] defines a set of contractions for
    // term[t][], while node[] indicates the nodes (vertices) to which fields
    // (and states) are attached.
    int i,j, n, m;
    int pairs = 0,  // counts nodes that have a pair of final states
        ibyxs = 0,  // counts nodes that have a pair of external states
        loops = 0,  // counts nodes that share two contractions
```

```
        seats = 0,   // are final states are adjacent or cate-corner?
        conxs,       // number of connections between two nodes
        biloop= 0;   // 0 or 1, number of biloops

int n1, n2, n3, n4;
int ibeg, jbeg;
int kernel = 0,
    prop1 = 0,
    prop2 = 0;

// nodes to which the external states are attached
n1 = node[field[12]];
n2 = node[field[13]];
n3 = node[field[14]];
n4 = node[field[15]];

// printdiagram(t);

// count ibyxs, pairs of external states (an ibyx is either an in-out or
// a pair)
for(i=12; i<16; i++)
    for(j=i+1; j<16; j++)
    {
        if( node[ field[i]] == node[field[j]])
        ++ibyxs;
    }

// count pairs (each pair indicates presence of an s-channel)
if(n3 == n4) // do final states share a vertex?
        ++pairs;
if(n1 == n2) // do initial states share a vertex?
        ++pairs;

// count loops and bi-loops
for(n=1; n<=4; n++) // for each node n
    for(m=n+1; m<=4; m++) // for each node m > n
    {
        conxs = 0;
        ibeg = 3*(n-1);
        jbeg = 3*(m-1);
        for(i = ibeg; i < ibeg+3; i++) // for each state in node n
            for(j = jbeg; j < jbeg+3; j++) // for each state in node m
            {
```

```
                    if (field[i] == j) // we have a connection (contraction)
                        ++conxs;
                }
            if (conxs == 3)
                biloop = 1;
            else if (conxs == 2)
                ++loops;
        }

// determine type of seats (are final states adjacent or cate-corner?)
// if their nodes are connected by a contraction, they are adjacent.
if (!ibyxs) // then the diagram has one external state per node, thus is
{            // either a box or a cross
    ibeg = 3*(n3-1);
    jbeg = 3*(n4-1);

    for(i = ibeg; i < ibeg+3; i++)
        for(j = jbeg; j < jbeg+3; j++)
            if (field[i] == j && field[j] == i)
            {
                seats = ADJACENT; // its a box
                if (term[t][field[i]] == CFIELD ) // is AA,AB,BA or BB
                    kernel = CFIELD;
            }

    // determine propagator type for boxes
    if ( ibyxs == 0 && loops == 0 && seats == ADJACENT ) // its a box
        {
            if ( kernel == CFIELD ) // propagator is AA,AB,BA or BB
            {
                for(i = ibeg; i < ibeg+3; i++)
                    if ( field[i]<12 && term[t][field[i]] != CFIELD )
                        prop1 = term[t][field[i]];

                for(j = jbeg; j < jbeg+3; j++)
                    if ( field[j]<12 && term[t][field[j]] != CFIELD )
                        prop2 = term[t][field[j]];

                if ( prop1 == AFIELD )
                {
                    if ( prop2 == AFIELD )
                    {
                        boxprop[AAPROP] += 1;
```

```
                            //printdiagram(t);
                        }
                        else
                            boxprop[ABPROP] += 1;
                    }
                    else // prop1 is a BFIELD
                    {
                        if ( prop2 == AFIELD )
                        {
                            boxprop[BAPROP] += 1;
                            //printdiagram(t);
                        }
                        else
                            boxprop[BBPROP] += 1;
                    }
                }
                else // propagator is CC
                    boxprop[CCPROP] += 1;
            }
    else // its a cross
    {
    }
}

// attributes have been determined, now classify
if (ibyxs == 0)
{
    ++ibyxs0;
    if (loops == 0)
    {
        if (seats == ADJACENT)
        {
            ++boxes;
            // further classify boxes by propagator (AA, AB, BA, BB, CC)
            // n = boxproptype(t);
            // boxprop[n] += 1;
        }
        else
        {
            ++crosses;
            // further classify crosses by propagator
            // n = crossproptype(t);
            // crossprop[n] += 1;
```

```
            }
        }
        else if (loops == 2)
        {
            ++split_loops;
            // printdiagram(t);
        }
        else
        {
            ++others0;
            // printdiagram(t);
        }
    }
    else if (ibyxs == 1)
    {
        ++ibyxs1;
        if (loops == 0)
        {
//          if( pairs )
//              ++striangles;
//          else
                ++triangles;
        }
        else if (loops == 1)
        {
//          if (pairs)
//              ++sbeetles;
//          else
                ++beetles;
            // printdiagram(t);
        }
        else
        {
            ++others1;
            // printdiagram(t);
        }
    }
    else if(ibyxs == 2)
    {
        ++ibyxs2;
        if (loops == 1)
        {
            ++bowties;
```

```c
            // printdiagram(t);
        }
        else if (loops == 2)
        {
            ++others2;
            // printdiagram(t);
        }
        else // must be a biloop
        {
            if (pairs)
            {
                ++sbiloops;
                printdiagram(t);
            }
            else
            {
                ++biloops;
                // printdiagram(t);
            }

        }
    }
    else
        printf("invalid number of ibyxs\n");
}

void printresults(void)
{
    int i, sum, num;
    FILE* fh;
    char* propstr[6] = {"","AA", "AB", "BA", "BB", "CC"};

    fh = fopen("results_keep_dups.txt", "w+");

    sum = boxes + beetles + sbeetles + bowties + crosses + triangles +
        striangles + split_loops + biloops + sbiloops + others0 + others1
        + others2;

    num = boxes/24 + beetles/12 + sbeetles/12 + bowties/24 + crosses/24
        + triangles/12 + striangles/12 + split_loops/24 + biloops/12
        + sbiloops/12;
```

```
        fprintf(fh, "ext contractions done = %i\n", extconxdone);
        fprintf(fh, "goodcount = %i\n", goodcount);
        fprintf(fh, "numdiagrams = %i\n", numdiagrams);
        fprintf(fh, "boxes = %i\n", boxes);
        for(i=1; i<6; i++)
            fprintf(fh, "%s box props = %i\n", propstr[i], boxprop[i]);
        fprintf(fh, "beetles = %i\n", beetles);
//      fprintf(fh, "sbeetles = %i\n", sbeetles);
        fprintf(fh, "bowties = %i\n", bowties);
        fprintf(fh, "crosses = %i\n", crosses);
        fprintf(fh, "triangles = %i\n", triangles);
//      fprintf(fh, "striangles = %i\n", striangles);
        fprintf(fh, "split_loops = %i\n", split_loops);
        fprintf(fh, "biloops = %i\n", biloops);
        fprintf(fh, "sbiloops = %i\n", sbiloops);
        fprintf(fh, "others0 = %i\n", others0);
        fprintf(fh, "others1 = %i\n", others1);
        fprintf(fh, "others2 = %i\n", others2);
        fprintf(fh, "sum others = %i\n", others0 + others1 + others2);
        fprintf(fh, "sum all = %i\n\n", sum);

        fprintf(fh, "ibyxs0 = %i\n", ibyxs0);
        fprintf(fh, "ibyxs1 = %i\n", ibyxs1);
        fprintf(fh, "ibyxs2 = %i\n", ibyxs2);
        fprintf(fh, "sum ibyxs = %i\n", ibyxs0 + ibyxs1 + ibyxs2);

//      fprintf(fh, "numdiagrams mod 24 = %i\n", numdiagrams%24);
        fprintf(fh, "boxes mod 24 = %i\n", boxes%24);
        for(i=1; i<6; i++)
            fprintf(fh, "%s box props mod 24 = %i\n", propstr[i], boxprop[i]%24);
        fprintf(fh, "beetles mod 12 = %i\n", beetles%12);
//      fprintf(fh, "sbeetles mod 12 = %i\n", sbeetles%12);
        fprintf(fh, "bowties mod 24 = %i\n", bowties%24);
        fprintf(fh, "crosses mod 24 = %i\n", crosses%24);
        fprintf(fh, "triangles mod 12 = %i\n", triangles%12);
//      fprintf(fh, "striangles mod 12 = %i\n", striangles%12);
        fprintf(fh, "split_loops mod 24 = %i\n", split_loops%24);
        fprintf(fh, "biloops mod 12 = %i\n\n", biloops%12);
        fprintf(fh, "sbiloops mod 12 = %i\n\n", sbiloops%12);

//      fprintf(fh, "numdiagrams/24 = %i\n", numdiagrams/24);
        fprintf(fh, "boxes/24 = %i\n", boxes/24);
        for(i=1; i<6; i++)
```

```c
        fprintf(fh, "%s box props/24 = %i\n", propstr[i], boxprop[i]/24);
    fprintf(fh, "beetles/12 = %i\n", beetles/12);
//  fprintf(fh, "sbeetles/12 = %i\n", sbeetles/12);
    fprintf(fh, "bowties/24 = %i\n", bowties/24);
    fprintf(fh, "crosses/24 = %i\n", crosses/24);
    fprintf(fh, "triangles/12 = %i\n", triangles/12);
//  fprintf(fh, "striangles/12 = %i\n", striangles/12);
    fprintf(fh, "split_loops/24 = %i\n", split_loops/24);
    fprintf(fh, "biloops/12 = %i\n", biloops/12);
    fprintf(fh, "sbiloops/12 = %i\n", sbiloops/12);
    fprintf(fh, "num (no dups) = %i\n", num);



    fclose(fh);
}

void printdiagram(int t)
{
    int i,j, k=0;

    // print the term
    for(i=0; i<4; i++)
    {
        for(j=0; j<3; j++)
            fprintf(fh, "%c", (char) term[t][field[3*i+j]]+64);
        fprintf(fh, " ");
    }

    // external connections
    fprintf(fh, "%c->%c%i  ", term[t][12]+64, term[t][field[12]]+64,
        node[field[12]] );
    fprintf(fh, "%c->%c%i  ", term[t][13]+64, term[t][field[13]]+64,
        node[field[13]] );
    fprintf(fh, "%c'->%c%i  ", term[t][14]+64, term[t][field[14]]+64,
        node[field[14]] );
    fprintf(fh, "%c'->%c%i  ", term[t][15]+64, term[t][field[15]]+64,
        node[field[15]] );

    // internal connections
    for(i=0; i<12; i++)
    {
        if ( field[i]<12 && field[i]>i )
            fprintf(fh, "%c%i->%c%i  ", term[t][i]+64, node[i],
```

```
                term[t][field[i]]+64, node[field[i]]);
        }
        fprintf(fh, "\n");
}
```

6.1.1 results.txt

The results below are self-explanatory. Counts of the various types of diagrams are given. Of particular importance are the counts of the five types of box diagrams, and verification that these counts are divisible by 4!, leaving 2 (direct and exchange) of each of the four types of box diagrams AA, AB, BA and BB.

```
ext contractions done = 1236
goodcount = 36
numdiagrams = 3204
boxes = 384
AA box props = 48
AB box props = 48
BA box props = 48
BB box props = 48
CC box props = 192
beetles = 1344
bowties = 216
crosses = 192
triangles = 672
split_loops = 288
biloops = 72
sbiloops = 36
others0 = 0
others1 = 0
others2 = 0
sum others = 0
sum all = 3204

ibyxs0 = 864
ibyxs1 = 2016
ibyxs2 = 324
sum ibyxs = 3204
boxes mod 24 = 0
AA box props mod 24 = 0
AB box props mod 24 = 0
BA box props mod 24 = 0
```

```
BB box props mod 24 = 0
CC box props mod 24 = 0
beetles mod 12 = 0
bowties mod 24 = 0
crosses mod 24 = 0
triangles mod 12 = 0
split_loops mod 24 = 0
biloops mod 12 = 0

sbiloops mod 12 = 0

boxes/24 = 16
AA box props/24 = 2
AB box props/24 = 2
BA box props/24 = 2
BB box props/24 = 2
CC box props/24 = 8
beetles/12 = 112
bowties/24 = 9
crosses/24 = 8
triangles/12 = 56
split_loops/24 = 12
biloops/12 = 6
sbiloops/12 = 3
num (no dups) = 222
```

6.1.2 terms.txt

In S-matrix component S_4, the product of four Hamiltonians

$$\mathcal{H}^4 \;\; = \;\; (AAC + ABC + BBC)^4 \tag{301}$$

produces 81 terms. These are listed below. Each term is a product of twelve fields, three fields from each of four vertices.

```
ABC ABC ABC ABC
ABC ABC ABC AAC
ABC ABC ABC BBC
ABC ABC AAC ABC
ABC ABC AAC AAC
ABC ABC AAC BBC
ABC ABC BBC ABC
ABC ABC BBC AAC
```

```
ABC ABC BBC BBC
ABC AAC ABC ABC
ABC AAC ABC AAC
ABC AAC ABC BBC
ABC AAC AAC ABC
ABC AAC AAC AAC
ABC AAC AAC BBC
ABC AAC BBC ABC
ABC AAC BBC AAC
ABC AAC BBC BBC
ABC BBC ABC ABC
ABC BBC ABC AAC
ABC BBC ABC BBC
ABC BBC AAC ABC
ABC BBC AAC AAC
ABC BBC AAC BBC
ABC BBC BBC ABC
ABC BBC BBC AAC
ABC BBC BBC BBC
AAC ABC ABC ABC
AAC ABC ABC AAC
AAC ABC ABC BBC
AAC ABC AAC ABC
AAC ABC AAC AAC
AAC ABC AAC BBC
AAC ABC BBC ABC
AAC ABC BBC AAC
AAC ABC BBC BBC
AAC AAC ABC ABC
AAC AAC ABC AAC
AAC AAC ABC BBC
AAC AAC AAC ABC
AAC AAC AAC AAC
AAC AAC AAC BBC
AAC AAC BBC ABC
AAC AAC BBC AAC
AAC AAC BBC BBC
AAC BBC ABC ABC
AAC BBC ABC AAC
AAC BBC ABC BBC
AAC BBC AAC ABC
AAC BBC AAC AAC
AAC BBC AAC BBC
```

```
AAC BBC BBC ABC
AAC BBC BBC AAC
AAC BBC BBC BBC
BBC ABC ABC ABC
BBC ABC ABC AAC
BBC ABC ABC BBC
BBC ABC AAC ABC
BBC ABC AAC AAC
BBC ABC AAC BBC
BBC ABC BBC ABC
BBC ABC BBC AAC
BBC ABC BBC BBC
BBC AAC ABC ABC
BBC AAC ABC AAC
BBC AAC ABC BBC
BBC AAC AAC ABC
BBC AAC AAC AAC
BBC AAC AAC BBC
BBC AAC BBC ABC
BBC AAC BBC AAC
BBC AAC BBC BBC
BBC BBC ABC ABC
BBC BBC ABC AAC
BBC BBC ABC BBC
BBC BBC AAC ABC
BBC BBC AAC AAC
BBC BBC AAC BBC
BBC BBC BBC ABC
BBC BBC BBC AAC
BBC BBC BBC BBC
```

6.1.3   diagrams.txt

The listing below gives the specifications for all 48 AA box diagrams generated by program *FindFeynmanDiagrams* for the reaction $A + A \rightarrow A + B$. Many of the diagrams are duplicates. The diagrams are 4th order, and are derived from the S-matrix component S_4, which contains the factor 1/4!. This factor cancels the multiplicity, leaving two unique diagrams, the direct and exchange AA box diagrams. The first diagram specification is

```
ABC AAC AAC AAC A->A2  A->A3  A'->A4  B'->B1  A1->A2  C1->C4  C2->C3 A3->A4
```

The specifier "ABC AAC AAC AAC" on the left identifies the term which produced the diagram (see list of terms in the preceding section). The next specifier indicates that the first initial state particle A enters vertex 2. The following three specifiers similarly

indicate that the second initial state particle A enters vertex 3, and the final state particles A' and B' exit from vertices 4 and 1, respectively. The last four specifiers indicate virtual A-particles and C-particles propagating on internal lines between pairs of vertices. The two internal C-particles are the two C-rungs of the box diagram, while the two internal A-particles together from the G_A^A propagator.

```
ABC AAC AAC AAC A->A2  A->A3  A'->A4  B'->B1  A1->A2  C1->C4  C2->C3  A3->A4
ABC AAC AAC AAC A->A2  A->A3  A'->A4  B'->B1  A1->A3  C1->C4  A2->A4  C2->C3
ABC AAC AAC AAC A->A2  A->A4  A'->A3  B'->B1  A1->A2  C1->C3  C2->C4  A3->A4
ABC AAC AAC AAC A->A2  A->A4  A'->A3  B'->B1  A1->A4  C1->C3  A2->A3  C2->C4
ABC AAC AAC AAC A->A3  A->A2  A'->A4  B'->B1  A1->A2  C1->C4  C2->C3  A3->A4
ABC AAC AAC AAC A->A3  A->A2  A'->A4  B'->B1  A1->A3  C1->C4  A2->A4  C2->C3
ABC AAC AAC AAC A->A3  A->A4  A'->A2  B'->B1  A1->A3  C1->C2  A2->A4  C3->C4
ABC AAC AAC AAC A->A3  A->A4  A'->A2  B'->B1  A1->A4  C1->C2  A2->A3  C3->C4
ABC AAC AAC AAC A->A4  A->A2  A'->A3  B'->B1  A1->A2  C1->C3  C2->C4  A3->A4
ABC AAC AAC AAC A->A4  A->A2  A'->A3  B'->B1  A1->A4  C1->C3  A2->A3  C2->C4
ABC AAC AAC AAC A->A4  A->A3  A'->A2  B'->B1  A1->A3  C1->C2  A2->A4  C3->C4
ABC AAC AAC AAC A->A4  A->A3  A'->A2  B'->B1  A1->A4  C1->C2  A2->A3  C3->C4
AAC ABC AAC AAC A->A1  A->A3  A'->A4  B'->B2  A1->A2  C1->C3  C2->C4  A3->A4
AAC ABC AAC AAC A->A1  A->A3  A'->A4  B'->B2  A1->A4  C1->C3  A2->A3  C2->C4
AAC ABC AAC AAC A->A1  A->A4  A'->A3  B'->B2  A1->A2  C1->C4  C2->C3  A3->A4
AAC ABC AAC AAC A->A1  A->A4  A'->A3  B'->B2  A1->A3  C1->C4  A2->A4  C2->C3
AAC ABC AAC AAC A->A3  A->A1  A'->A4  B'->B2  A1->A2  C1->C3  C2->C4  A3->A4
AAC ABC AAC AAC A->A3  A->A1  A'->A4  B'->B2  A1->A4  C1->C3  A2->A3  C2->C4
AAC ABC AAC AAC A->A3  A->A4  A'->A1  B'->B2  A1->A3  C1->C2  A2->A4  C3->C4
AAC ABC AAC AAC A->A3  A->A4  A'->A1  B'->B2  A1->A4  C1->C2  A2->A3  C3->C4
AAC ABC AAC AAC A->A4  A->A1  A'->A3  B'->B2  A1->A2  C1->C4  C2->C3  A3->A4
AAC ABC AAC AAC A->A4  A->A1  A'->A3  B'->B2  A1->A3  C1->C4  A2->A4  C2->C3
AAC ABC AAC AAC A->A4  A->A3  A'->A1  B'->B2  A1->A3  C1->C2  A2->A4  C3->C4
AAC ABC AAC AAC A->A4  A->A3  A'->A1  B'->B2  A1->A4  C1->C2  A2->A3  C3->C4
AAC AAC ABC AAC A->A1  A->A2  A'->A4  B'->B3  A1->A3  C1->C2  A2->A4  C3->C4
AAC AAC ABC AAC A->A1  A->A2  A'->A4  B'->B3  A1->A4  C1->C2  A2->A3  C3->C4
AAC AAC ABC AAC A->A1  A->A4  A'->A2  B'->B3  A1->A2  C1->C4  C2->C3  A3->A4
AAC AAC ABC AAC A->A1  A->A4  A'->A2  B'->B3  A1->A3  C1->C4  A2->A4  C2->C3
AAC AAC ABC AAC A->A2  A->A1  A'->A4  B'->B3  A1->A3  C1->C2  A2->A4  C3->C4
AAC AAC ABC AAC A->A2  A->A1  A'->A4  B'->B3  A1->A4  C1->C2  A2->A3  C3->C4
AAC AAC ABC AAC A->A2  A->A4  A'->A1  B'->B3  A1->A2  C1->C3  C2->C4  A3->A4
AAC AAC ABC AAC A->A2  A->A4  A'->A1  B'->B3  A1->A4  C1->C3  A2->A3  C2->C4
AAC AAC ABC AAC A->A4  A->A1  A'->A2  B'->B3  A1->A2  C1->C4  C2->C3  A3->A4
AAC AAC ABC AAC A->A4  A->A1  A'->A2  B'->B3  A1->A3  C1->C4  A2->A4  C2->C3
AAC AAC ABC AAC A->A4  A->A2  A'->A1  B'->B3  A1->A2  C1->C3  C2->C4  A3->A4
AAC AAC ABC AAC A->A4  A->A2  A'->A1  B'->B3  A1->A4  C1->C3  A2->A3  C2->C4
```

```
AAC AAC AAC ABC A->A1  A->A2  A'->A3  B'->B4  A1->A3  C1->C2  A2->A4  C3->C4
AAC AAC AAC ABC A->A1  A->A2  A'->A3  B'->B4  A1->A4  C1->C2  A2->A3  C3->C4
AAC AAC AAC ABC A->A1  A->A3  A'->A2  B'->B4  A1->A2  C1->C3  C2->C4  A3->A4
AAC AAC AAC ABC A->A1  A->A3  A'->A2  B'->B4  A1->A4  C1->C3  A2->A3  C2->C4
AAC AAC AAC ABC A->A2  A->A1  A'->A3  B'->B4  A1->A3  C1->C2  A2->A4  C3->C4
AAC AAC AAC ABC A->A2  A->A1  A'->A3  B'->B4  A1->A4  C1->C2  A2->A3  C3->C4
AAC AAC AAC ABC A->A2  A->A3  A'->A1  B'->B4  A1->A2  C1->C4  C2->C3  A3->A4
AAC AAC AAC ABC A->A2  A->A3  A'->A1  B'->B4  A1->A3  C1->C4  A2->A4  C2->C3
AAC AAC AAC ABC A->A3  A->A1  A'->A2  B'->B4  A1->A2  C1->C3  C2->C4  A3->A4
AAC AAC AAC ABC A->A3  A->A1  A'->A2  B'->B4  A1->A4  C1->C3  A2->A3  C2->C4
AAC AAC AAC ABC A->A3  A->A2  A'->A1  B'->B4  A1->A2  C1->C4  C2->C3  A3->A4
AAC AAC AAC ABC A->A3  A->A2  A'->A1  B'->B4  A1->A3  C1->C4  A2->A4  C2->C3
```

6.2 Program *CalcGBSE*

The Mathematica file CalcGBSE.nb is listed below, along with output file CalcGBSEresults.txt.

```
In[1]:=
(* Calculate box diagrams for CBSE, GBSEnoBB and GBSEft *)
(* Frank Dick, WPI Physics, 2007 *)
Clear["Global'*"];
SetDirectory["C:\WORK2\dissertation"];
strm=OpenWrite["CalcGBSEresults.txt"];

(* Initial and final state vectors *)
xAA = {1,0,0,0};
xAB = {0,1,0,0};
xBA = {0,0,1,0};
xBB = {0,0,0,1};
z={0,0,0,0};

(* Propagator coupling matrices *)
GAA = {xAA,z,z,z};
GAB = {z,xAB,z,z};
GBA = {z,z,xBA,z};
GBB = {z,z,z,xBB};
G={z,z,z,z};

(* propagator = coupling matrix / denominator *)
(* use abbreviated notation to match the formulas in the dissertation *)
G1 = GAA/d1;
G2 = GAB/d2;
G3 = GBA/d3;
G4 = GBB/d4;

(* propagator G has denominators Daa, Dab, Dba,and Dbb on the diagonal *)
(* G = G1 + G2 + G3 + G4 *)
G = {{1/d1,0,0,0},{0,1/d2,0,0},{0,0,1/d3,0},{0,0,0,1/d4}};

(* coupling constants are aa, ab=ba, bb *)

(* 2nd order M prime matrices are Mc for CBSE, and M for GBSEnoBB *)

(* zero the matrices, then populate *)
Mc = {z,z,z,z};
```

145

```
M = {z,z,z,z};
Mmc = {z,z,z,z};
Mm = {z,z,z,z};

(* 2nd order Mprime for CBSE *)
Mc[[1,1]]=aa*aa;
Mc[[1,3]]=aa*ab;
Mc[[1,4]]=ab*ab;
Mc[[2,1]]=aa*ab;
Mc[[2,3]]=ab*ab;
Mc[[3,1]]=aa*ab;
Mc[[3,2]]=ab*ab;
Mc[[4,1]]=ab*ab;

(* 2nd order Mprime for H = AAC + ABC *)
M[[1,1]]=aa*aa;
M[[1,2]]=aa*ab;
M[[1,3]]=aa*ab;
M[[1,4]]=ab*ab;
M[[2,1]]=aa*ab;
M[[2,3]]=ab*ab;
M[[3,1]]=aa*ab;
M[[3,2]]=ab*ab;
M[[4,1]]=ab*ab;

(* The kernel coupling matrices are equal to the 2nd order M prime matrices.
      Here couplers U contain only coupling
    constants. In practice, kernels U also have denominators. *)
Uc = Mc;
Ug = M;

(* compute box diagrams by expanding to 4th order *)

(* Use final state BA *)
Print["Cbse4=",Expand[I xAA.Uc.G.Uc.xBA]]
Print["Gbse4=",Expand[I xAA.Ug.G.Ug.xBA]]

(* 6th order, 3 rung ladders *)
Print["Cbse6=",Expand[-xAA.Uc.G.Uc.G.Uc.xBA]]
Print["Gbse6=",Expand[-xAA.Ug.G.Ug.G.Ug.xBA]]

(* 8th order, 4 rung ladders *)
Print["Cbse8=",Expand[-I xAA.Uc.G.Uc.G.Uc.G.Uc.xBA]]
```

146

```
Print["Gbse8=",Expand[-I xAA.Ug.G.Ug.G.Ug.G.Ug.xBA]]

(* Expand the CBSE to 6th order *)
(* u = kernel, f1 = G1, m1 = M11, m2 = M13, m3 = M14 *)
(* m1 *)
u + I(m1)*f1*u + I(m2)*f3*u + I(m3)*f4*u
(* m2 *)
u + I(n2)*f2*u + I(m1)*f1*u
(* n2 = m2 flipped, since Faassen-Tjon put M12 into M13 *)
u + I(m2)*f3*u + I(m1)*f1*u
(* m3 *)
u + I(m1)*f1*u

(* Substitute m1, m2, n2, m3 into m2 through third iteration *)
Write[strm,
    Expand[u +
        I(u + I(u + I(n2)*f2*u + I(m1)*f1*u)*f3*u +
            I(u + I(m1)*f1*u + I(m2)*f3*u + I(m3)*f4*u)*f1*u)*f2*u +
        I(u + I(u + I(m1)*f1*u + I(m2)*f3*u + I(m3)*f4*u)*f1*u +
            I(u + I(m2)*f3*u + I(m1)*f1*u)*f3*u + I(u + I(m1)*f1*u)*f4*u)*
          f1*u
      ]];

(* Find the form of the coupled equations *)
Mmc[[1,1]]=m11;
Mmc[[1,3]]=m13;
Mmc[[1,4]]=m14;
Mmc[[2,1]]=m21;
Mmc[[2,3]]=m23;
Mmc[[3,1]]=m31;
Mmc[[3,2]]=m32;
Mmc[[4,1]]=m41;

Mm[[1,1]]=m11;
Mm[[1,2]]=m12;
Mm[[1,3]]=m13;
Mm[[1,4]]=m14;
Mm[[2,1]]=m21;
Mm[[2,3]]=m23;
Mm[[3,1]]=m31;
Mm[[3,2]]=m32;
Mm[[4,1]]=m41;
```

```
(* The elements of Nmc and Nm1 give the coupled equations. *)

(* 1st iteration *)
Nm1=Ug+ I Ug.G.Mm;
Nm1transpose=Ug+ I Mm.G.Ug;
Nmc=Uc+ I Uc.G.Mmc;
Write[strm,"\n** 1st **"];
Write[strm,"Nm1 = ",Expand[Nm1]];
(*Print["Nm1transpose = ",Expand[Nm1transpose]];*)
Write[strm,"Nmc = ",Expand[Nmc]];

(* 2nd iteration *)
Nm11=Ug+ I Ug.G.Nm1;
Nmc1=Uc+ I Uc.G.Nmc;
Write[strm,"** 2nd **"];
Write[strm,"Nm11 = ",Expand[Nm11], "\n"];
Write[strm,"Nmc1 = ",Expand[Nmc1], "\n"];

(* 3rd iteration *)
Nm12=Ug+ I Ug.G.Nm11;
Nmc2=Uc+ I Uc.G.Nmc1;
Write[strm,"** 3rd **"];
(*
  Print["Nm12 = ",Expand[Nm12], "\n"];
  Print["Nmc2 = ",Expand[Nmc2], "\n"];
  *)
Write[strm,"Nm(3,1) = ",Expand[Nm12[[3,1]]]];
Write[strm,"Nmc(3,1) = ",Expand[Nmc2[[3,1]]]];

(* 4th iteration *)
Nm13=Ug+ I Ug.G.Nm12;
Nmc3=Uc+ I Uc.G.Nmc2;
Write[strm,"** 4th **"];
(*
  Print["Nm13 = ",Expand[Nm13], "\n"];
  Print["Nmc3 = ",Expand[Nmc3], "\n"];
  *)
Write[strm,"Nm(3,1) = ",Expand[Nm13[[3,1]]]];
Write[strm,"Nmc(3,1) = ",Expand[Nmc3[[3,1]]]];

(* **** Uncomment at your own peril! Produces many pages of symbols

      (* 5th iteration *)
```

```
    Nm14=Ug+ I Ug.G.Nm13;
Print["** 5th **"];
Print["Nm14 = ",Expand[Nm14], "\n"];
(*Print["Nmc4 = ",Expand[Nmc4], "\n"];*)
Print[" "];

(* 6th iteration *)
Nm15=Ug+ I Ug.G.Nm14;
Print["** 6th **"];
Print["Nm15 = ",Expand[Nm15], "\n"];
(*Print["Nmc5 = ",Expand[Nmc5], "\n"];*)
Print[" "];

(* 7th iteration *)
Nm16=Ug+ I Ug.G.Nm15;
Print["** 7th **"];
Print["Nm16 = ",Expand[Nm16], "\n"];
(*Print["Nmc6 = ",Expand[Nmc6], "\n"];*)
Print[" "];

(* 8th iteration *)
Nm17=Ug+ I Ug.G.Nm16;
Print["** 8th **"];
Print["Nm17 = ",Expand[Nm17], "\n"];
(*Print["Nmc7 = ",Expand[Nmc7], "\n"];*)
Print[" "];

(* 9th iteration *)
Nm18=Ug+ I Ug.G.Nm17;
Print["** 9th **"];
Print["Nm18 = ",Expand[Nm18], "\n"];
(*Print["Nmc8 = ",Expand[Nmc8], "\n"];*)
Print[" "];

(* 10th iteration *)
Nm19=Ug+ I Ug.G.Nm18;
Print["** 10th **"];
Print["Nm19 = ",Expand[Nm19], "\n"];
(*Print["Nmc9 = ",Expand[Nmc9], "\n"];*)
Print[" "];

    **** See comment above. *)
```

```
Close[strm];
(**)
```

6.2.1 CalcGBSEresults.txt

The first result in the listing below, written in terms of u and the f_i, is the iterative expansion of the CBSE equations to 6th order. The f_i represent the propagators, and serve to define the ladders. Referencing the V, H notation introduced in section 4.10, propagator $f1$ is H_1, $f2$ is $H2$, $f3$ is $H3$ and $f4$ is $H4$. The u's are C-kernels, and since the f_i define the ladders, the kernels are relieved of that task, therefore do not contain coupling constants and are all the same. I is the square root of -1, $m1$ is $\mathcal{M}'_{11}$, $n2$ is $\mathcal{M}'_{21}$, $m2$ is $\mathcal{M}'_{31}$, and $m3$ is $\mathcal{M}'_{41}$.

The next results, $Nm1$ and Nmc, are the 2-vertex model $\mathcal{M}'$ and the CBSE $\mathcal{M}'$ to 2nd order, given by the first iteration of the expansion. These are followed by the 4th order $Nm11$ and $Nmc1$ given by the 2nd iteration. For 6th and 8th order, to conserve space only the $\mathcal{M}'_{31}$ elements $Nm(3,1)$ and $Nmc(3,1)$ are printed. In all of the Nm and Nmc terms above, the d_i are the denominators of the propagators H_i, the m_{ij} are elements of $\mathcal{M}'$, and aa and ab are the coupling constants g_{AA} and g_{AB}, respectively.

```
u + I*f1*u^2 + I*f2*u^2 - f1^2*u^3 - f1*f2*u^3 - f1*f3*u^3 - f2*f3*u^3 -
 f1*f4*u^3 - I*f1^3*m1*u^3 - I*f1^2*f2*m1*u^3 - I*f1^2*f3*m1*u^3 -
 I*f1*f2*f3*m1*u^3 - I*f1^2*f4*m1*u^3 - I*f1^2*f3*m2*u^3 -
 I*f1*f2*f3*m2*u^3 - I*f1*f3^2*m2*u^3 - I*f1^2*f4*m3*u^3 -
 I*f1*f2*f4*m3*u^3 - I*f2^2*f3*n2*u^3
"\n** 1st **"
"Nm1 = "{{aa^2 + (I*aa^2*m11)/d1 + (I*aa*ab*m21)/d2 + (I*aa*ab*m31)/d3 +
   (I*ab^2*m41)/d4, aa*ab + (I*aa^2*m12)/d1 + (I*aa*ab*m32)/d3,
  aa*ab + (I*aa^2*m13)/d1 + (I*aa*ab*m23)/d2, ab^2 + (I*aa^2*m14)/d1},
 {aa*ab + (I*aa*ab*m11)/d1 + (I*ab^2*m31)/d3,
  (I*aa*ab*m12)/d1 + (I*ab^2*m32)/d3, ab^2 + (I*aa*ab*m13)/d1,
  (I*aa*ab*m14)/d1}, {aa*ab + (I*aa*ab*m11)/d1 + (I*ab^2*m21)/d2,
  ab^2 + (I*aa*ab*m12)/d1, (I*aa*ab*m13)/d1 + (I*ab^2*m23)/d2,
  (I*aa*ab*m14)/d1}, {ab^2 + (I*ab^2*m11)/d1, (I*ab^2*m12)/d1,
  (I*ab^2*m13)/d1, (I*ab^2*m14)/d1}}
"Nmc = "{{aa^2 + (I*aa^2*m11)/d1 + (I*aa*ab*m31)/d3 + (I*ab^2*m41)/d4,
  (I*aa*ab*m32)/d3, aa*ab + (I*aa^2*m13)/d1, ab^2 + (I*aa^2*m14)/d1},
 {aa*ab + (I*aa*ab*m11)/d1 + (I*ab^2*m31)/d3, (I*ab^2*m32)/d3,
  ab^2 + (I*aa*ab*m13)/d1, (I*aa*ab*m14)/d1},
 {aa*ab + (I*aa*ab*m11)/d1 + (I*ab^2*m21)/d2, ab^2,
  (I*aa*ab*m13)/d1 + (I*ab^2*m23)/d2, (I*aa*ab*m14)/d1},
 {ab^2 + (I*ab^2*m11)/d1, 0, (I*ab^2*m13)/d1, (I*ab^2*m14)/d1}}
```

```
"** 2nd **"
"Nm11 = "{{aa^2 + (I*aa^4)/d1 + (I*aa^2*ab^2)/d2 + (I*aa^2*ab^2)/d3 +
    (I*ab^4)/d4 - (aa^4*m11)/d1^2 - (aa^2*ab^2*m11)/(d1*d2) -
    (aa^2*ab^2*m11)/(d1*d3) - (ab^4*m11)/(d1*d4) - (aa^3*ab*m21)/(d1*d2) -
    (aa*ab^3*m21)/(d2*d3) - (aa^3*ab*m31)/(d1*d3) - (aa*ab^3*m31)/(d2*d3) -
    (aa^2*ab^2*m41)/(d1*d4), aa*ab + (I*aa^3*ab)/d1 + (I*aa*ab^3)/d3 -
    (aa^4*m12)/d1^2 - (aa^2*ab^2*m12)/(d1*d2) - (aa^2*ab^2*m12)/(d1*d3) -
    (ab^4*m12)/(d1*d4) - (aa^3*ab*m32)/(d1*d3) - (aa*ab^3*m32)/(d2*d3),
  aa*ab + (I*aa^3*ab)/d1 + (I*aa*ab^3)/d2 - (aa^4*m13)/d1^2 -
    (aa^2*ab^2*m13)/(d1*d2) - (aa^2*ab^2*m13)/(d1*d3) - (ab^4*m13)/(d1*d4) -
    (aa^3*ab*m23)/(d1*d2) - (aa*ab^3*m23)/(d2*d3),
  ab^2 + (I*aa^2*ab^2)/d1 - (aa^4*m14)/d1^2 - (aa^2*ab^2*m14)/(d1*d2) -
    (aa^2*ab^2*m14)/(d1*d3) - (ab^4*m14)/(d1*d4)},
 {aa*ab + (I*aa^3*ab)/d1 + (I*aa*ab^3)/d3 - (aa^3*ab*m11)/d1^2 -
    (aa*ab^3*m11)/(d1*d3) - (aa^2*ab^2*m21)/(d1*d2) - (ab^4*m21)/(d2*d3) -
    (aa^2*ab^2*m31)/(d1*d3) - (aa*ab^3*m41)/(d1*d4),
  (I*aa^2*ab^2)/d1 + (I*ab^4)/d3 - (aa^3*ab*m12)/d1^2 -
    (aa*ab^3*m12)/(d1*d3) - (aa^2*ab^2*m32)/(d1*d3),
  ab^2 + (I*aa^2*ab^2)/d1 - (aa^3*ab*m13)/d1^2 - (aa*ab^3*m13)/(d1*d3) -
    (aa^2*ab^2*m23)/(d1*d2) - (ab^4*m23)/(d2*d3),
  (I*aa*ab^3)/d1 - (aa^3*ab*m14)/d1^2 - (aa*ab^3*m14)/(d1*d3)},
 {aa*ab + (I*aa^3*ab)/d1 + (I*aa*ab^3)/d2 - (aa^3*ab*m11)/d1^2 -
    (aa*ab^3*m11)/(d1*d2) - (aa^2*ab^2*m21)/(d1*d2) -
    (aa^2*ab^2*m31)/(d1*d3) - (ab^4*m31)/(d2*d3) - (aa*ab^3*m41)/(d1*d4),
  ab^2 + (I*aa^2*ab^2)/d1 - (aa^3*ab*m12)/d1^2 - (aa*ab^3*m12)/(d1*d2) -
    (aa^2*ab^2*m32)/(d1*d3) - (ab^4*m32)/(d2*d3),
  (I*aa^2*ab^2)/d1 + (I*ab^4)/d2 - (aa^3*ab*m13)/d1^2 -
    (aa*ab^3*m13)/(d1*d2) - (aa^2*ab^2*m23)/(d1*d2),
  (I*aa*ab^3)/d1 - (aa^3*ab*m14)/d1^2 - (aa*ab^3*m14)/(d1*d2)},
 {ab^2 + (I*aa^2*ab^2)/d1 - (aa^2*ab^2*m11)/d1^2 - (aa*ab^3*m21)/(d1*d2) -
    (aa*ab^3*m31)/(d1*d3) - (ab^4*m41)/(d1*d4),
  (I*aa*ab^3)/d1 - (aa^2*ab^2*m12)/d1^2 - (aa*ab^3*m32)/(d1*d3),
  (I*aa*ab^3)/d1 - (aa^2*ab^2*m13)/d1^2 - (aa*ab^3*m23)/(d1*d2),
  (I*ab^4)/d1 - (aa^2*ab^2*m14)/d1^2}}"\n"
"Nmc1 = "{{aa^2 + (I*aa^4)/d1 + (I*aa^2*ab^2)/d3 + (I*ab^4)/d4 -
    (aa^4*m11)/d1^2 - (aa^2*ab^2*m11)/(d1*d3) - (ab^4*m11)/(d1*d4) -
    (aa*ab^3*m21)/(d2*d3) - (aa^3*ab*m31)/(d1*d3) - (aa^2*ab^2*m41)/(d1*d4),
  (I*aa*ab^3)/d3 - (aa^3*ab*m32)/(d1*d3), aa*ab + (I*aa^3*ab)/d1 -
    (aa^4*m13)/d1^2 - (aa^2*ab^2*m13)/(d1*d3) - (ab^4*m13)/(d1*d4) -
    (aa*ab^3*m23)/(d2*d3), ab^2 + (I*aa^2*ab^2)/d1 - (aa^4*m14)/d1^2 -
    (aa^2*ab^2*m14)/(d1*d3) - (ab^4*m14)/(d1*d4)},
 {aa*ab + (I*aa^3*ab)/d1 + (I*aa*ab^3)/d3 - (aa^3*ab*m11)/d1^2 -
    (aa*ab^3*m11)/(d1*d3) - (ab^4*m21)/(d2*d3) - (aa^2*ab^2*m31)/(d1*d3) -
```

151

```
     (aa*ab^3*m41)/(d1*d4), (I*ab^4)/d3 - (aa^2*ab^2*m32)/(d1*d3),
   ab^2 + (I*aa^2*ab^2)/d1 - (aa^3*ab*m13)/d1^2 - (aa*ab^3*m13)/(d1*d3) -
    (ab^4*m23)/(d2*d3), (I*aa*ab^3)/d1 - (aa^3*ab*m14)/d1^2 -
    (aa*ab^3*m14)/(d1*d3)}, {aa*ab + (I*aa^3*ab)/d1 + (I*aa*ab^3)/d2 -
    (aa^3*ab*m11)/d1^2 - (aa*ab^3*m11)/(d1*d2) - (aa^2*ab^2*m31)/(d1*d3) -
    (ab^4*m31)/(d2*d3) - (aa*ab^3*m41)/(d1*d4),
   ab^2 - (aa^2*ab^2*m32)/(d1*d3) - (ab^4*m32)/(d2*d3),
   (I*aa^2*ab^2)/d1 + (I*ab^4)/d2 - (aa^3*ab*m13)/d1^2 -
    (aa*ab^3*m13)/(d1*d2), (I*aa*ab^3)/d1 - (aa^3*ab*m14)/d1^2 -
    (aa*ab^3*m14)/(d1*d2)}, {ab^2 + (I*aa^2*ab^2)/d1 - (aa^2*ab^2*m11)/d1^2 -
    (aa*ab^3*m31)/(d1*d3) - (ab^4*m41)/(d1*d4), -((aa*ab^3*m32)/(d1*d3)),
   (I*aa*ab^3)/d1 - (aa^2*ab^2*m13)/d1^2,
   (I*ab^4)/d1 - (aa^2*ab^2*m14)/d1^2}}"\n"
"** 3rd **"
"Nm(3,1) = "aa*ab - (aa^5*ab)/d1^2 + (I*aa^3*ab)/d1 + (I*aa*ab^3)/d2 -
 (2*aa^3*ab^3)/(d1*d2) - (aa^3*ab^3)/(d1*d3) - (aa*ab^5)/(d2*d3) -
 (aa*ab^5)/(d1*d4) - (I*aa^5*ab*m11)/d1^3 - ((2*I)*aa^3*ab^3*m11)/(d1^2*d2) -
 (I*aa^3*ab^3*m11)/(d1^2*d3) - (I*aa*ab^5*m11)/(d1*d2*d3) -
 (I*aa*ab^5*m11)/(d1^2*d4) - (I*aa^2*ab^4*m21)/(d1*d2^2) -
 (I*aa^4*ab^2*m21)/(d1^2*d2) - (I*ab^6*m21)/(d2^2*d3) -
 (I*aa^2*ab^4*m21)/(d1*d2*d3) - (I*aa^4*ab^2*m31)/(d1^2*d3) -
 ((2*I)*aa^2*ab^4*m31)/(d1*d2*d3) - (I*aa^3*ab^3*m41)/(d1^2*d4) -
 (I*aa*ab^5*m41)/(d1*d2*d4)
"Nmc(3,1) = "aa*ab - (aa^5*ab)/d1^2 + (I*aa^3*ab)/d1 + (I*aa*ab^3)/d2 -
 (aa^3*ab^3)/(d1*d2) - (aa^3*ab^3)/(d1*d3) - (aa*ab^5)/(d2*d3) -
 (aa*ab^5)/(d1*d4) - (I*aa^5*ab*m11)/d1^3 - (I*aa^3*ab^3*m11)/(d1^2*d2) -
 (I*aa^3*ab^3*m11)/(d1^2*d3) - (I*aa*ab^5*m11)/(d1*d2*d3) -
 (I*aa*ab^5*m11)/(d1^2*d4) - (I*ab^6*m21)/(d2^2*d3) -
 (I*aa^2*ab^4*m21)/(d1*d2*d3) - (I*aa^4*ab^2*m31)/(d1^2*d3) -
 (I*aa^2*ab^4*m31)/(d1*d2*d3) - (I*aa^3*ab^3*m41)/(d1^2*d4) -
 (I*aa*ab^5*m41)/(d1*d2*d4)
"** 4th **"
"Nm(3,1) = "aa*ab - (I*aa^7*ab)/d1^3 - (aa^5*ab)/d1^2 + (I*aa^3*ab)/d1 -
 (I*aa^3*ab^5)/(d1*d2^2) + (I*aa*ab^3)/d2 - ((3*I)*aa^5*ab^3)/(d1^2*d2) -
 (2*aa^3*ab^3)/(d1*d2) - ((2*I)*aa^5*ab^3)/(d1^2*d3) - (aa^3*ab^3)/(d1*d3) -
 (I*aa*ab^7)/(d2^2*d3) - (aa*ab^5)/(d2*d3) - ((4*I)*aa^3*ab^5)/(d1*d2*d3) -
 ((2*I)*aa^3*ab^5)/(d1^2*d4) - (aa*ab^5)/(d1*d4) - (I*aa*ab^7)/(d1*d2*d4) +
 (aa^7*ab*m11)/d1^4 + (aa^3*ab^5*m11)/(d1^2*d2^2) +
 (3*aa^5*ab^3*m11)/(d1^3*d2) + (2*aa^5*ab^3*m11)/(d1^3*d3) +
 (aa*ab^7*m11)/(d1*d2^2*d3) + (4*aa^3*ab^5*m11)/(d1^2*d2*d3) +
 (2*aa^3*ab^5*m11)/(d1^3*d4) + (aa*ab^7*m11)/(d1^2*d2*d4) +
 (2*aa^4*ab^4*m21)/(d1^2*d2^2) + (aa^6*ab^2*m21)/(d1^3*d2) +
 (3*aa^2*ab^6*m21)/(d1*d2^2*d3) + (2*aa^4*ab^4*m21)/(d1^2*d2*d3) +
```

152

```
(aa^2*ab^6*m21)/(d1^2*d2*d4) + (aa^4*ab^4*m31)/(d1^2*d3^2) +
(ab^8*m31)/(d2^2*d3^2) + (2*aa^2*ab^6*m31)/(d1*d2*d3^2) +
(aa^6*ab^2*m31)/(d1^3*d3) + (aa^2*ab^6*m31)/(d1*d2^2*d3) +
(3*aa^4*ab^4*m31)/(d1^2*d2*d3) + (aa^2*ab^6*m31)/(d1^2*d3*d4) +
(aa*ab^7*m41)/(d1^2*d4^2) + (aa^5*ab^3*m41)/(d1^3*d4) +
(2*aa^3*ab^5*m41)/(d1^2*d2*d4) + (aa^3*ab^5*m41)/(d1^2*d3*d4) +
(aa*ab^7*m41)/(d1*d2*d3*d4)
"Nmc(3,1) = "aa*ab - (I*aa^7*ab)/d1^3 - (aa^5*ab)/d1^2 + (I*aa^3*ab)/d1 +
(I*aa*ab^3)/d2 - (I*aa^5*ab^3)/(d1^2*d2) - (aa^3*ab^3)/(d1*d2) -
((2*I)*aa^5*ab^3)/(d1^2*d3) - (aa^3*ab^3)/(d1*d3) - (I*aa*ab^7)/(d2^2*d3) -
(aa*ab^5)/(d2*d3) - ((3*I)*aa^3*ab^5)/(d1*d2*d3) -
((2*I)*aa^3*ab^5)/(d1^2*d4) - (aa*ab^5)/(d1*d4) - (I*aa*ab^7)/(d1*d2*d4) +
(aa^7*ab*m11)/d1^4 + (aa^5*ab^3*m11)/(d1^3*d2) +
(2*aa^5*ab^3*m11)/(d1^3*d3) + (aa*ab^7*m11)/(d1*d2^2*d3) +
(3*aa^3*ab^5*m11)/(d1^2*d2*d3) + (2*aa^3*ab^5*m11)/(d1^3*d4) +
(aa*ab^7*m11)/(d1^2*d2*d4) + (aa^2*ab^6*m21)/(d1*d2^2*d3) +
(aa^4*ab^4*m21)/(d1^2*d2*d3) + (aa^4*ab^4*m31)/(d1^2*d3^2) +
(ab^8*m31)/(d2^2*d3^2) + (2*aa^2*ab^6*m31)/(d1*d2*d3^2) +
(aa^6*ab^2*m31)/(d1^3*d3) + (aa^4*ab^4*m31)/(d1^2*d2*d3) +
(aa^2*ab^6*m31)/(d1^2*d3*d4) + (aa*ab^7*m41)/(d1^2*d4^2) +
(aa^5*ab^3*m41)/(d1^3*d4) + (aa^3*ab^5*m41)/(d1^2*d2*d4) +
(aa^3*ab^5*m41)/(d1^2*d3*d4) + (aa*ab^7*m41)/(d1*d2*d3*d4)
```

6.3 Program *FullMprime*

The Mathematica file FullMprime.nb is listed below, along with output file FullMprimeResults.txt. The complete solution of $\mathcal{M}'$ may be expressed as sixteen coupled equations. These equations are given by the 1st iteration of the GBSE.

```
In[1]:=
(* Generate the sixteen 2nd Order Coupled equations for the 2-
    vertex model *)
(* Frank Dick, WPI Physics, 2007 *)
Clear["Global'*"];

(* zero the matrices, then populate *)
z={0,0,0,0};
G={z,z,z,z};
M={z,z,z,z};
U={z,z,z,z};

(* propagator G has denominators Daa, Dab, Dba,and Dbb on the diagonal *)
G = {{1/d1,0,0,0},{0,1/d2,0,0},{0,0,1/d3,0},{0,0,0,1/d4}};

(* coupling constants are aa, ab=ba, bb *)

(* The U coupling matrix. *)
U[[1,1]]=aa*aa;
U[[1,2]]=aa*ab;
U[[1,3]]=aa*ab;
U[[1,4]]=ab*ab;
U[[2,1]]=aa*ab;
U[[2,3]]=ab*ab;
U[[3,1]]=aa*ab;
U[[3,2]]=ab*ab;
U[[4,1]]=ab*ab;

(* Assign element variable names to Mprime *)
M[[1,1]]=m11;
M[[1,2]]=m12;
M[[1,3]]=m13;
M[[1,4]]=m14;
M[[2,1]]=m21;
M[[2,2]]=m22;
M[[2,3]]=m23;
M[[2,4]]=m24;
```

```
M[[3,1]]=m31;
M[[3,2]]=m32;
M[[3,3]]=m33;
M[[3,4]]=m34;
M[[4,1]]=m41;
M[[4,2]]=m42;
M[[4,3]]=m43;
M[[4,4]]=m44;

(* The elements of M1 give the coupled equations. *)

(* 1st iteration *)
M1=U+  U.G.M;
Print["\n** 1st **"];
Print["M1 = ",Expand[M1]];

(**)
```

6.3.1   FullMprimeResults.txt

In the listing below, $M1$ is the matrix $\mathcal{M}'$ to 2nd order. The m_{ij} are the elements of $\mathcal{M}'$, the d_i are the denominators of the propagators, and aa and ab are the coupling constants g_{AA} and g_{AB}, respectively.

```
"\n** 1st **"
"M1 = "{{aa^2 + (aa^2*m11)/d1 + (aa*ab*m21)/d2 + (aa*ab*m31)/d3 +
   (ab^2*m41)/d4, aa*ab + (aa^2*m12)/d1 + (aa*ab*m22)/d2 + (aa*ab*m32)/d3 +
   (ab^2*m42)/d4, aa*ab + (aa^2*m13)/d1 + (aa*ab*m23)/d2 + (aa*ab*m33)/d3 +
   (ab^2*m43)/d4, ab^2 + (aa^2*m14)/d1 + (aa*ab*m24)/d2 + (aa*ab*m34)/d3 +
   (ab^2*m44)/d4}, {aa*ab + (aa*ab*m11)/d1 + (ab^2*m31)/d3,
  (aa*ab*m12)/d1 + (ab^2*m32)/d3, ab^2 + (aa*ab*m13)/d1 + (ab^2*m33)/d3,
  (aa*ab*m14)/d1 + (ab^2*m34)/d3}, {aa*ab + (aa*ab*m11)/d1 + (ab^2*m21)/d2,
  ab^2 + (aa*ab*m12)/d1 + (ab^2*m22)/d2, (aa*ab*m13)/d1 + (ab^2*m23)/d2,
  (aa*ab*m14)/d1 + (ab^2*m24)/d2}, {ab^2 + (ab^2*m11)/d1, (ab^2*m12)/d1,
  (ab^2*m13)/d1, (ab^2*m14)/d1}}
```

6.4 Program *3VertexMprime*

3VertexMprime determines at what order the A and B kernels begin to contribute to the reaction $A + A \rightarrow A + B$. In the listing below, G is the propagator, U is the kernel coupling matrix (denominators not shown), and M is $\mathcal{M}'$. The value of $\mathcal{M}'_{12}$ is written to the output file *3VertexMprimeResults.txt* for the 1st, 2nd and 3rd iterations of the expansion. The presence of the A and B kernels is indicated by the coupling constant cd (which is actually coupling constant ab, but re-labeled to flag the A and B kernels).

```
(* Iterate the 3-vertex Mprime *)
(* Frank Dick, WPI Physics, 2007 *)
Clear["Global'*"]
SetDirectory["C:\WORK2\dissertation"];
strm=OpenWrite["3VertexMprimeResults.txt"];


(* zero the matrices, then populate *)
z={0,0,0,0,0,0,0,0,0};
G={z,z,z,z,z,z,z,z,z};
M={z,z,z,z,z,z,z,z,z};
U={z,z,z,z,z,z,z,z,z};

(* propagator G has denominators on the diagonal *)
G = {{1/d1,0,0,0,0,0,0,0,0},{0,1/d2,0,0,0,0,0,0,0},{0,0,1/d3,0,0,0,0,0,0},{0,
        0,0,1/d4,0,0,0,0,0},{0,0,0,0,1/d5,0,0,0,0},{0,0,0,0,0,1/d6,0,0,0},{0,
        0,0,0,0,0,1/d7,0,0},{0,0,0,0,0,0,0,1/d8,0},{0,0,0,0,0,0,0,0,1/d9}};

(* coupling constants are aa, ab=ba, bb, cd=ab, cd marks A,B kernels *)

(* The U coupling matrix. *)
U[[1,1]]=aa*aa;
U[[1,2]]=aa*ab;
U[[1,3]]=aa*ab;
U[[1,4]]=ab*ab;
U[[1,7]]=cd*cd;

U[[2,1]]=aa*ab;
U[[2,2]]=aa*bb;
U[[2,3]]=ab*ab;
U[[2,4]]=ab*bb;

U[[3,1]]=aa*ab;
U[[3,2]]=ab*ab;
```

```
U[[3,3]]=aa*bb;
U[[3,4]]=ab*bb;

U[[4,1]]=ab*ab;
U[[4,2]]=ab*bb;
U[[4,3]]=ab*bb;
U[[4,4]]=bb*bb;
U[[4,7]]=cd*cd;

U[[5,6]]=cd*cd;
U[[6,5]]=cd*cd;

U[[7,1]]=cd*cd;
U[[7,4]]=cd*cd;

U[[8,9]]=cd*cd;
U[[9,8]]=cd*cd;

(* Assign element variable names to Mprime *)
M[[1,1]]=m11;M[[1,2]]=m12;M[[1,3]]=m13;M[[1,4]]=m14;M[[1,5]]=m15;M[[1,6]]=m16;
M[[1,7]]=m17;M[[1,8]]=m18;M[[1,9]]=m19;

M[[2,1]]=m21;M[[2,2]]=m22;M[[2,3]]=m23;M[[2,4]]=m24;M[[2,5]]=m25;M[[2,6]]=m26;
M[[2,7]]=m27;M[[2,8]]=m28;M[[2,9]]=m29;

M[[3,1]]=m31;M[[3,2]]=m32;M[[3,3]]=m33;M[[3,4]]=m34;M[[3,5]]=m35;M[[3,6]]=m36;
M[[3,7]]=m37;M[[3,8]]=m38;M[[3,9]]=m39;

M[[4,1]]=m41;M[[4,2]]=m42;M[[4,3]]=m43;M[[4,4]]=m44;M[[4,5]]=m45;M[[4,6]]=m46;
M[[4,7]]=m47;M[[4,8]]=m48;M[[4,9]]=m49;

M[[5,1]]=m51;M[[5,2]]=m52;M[[5,3]]=m53;M[[5,4]]=m54;M[[5,5]]=m55;M[[5,6]]=m56;
M[[5,7]]=m57;M[[5,8]]=m58;M[[5,9]]=m59;

M[[6,1]]=m61;M[[6,2]]=m62;M[[6,3]]=m63;M[[6,4]]=m64;M[[6,5]]=m65;M[[6,6]]=m66;
M[[6,7]]=m67;M[[6,8]]=m68;M[[6,9]]=m69;

M[[7,1]]=m71;M[[7,2]]=m72;M[[7,3]]=m73;M[[7,4]]=m74;M[[7,5]]=m75;M[[7,6]]=m76;
M[[7,7]]=m77;M[[7,8]]=m78;M[[7,9]]=m79;

M[[8,1]]=m81;M[[8,2]]=m82;M[[8,3]]=m83;M[[8,4]]=m84;M[[8,5]]=m85;M[[8,6]]=m86;
M[[8,7]]=m87;M[[8,8]]=m88;M[[8,9]]=m89;
```

```
M[[9,1]]=m91;M[[9,2]]=m92;M[[9,3]]=m93;M[[9,4]]=m94;M[[9,5]]=m95;M[[9,6]]=m96;
M[[9,7]]=m97;M[[9,8]]=m98;M[[9,9]]=m99;

(* 1st iteration *)
M1=U+  U.G.M;
Write[strm,"\n** 1st **"];
Write[strm,"M1[1,2] = ",Expand[   M1[[1,2]]   ]];


M2=U+  U.G.M1;
Write[strm,"\n** 2st **"];
Write[strm,"M2[1,2] = ",Expand[   M2[[1,2]]   ]];


M3=U+  U.G.M2;
Write[strm,"\n** 3st **"];
Write[strm,"M3[1,2] = ",Expand[   M3[[1,2]]   ]];


(*
  M4=U+  U.G.M3;
  Write[strm,"\n** 4st **"];
  Write[strm,"M4[1,2] = ",Expand[   M4[[1,2]]   ]];
  *)

Close[strm];
(**)
```

6.4.1   3VertexMprimeResults.txt

In the listing below, the coupling constant *cd* appears on the 7th line of M3[1,2] along with propagator denominator *d*7, indicating that the A and B kernels and the G_{CC} propagator begin to contribute to the reaction $A + A \rightarrow A + B$ at 6th order in coupling constants (3-rung ladders).


```
"\n** 1st **"
"M1[1,2] = "aa*ab + (aa^2*m12)/d1 + (aa*ab*m22)/d2 + (aa*ab*m32)/d3 +
 (ab^2*m42)/d4 + (cd^2*m72)/d7
"\n** 2st **"
"M2[1,2] = "aa*ab + (aa^3*ab)/d1 + (aa^2*ab*bb)/d2 + (aa*ab^3)/d3 +
 (ab^3*bb)/d4 + (aa^4*m12)/d1^2 + (aa^2*ab^2*m12)/(d1*d2) +
 (aa^2*ab^2*m12)/(d1*d3) + (ab^4*m12)/(d1*d4) + (cd^4*m12)/(d1*d7) +
 (aa^2*ab*bb*m22)/d2^2 + (aa^3*ab*m22)/(d1*d2) + (aa*ab^3*m22)/(d2*d3) +
 (ab^3*bb*m22)/(d2*d4) + (aa^2*ab*bb*m32)/d3^2 + (aa^3*ab*m32)/(d1*d3) +
 (aa*ab^3*m32)/(d2*d3) + (ab^3*bb*m32)/(d3*d4) + (ab^2*bb^2*m42)/d4^2 +
```

```
(aa^2*ab^2*m42)/(d1*d4) + (aa*ab^2*bb*m42)/(d2*d4) +
(aa*ab^2*bb*m42)/(d3*d4) + (cd^4*m42)/(d4*d7) + (aa^2*cd^2*m72)/(d1*d7) +
(ab^2*cd^2*m72)/(d4*d7)
"\n** 3st **"
"M3[1,2] = "aa*ab + (aa^5*ab)/d1^2 + (aa^3*ab)/d1 + (aa^3*ab*bb^2)/d2^2 +
(aa^2*ab*bb)/d2 + (aa^3*ab^3)/(d1*d2) + (aa^4*ab*bb)/(d1*d2) +
(aa^2*ab^3*bb)/d3^2 + (aa*ab^3)/d3 + (2*aa^3*ab^3)/(d1*d3) +
(aa*ab^5)/(d2*d3) + (aa^2*ab^3*bb)/(d2*d3) + (ab^3*bb^3)/d4^2 +
(ab^3*bb)/d4 + (aa*ab^5)/(d1*d4) + (aa^2*ab^3*bb)/(d1*d4) +
(2*aa*ab^3*bb^2)/(d2*d4) + (ab^5*bb)/(d3*d4) + (aa*ab^3*bb^2)/(d3*d4) +
(aa*ab*cd^4)/(d1*d7) + (ab*bb*cd^4)/(d4*d7) + (aa^6*m12)/d1^3 +
(aa^3*ab^2*bb*m12)/(d1*d2^2) + (2*aa^4*ab^2*m12)/(d1^2*d2) +
(aa^3*ab^2*bb*m12)/(d1*d3^2) + (2*aa^4*ab^2*m12)/(d1^2*d3) +
(2*aa^2*ab^4*m12)/(d1*d2*d3) + (ab^4*bb^2*m12)/(d1*d4^2) +
(2*aa^2*ab^4*m12)/(d1^2*d4) + (2*aa*ab^4*bb*m12)/(d1*d2*d4) +
(2*aa*ab^4*bb*m12)/(d1*d3*d4) + (2*aa^2*cd^4*m12)/(d1^2*d7) +
(2*ab^2*cd^4*m12)/(d1*d4*d7) + (aa^3*ab*bb^2*m22)/d2^3 +
(aa^3*ab^3*m22)/(d1*d2^2) + (aa^4*ab*bb*m22)/(d1*d2^2) +
(aa^5*ab*m22)/(d1^2*d2) + (aa^2*ab^3*bb*m22)/(d2*d3^2) +
(aa*ab^5*m22)/(d2^2*d3) + (aa^2*ab^3*bb*m22)/(d2^2*d3) +
(2*aa^3*ab^3*m22)/(d1*d2*d3) + (ab^3*bb^3*m22)/(d2*d4^2) +
(2*aa*ab^3*bb^2*m22)/(d2^2*d4) + (aa*ab^5*m22)/(d1*d2*d4) +
(aa^2*ab^3*bb*m22)/(d1*d2*d4) + (ab^5*bb*m22)/(d2*d3*d4) +
(aa*ab^3*bb^2*m22)/(d2*d3*d4) + (aa*ab*cd^4*m22)/(d1*d2*d7) +
(ab*bb*cd^4*m22)/(d2*d4*d7) + (aa^3*ab*bb^2*m32)/d3^3 +
(aa^3*ab^3*m32)/(d1*d3^2) + (aa^4*ab*bb*m32)/(d1*d3^2) +
(aa*ab^5*m32)/(d2*d3^2) + (aa^2*ab^3*bb*m32)/(d2*d3^2) +
(aa^5*ab*m32)/(d1^2*d3) + (aa^2*ab^3*bb*m32)/(d2^2*d3) +
(2*aa^3*ab^3*m32)/(d1*d2*d3) + (ab^3*bb^3*m32)/(d3*d4^2) +
(2*aa*ab^3*bb^2*m32)/(d3^2*d4) + (aa*ab^5*m32)/(d1*d3*d4) +
(aa^2*ab^3*bb*m32)/(d1*d3*d4) + (ab^5*bb*m32)/(d2*d3*d4) +
(aa*ab^3*bb^2*m32)/(d2*d3*d4) + (aa*ab*cd^4*m32)/(d1*d3*d7) +
(ab*bb*cd^4*m32)/(d3*d4*d7) + (ab^2*bb^4*m42)/d4^3 + (ab^6*m42)/(d1*d4^2) +
(aa^2*ab^2*bb^2*m42)/(d1*d4^2) + (ab^4*bb^2*m42)/(d2*d4^2) +
(aa*ab^2*bb^3*m42)/(d2*d4^2) + (ab^4*bb^2*m42)/(d3*d4^2) +
(aa*ab^2*bb^3*m42)/(d3*d4^2) + (aa^4*ab^2*m42)/(d1^2*d4) +
(aa^2*ab^2*bb^2*m42)/(d2^2*d4) + (aa^2*ab^4*m42)/(d1*d2*d4) +
(aa^3*ab^2*bb*m42)/(d1*d2*d4) + (aa^2*ab^2*bb^2*m42)/(d3^2*d4) +
(aa^2*ab^4*m42)/(d1*d3*d4) + (aa^3*ab^2*bb*m42)/(d1*d3*d4) +
(2*aa*ab^4*bb*m42)/(d2*d3*d4) + (ab^2*cd^4*m42)/(d4^2*d7) +
(bb^2*cd^4*m42)/(d4^2*d7) + (aa^2*cd^4*m42)/(d1*d4*d7) +
(ab^2*cd^4*m42)/(d1*d4*d7) + (cd^6*m72)/(d1*d7^2) + (cd^6*m72)/(d4*d7^2) +
(aa^4*cd^2*m72)/(d1^2*d7) + (aa^2*ab^2*cd^2*m72)/(d1*d2*d7) +
```

159

```
(aa^2*ab^2*cd^2*m72)/(d1*d3*d7) + (ab^2*bb^2*cd^2*m72)/(d4^2*d7) +
(aa^2*ab^2*cd^2*m72)/(d1*d4*d7) + (ab^4*cd^2*m72)/(d1*d4*d7) +
(aa*ab^2*bb*cd^2*m72)/(d2*d4*d7) + (aa*ab^2*bb*cd^2*m72)/(d3*d4*d7)
```

References

[1] F. Dick and J. Norbury, *Pion Cross-Sections from Scalar Theory.* (NASA/TP-2006-XXXXXX).

[2] E.E. van Faassen and J.A. Tjon, *Relativistic NN scattering calculations with Δ degrees of freedom*, Phys. Rev. C, **30**, 285-297 (1984).

[3] H. Yukawa, *On the interaction of elementary particles*, Proceedings of the Physico-Mathematical Society of Japan, **17**, 48 (1935).

[4] R.P. Feynman, *Space-Time Approach to Quantum Electrodynamics*, Phys. Rev., **76** No. 6, 769 (1949).

[5] A. Zee, *Quantum Field Theory in a Nutshell*, Princeton University Press, Princeton (2003).

[6] G. Wanders, *Nonrelativistic Limit of a Bethe-Salpeter Equation*, Phys. Rev. **104**, 1782 - 1783 (1956).

[7] M. Fortes and A. D. Jackson, *Relativistic effects in low-energy nucleon-nucleon scattering*, Nuc. Phys. A, **175**, pgs 449-461 (1971).

[8] Mohsen Emami-Razavi and Jurij W Darewych, *Relativistic two-, three- and four-body wave equations in scalar QFT*, J. Phys. G, **31**, 1095-1109 (2005).

[9] W. Glöckle and L. Müller, *Relativistic theory of interacting particles*, Phys. Rev. C **23** 1183 (1981).

[10] K. Kusaka and A.G. Williams, *Solving the Bethe-Salpeter equation for scalar theories in Minkowski space*, Phys. Rev. D, **51** No. 1, 7026 (1995).

[11] V. Sauli and J. Adam, Jr., *Study of relativistic bound states for scalar theories in the Bethe-Salpeter Dyson-Schwinger formalism*, Phys. Rev. D **67** 085007-1 (2003).

[12] N. Nakanishi, *A General Survey of the Theory of the Bethe-Salpeter Equation*, Suppl. Prog. Theor. Phys. **43**, 1 (1969).

[13] R. Vinh Mau, *The theory of the nucleon-nucleon interaction*, An advanced course in modern nuclear physics, pp. 1-38, Springer, New York (2001).

[14] T.H.R. Skyrme: Proc. Roy. Soc. **A260**, 127 (1961). Nucl. Phys. **31**, 556 (1973).

[15] F. Gross, *Relativistic Quantum Mechanics and Field Theory*, Wiley, New York (1993).

[16] J.W. Norbury, *Quantum Field Theory*, unpublished.

[17] I.J.R.Aitchison and A.J.G Hey, Gauge Theories in Particles Physics, Vol 1, Institute of Physics Publishing, Philadelphia (2003).

[18] M.E. Peskin and D. V. Schroeder, *An Introduction to Quantum Field Theory*, Perseus Books, Cambridge (1995).

[19] M. Maggiore, *A Modern Introduction to Quantum Field Theory*, Oxford University Press, Oxford (2005).

[20] B. Hatfield, Quantum Field Theory of Point Particles and Strings, Westview Press, Boulder (1992).

[21] L.S. Brown, Quantum Field Theory, Cambridge University Press, Cambridge (1992)

[22] N.N.Bogoliubov and D.V. Shirkov, Introduction to the Theory of Quantized Fields, John Wiley and Sons, New York (1980).

[23] W.Greiner and J. Reinhardt, *Field Quantization*, Springer, Berlin (1996).

[24] F. Schwabl, *Advanced Quantum Mechanics*, Springer, (2005).

[25] S. Weinberg, *The Quantum Theory of Fields*, Cambridge University Press, Cambridge (2002).

[26] C. Itzykson and J.B. Zuber, *Quantum Field Theory*, Dover, Minneola, NY (2005).

[27] J.D. Bjorken and S.D. Drell, *Relativistic Quantum Fields*, McGraw-Hill, New York (1965).

[28] F. Mandl and G. Shaw, *Quantum Field Theory*, Wiley, New York (1984).

[29] L.H. Ryder, *Quantum Field Theory*, Cambridge University Press, Cambridge (2005).

[30] F. Dick and J. Norbury, *Differential Cross Section Kinematics for 3-dimensional Transport Codes.* (NASA/TP-2006-XXXXXX).

[31] V. Dmitriev and O. Sushkov, Δ-*formation in the* $^1H(^3He, {}^3H)\Delta^{++}$ *reaction at intermediate energies*, Nuc. Phys. A **459**, 503 (1986).

[32] S. Huber and J. Aichelin, *Production of Δ- and N^*-resonances in the one-boson exchange model*, Nuc. Phys. A **573**, 587 (1994).

[33] E.E. van Faassen and J.A. Tjon *Relativistic calculations for $NN - N\Delta$ scattering with pion and ρ exchange* Physical Review C **28** 2354 (1983).

[34] J.A. Tjon and E.E. van Faassen, *Relativistic One-Boson Exchange Calculations for Coupled $NN \Rightarrow N\Delta$ Scattering*, Phys. Let., **120B**, 39-43 (1983).

[35] F. Gross, J.W. Van Orden and K. Holinde, *Relativistic one-boson-exchange model for the nucleon-nucleon interaction*, Phys. Rev. C, **45**, pgs 2094-2132 (1992).

[36] W.M. Yao et al, *Review of Particle Physics*, J. Phys. G, **33**, 1 (2006).

[37] E.E. Salpeter and H.A. Bethe, *A Relativistic Equation for Bound-state Problems* Phys. Rev., **84** No. 6, 1232 (1951).

[38] A.D. Lahiff and I.R. Afnan, *Solution of the Bethe-Salpeter equation for pion-nucleon scattering*, Phys. Rev. C, **60**, 024608-1 (1999).

[39] J.J. Kubis, *Partial-Wave Analysis of Spinor Bethe-Salpeter Equations for Single Particle Exchange*, Phys. Rev. D, **6**, pgs 547-564 (1972).

[40] M.L. Goldberger, M.T. Grisaru, S.W. MacDowell and D.Y. Wong, *Theory of Low-Energy Nucleon-Nucleon Scattering*, Phys. Rev., **120**, pgs 2250-2276 (1960).

[41] R.E. Cutkosky, *Solutions of a Bethe-Salpeter Equation*, Phys. Rev., **96** No.4, 1135 (1954).

[42] N. Seto, Suppl. Prog. Theor. Phys. **95**, 25 (1988).